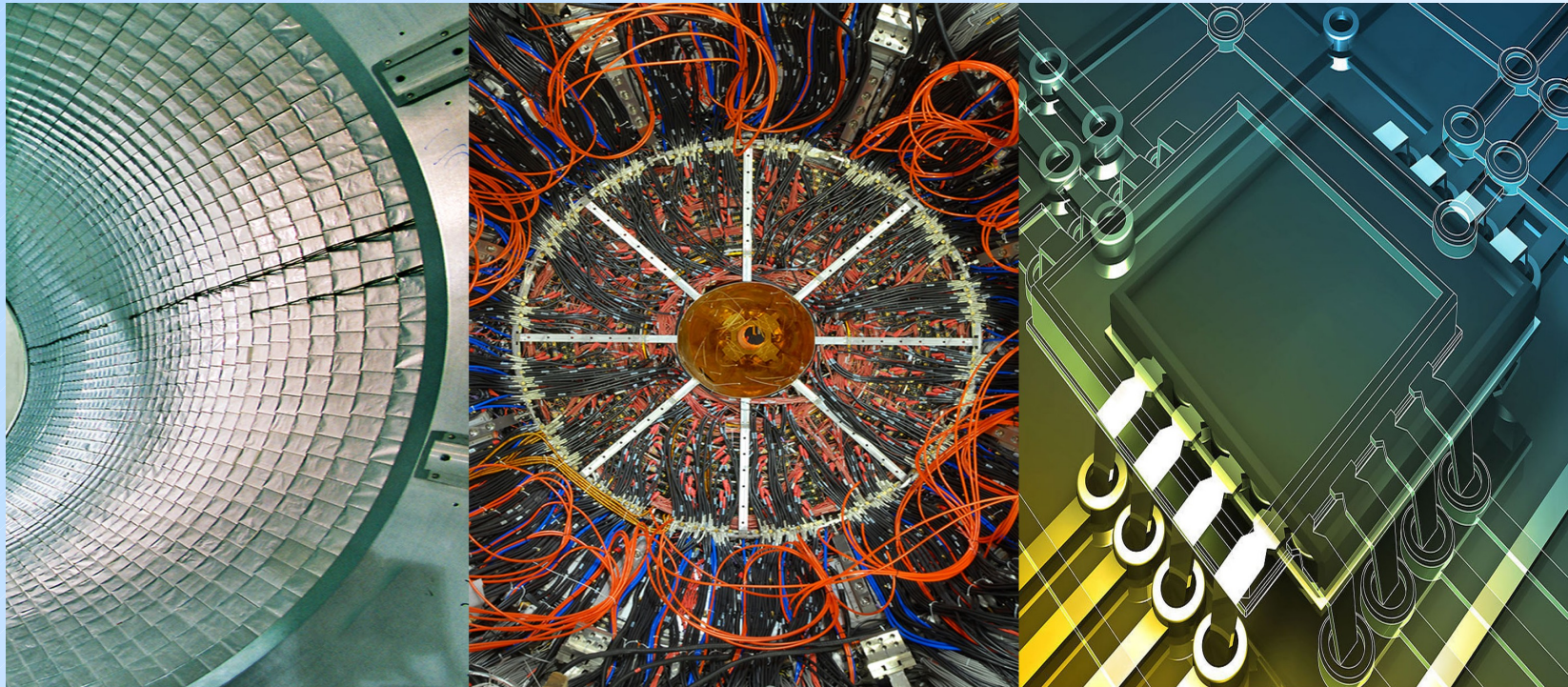


Photon detectors 2/2

Samo Korpar

University of Maribor and J. Stefan Institute, Ljubljana

8th Summer Topical Seminar on Frontier of Particle Physics -
Detector and Electronics
August 18 – 22, 2011, Beijing, China



Detector types

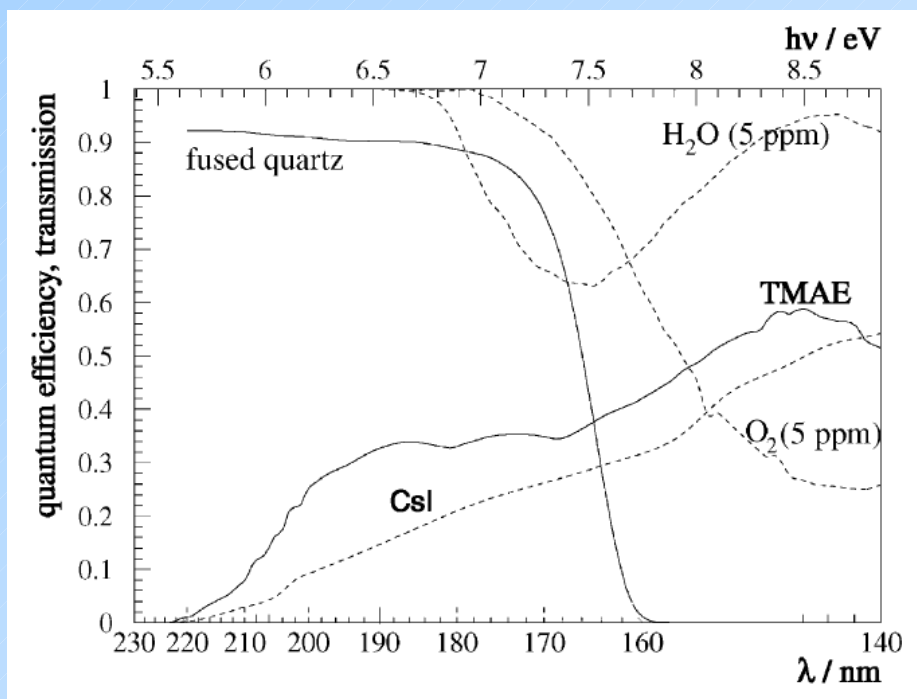
- PMT
- MAPMT, Flat-panel PMT
- MCP-PMT
- Photosensitive gas detectors (MWPC / MPGD)
- PIN diode
- APD
- VLPC
- HPD, HAPD
- G-APD / SiPM

Gaseous detectors

Two ways to achieve photo-sensitivity:

- Addition of photosensitive molecules to the counter gas (TMAE, TEA)
- Solid photocatode (CsI, bialkali ...)

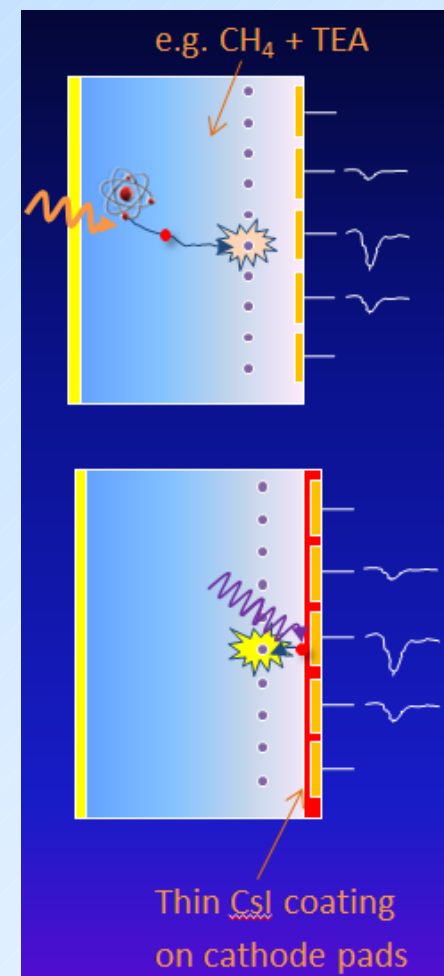
Released photoelectron drifts toward the high field region and produces the avalanche → multiplication → detectable signal



- TMAE, TEA, CsI sensitive in deep UV
- Bialkali sensitive also in visible but **requires very clean gas** – long term operation not yet demonstrated

Difficulties:

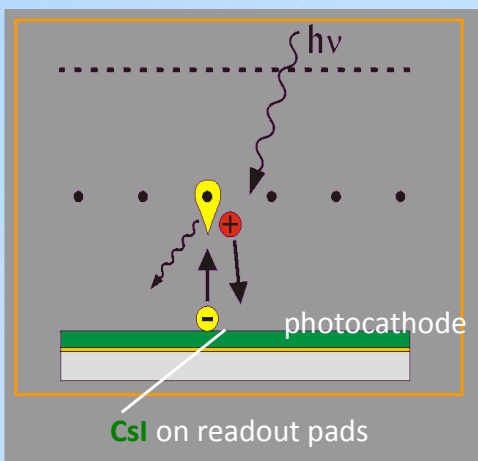
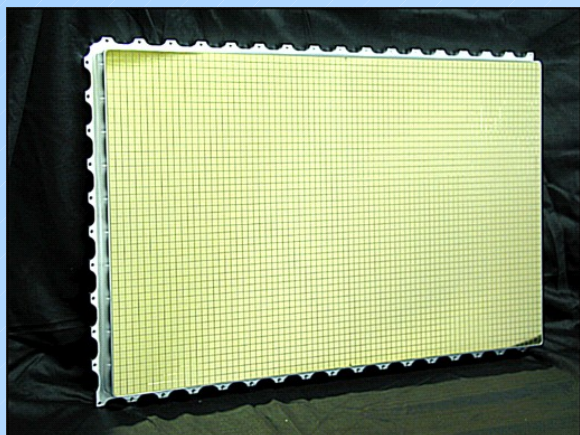
- High gain operation (ion feedback and light emission from avalanche)
- Gas purity → UV transparency
- Aging (ion feedback, impurities)



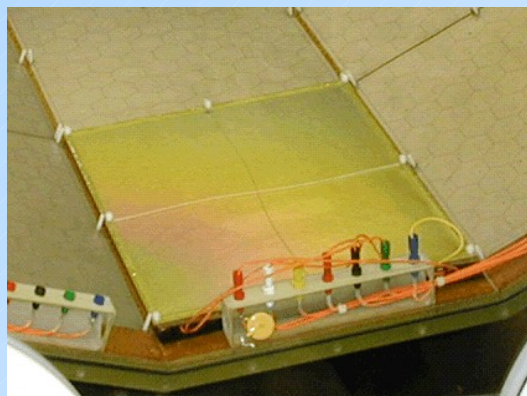
Gaseous detectors: some applications

Proven technology:

Cherenkov detectors in ALICE, HADES, COMPASS, J-LAB.... Many m² of CsI photo-cathodes

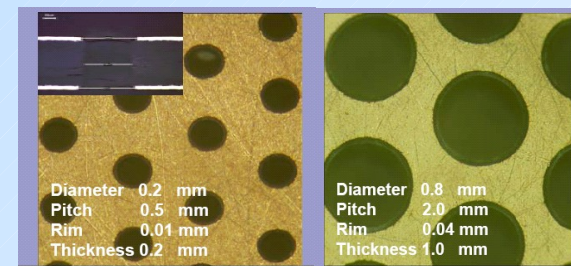


Recently installed:
HBD (threshold Cherenkov counter) of PHENIX.



R&D:

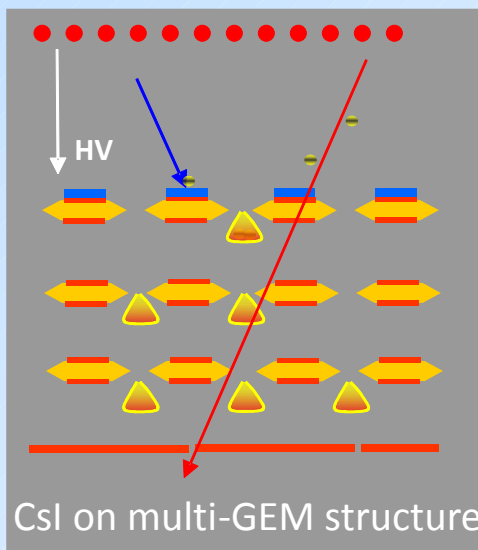
- Thick GEMs (ALICE, COMPASS)

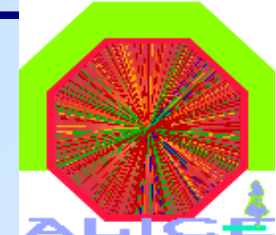


- Sealed gaseous devices



Sealed gaseous photo-detector with bi-alkali PC. (Weizmann Inst., Israel)





High Momentum Particle ID at ALICE uses MWPCs with CsI photocathode.

Radiator:

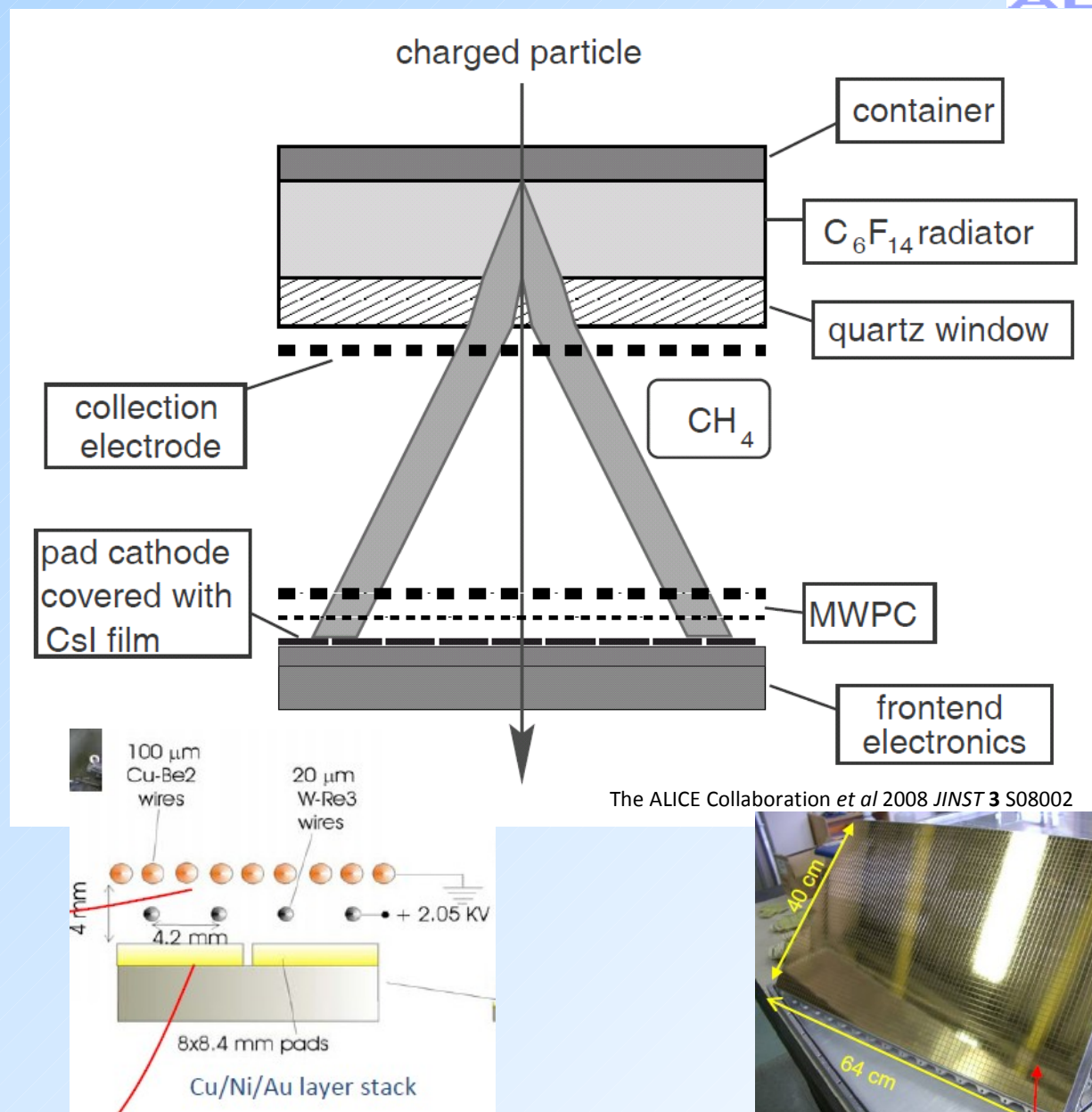
15 mm liquid C_6F_{14} ,
 $n \sim 1.2989$ @ 175nm,
 $\beta_{th} = 0.77$

Photon converter:

Reflective layer of CsI
 QE $\sim 25\%$ @ 175 nm.

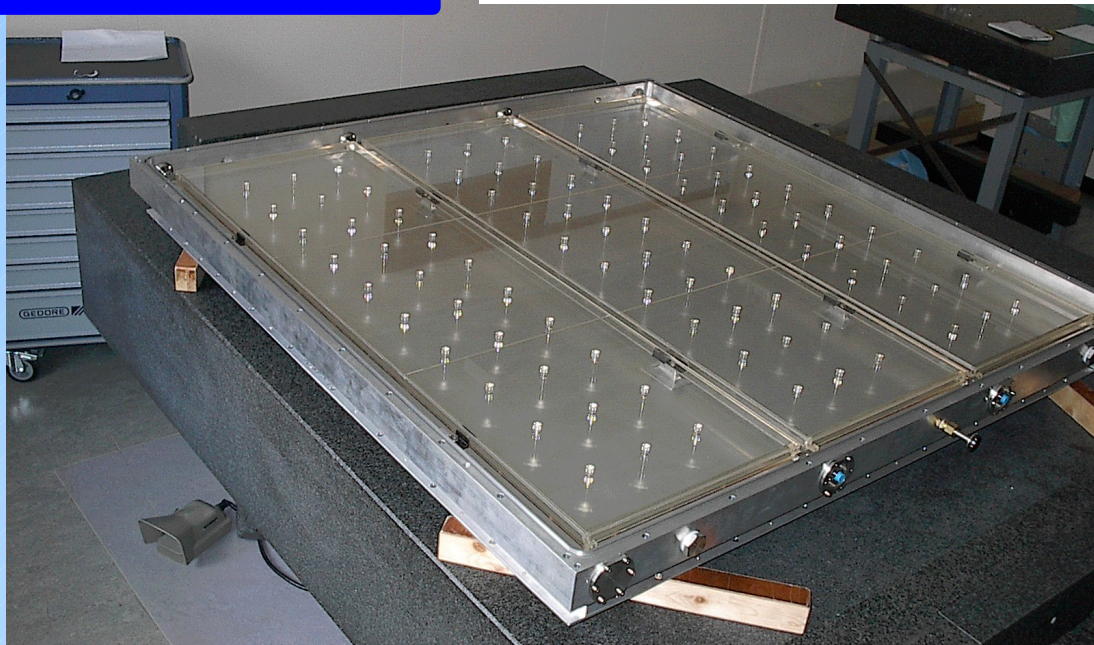
Photoelectron detector:

MWPC with CH_4 at
 atmospheric pressure (4 mm
 gap, HV = 2050 V)
 + analogue pad readout.

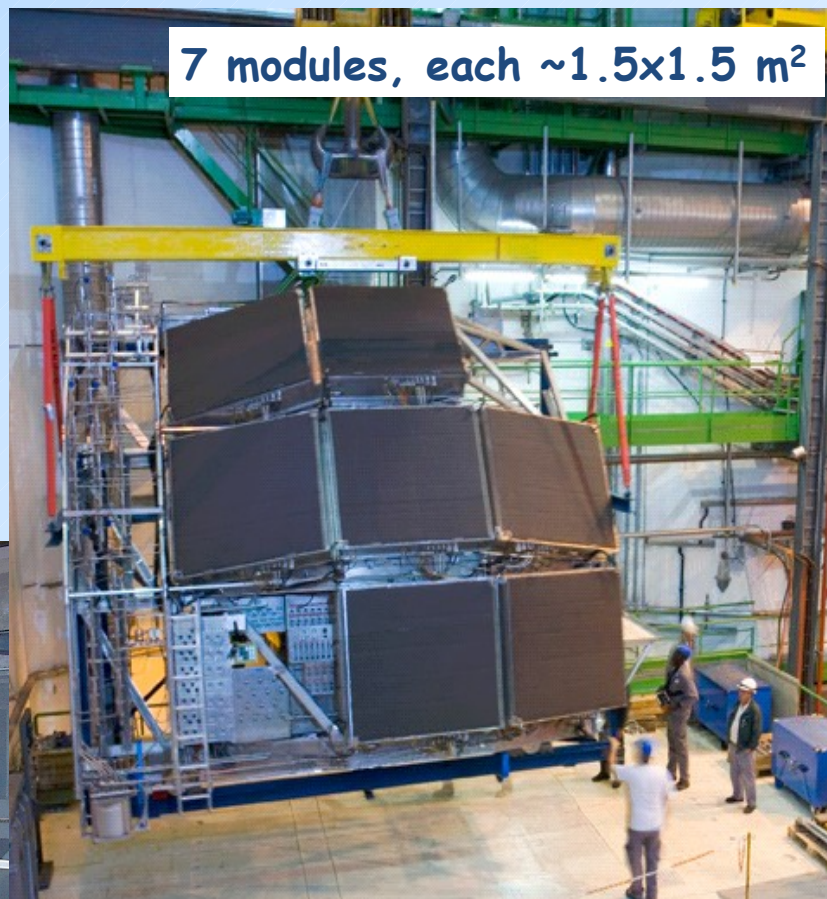


ALICE HMPID

3 radiators/module, 8l each



7 modules, each $\sim 1.5 \times 1.5 \text{ m}^2$



6 CsI photo-cathodes/module, total area $> 10 \text{ m}^2$

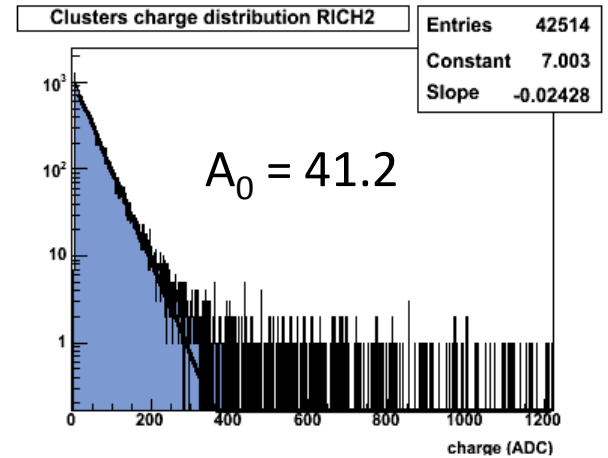
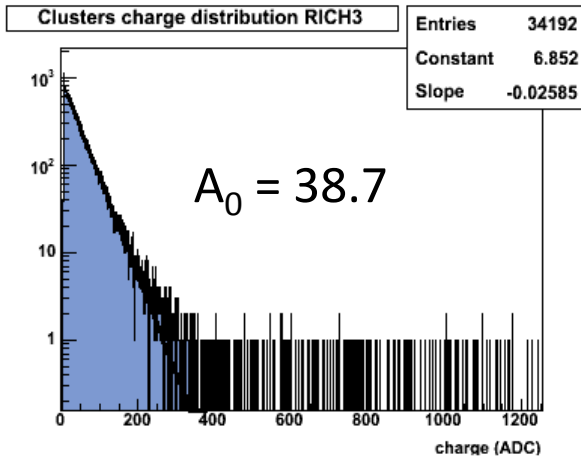
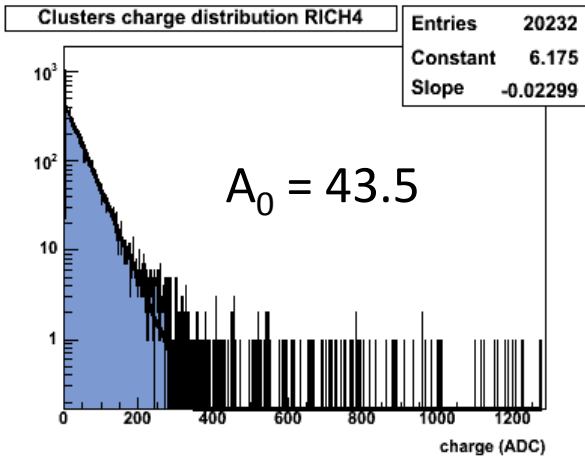
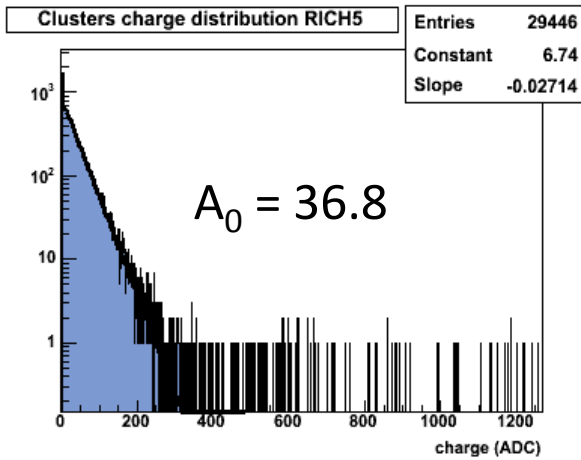
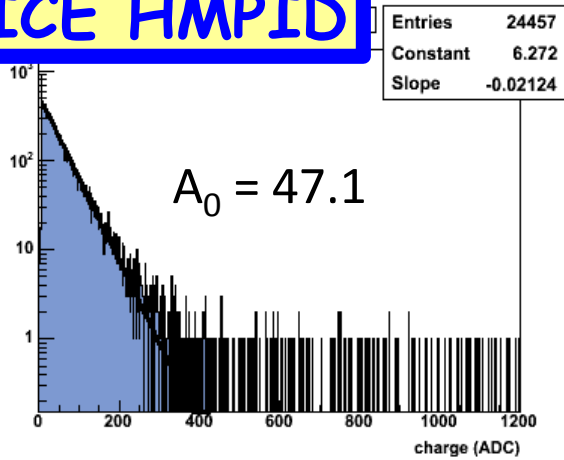
ALICE HMPID

Typical single photo-electron spectra in a MWPC

$$f(z) \propto z^{m-1} e^{-mz}$$

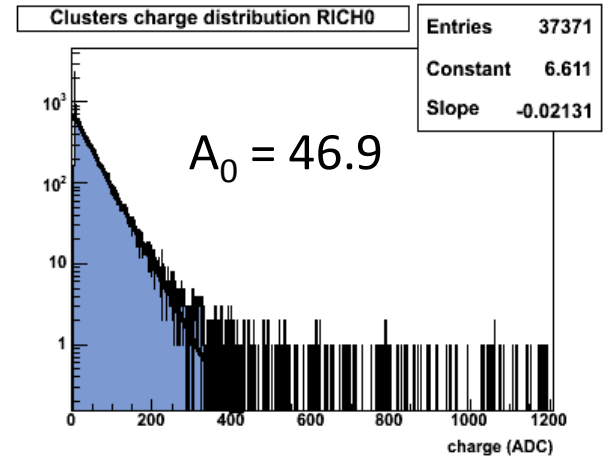
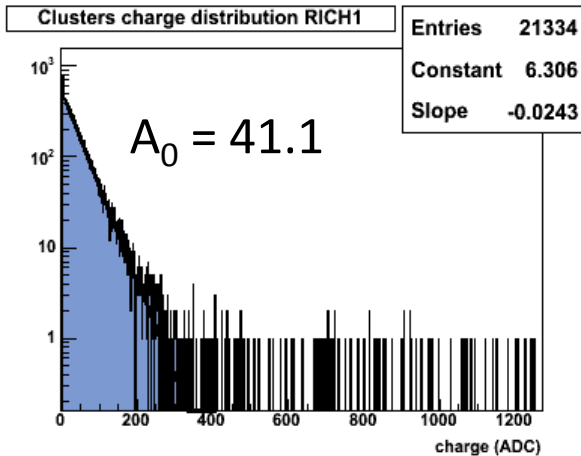
$$z = A/A_0 \quad A = \text{charge}$$

$$m = \text{Polya parameter}$$

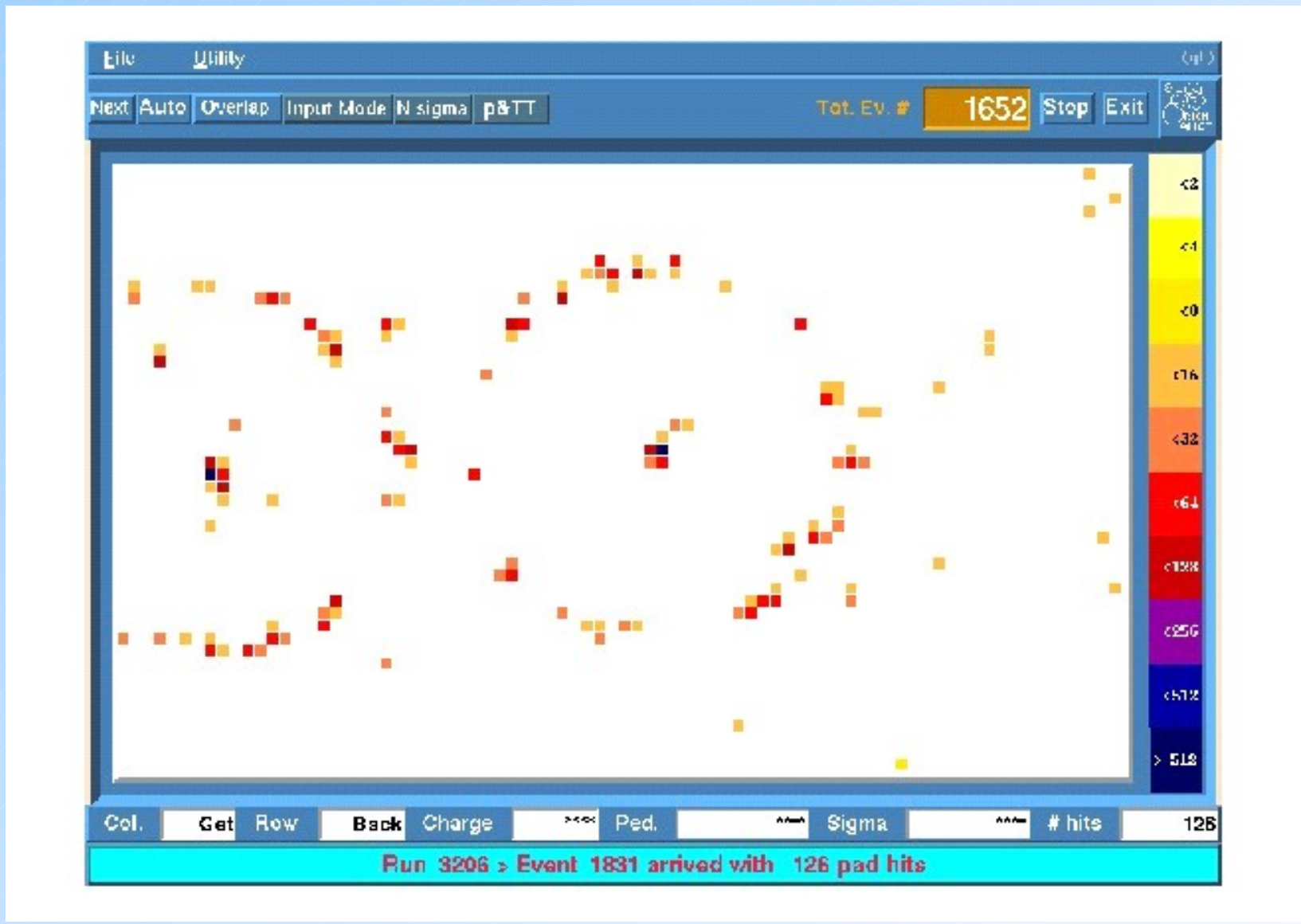


Here: fit with $m = 1$
 \rightarrow exponential distribution

$$P(A) = \frac{1}{A_0} e^{-\frac{A}{A_0}}$$



ALICE HMPID

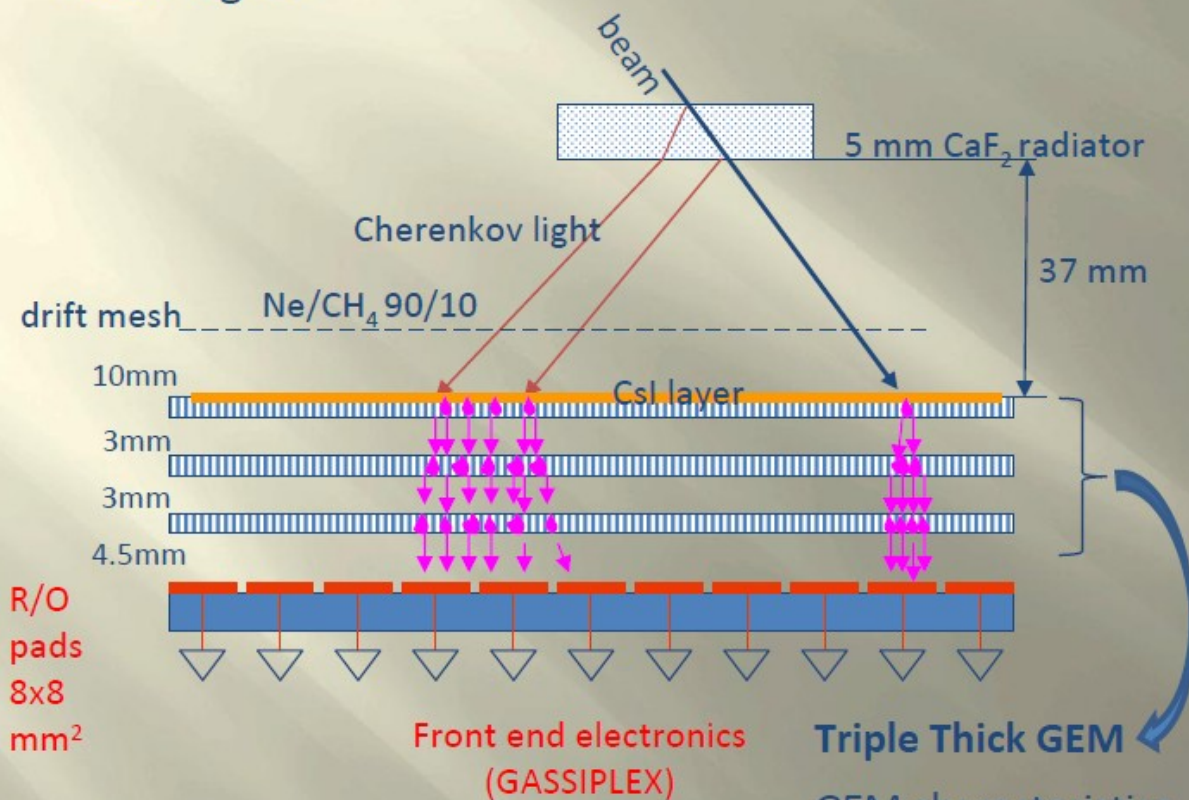




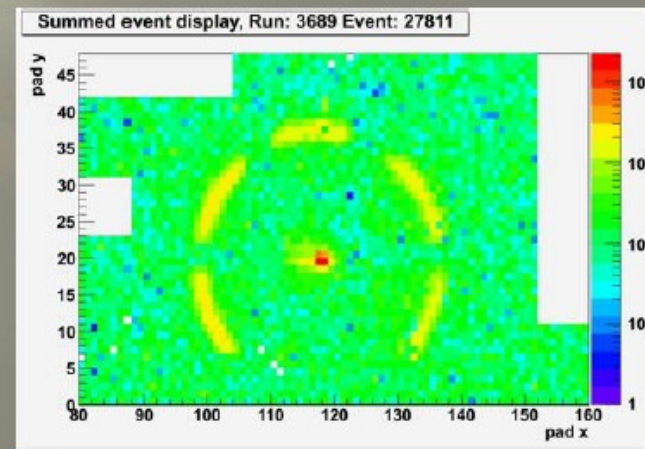
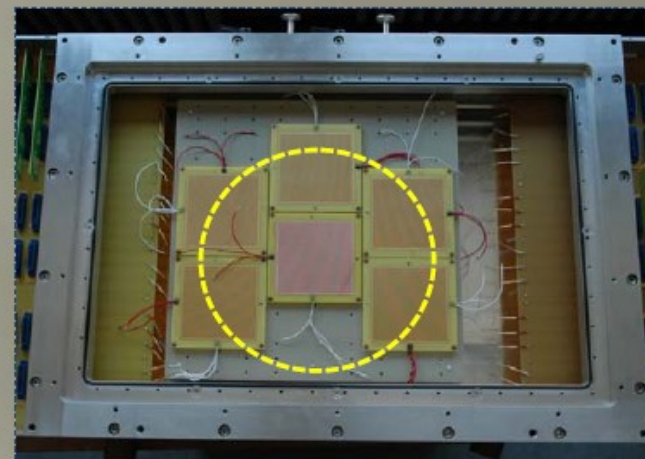
Principle of a 3-TGEM chamber



R&D on CsI-TTGEM option, to achieve better spatial resolution and exploit intrinsically faster signal



CERN PS/T10 testbeam (May 2011)



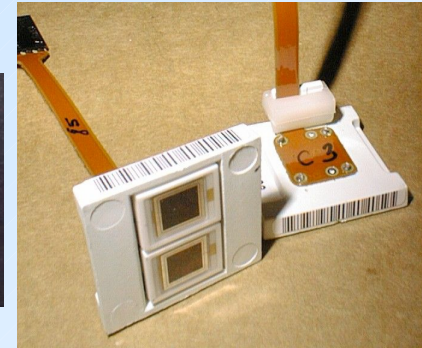
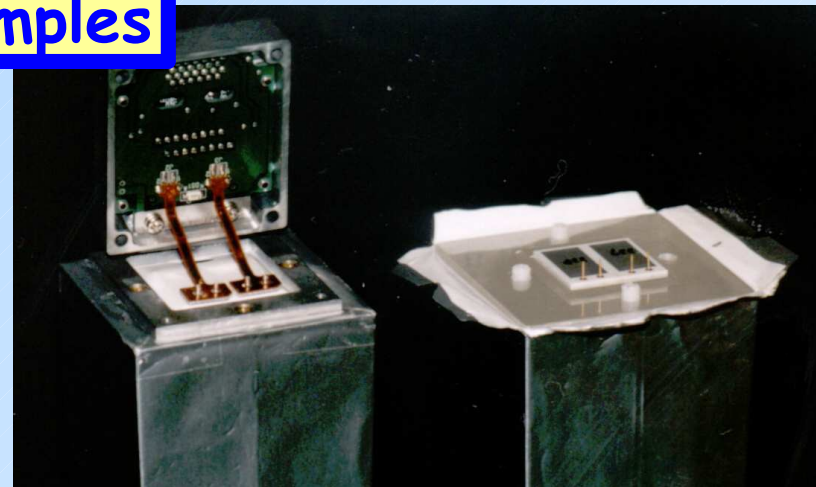
See talk by Vladimir PESKOV, in session S11 Gaseous



Solid state detectors - application examples

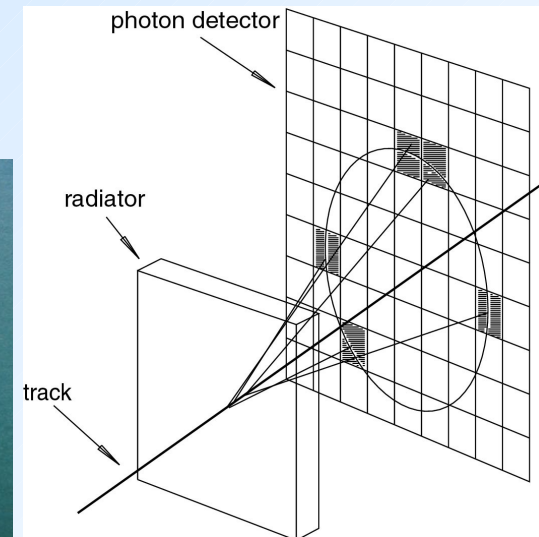
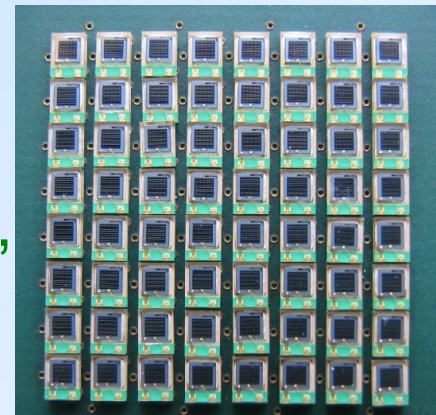
Calorimeters:

- Belle calorimeter with PIN photodiodes
~ 50000 photons/MeV
- CMS calorimeter with APDs
~ 100 photons/MeV



Cherenkov light detection:

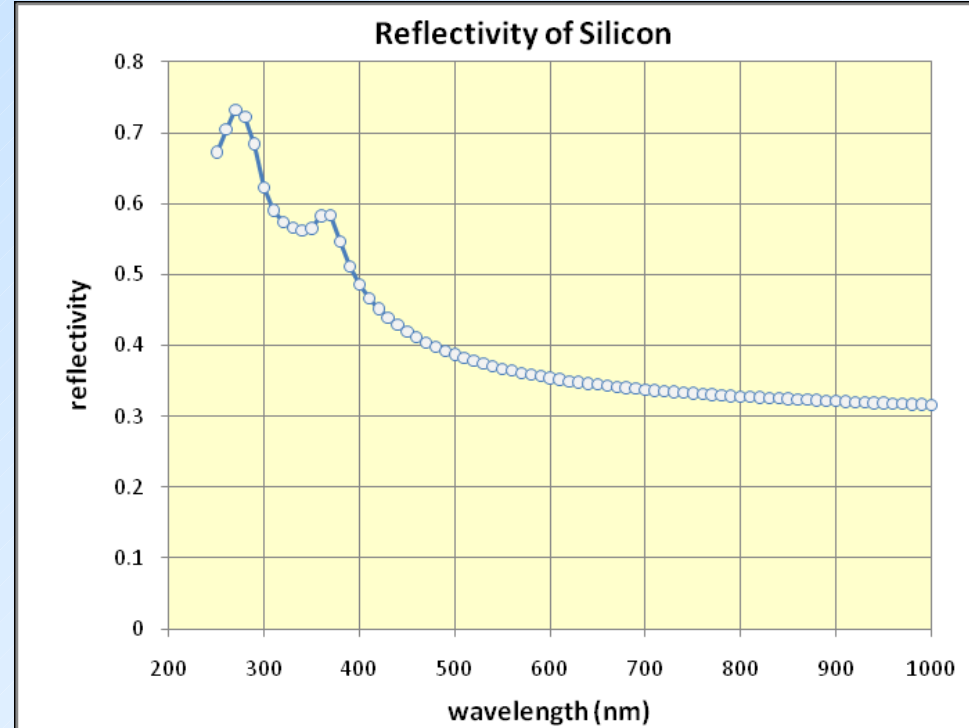
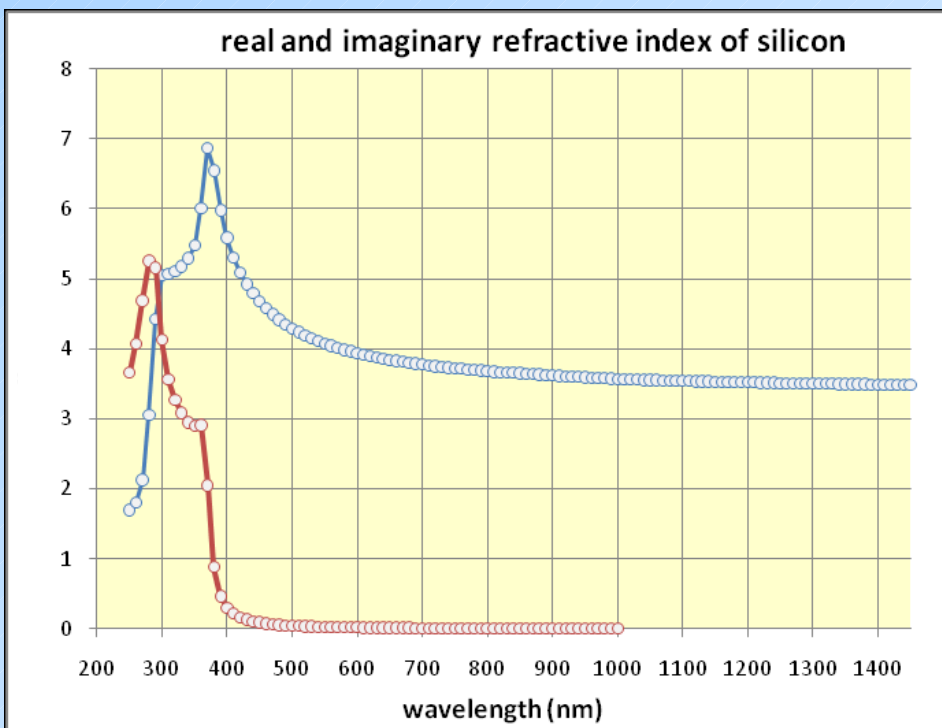
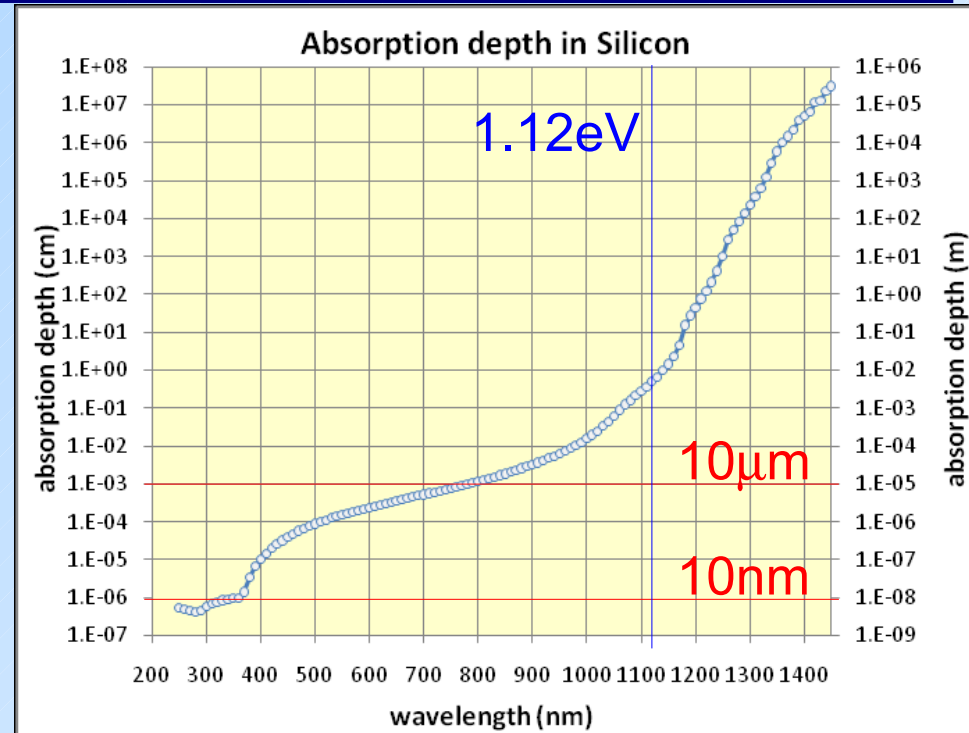
- Belle-II aerogel RICH prototype module with SiPMs – detection of single photons



Fiber trackers, medical imaging (PET), TOF ...

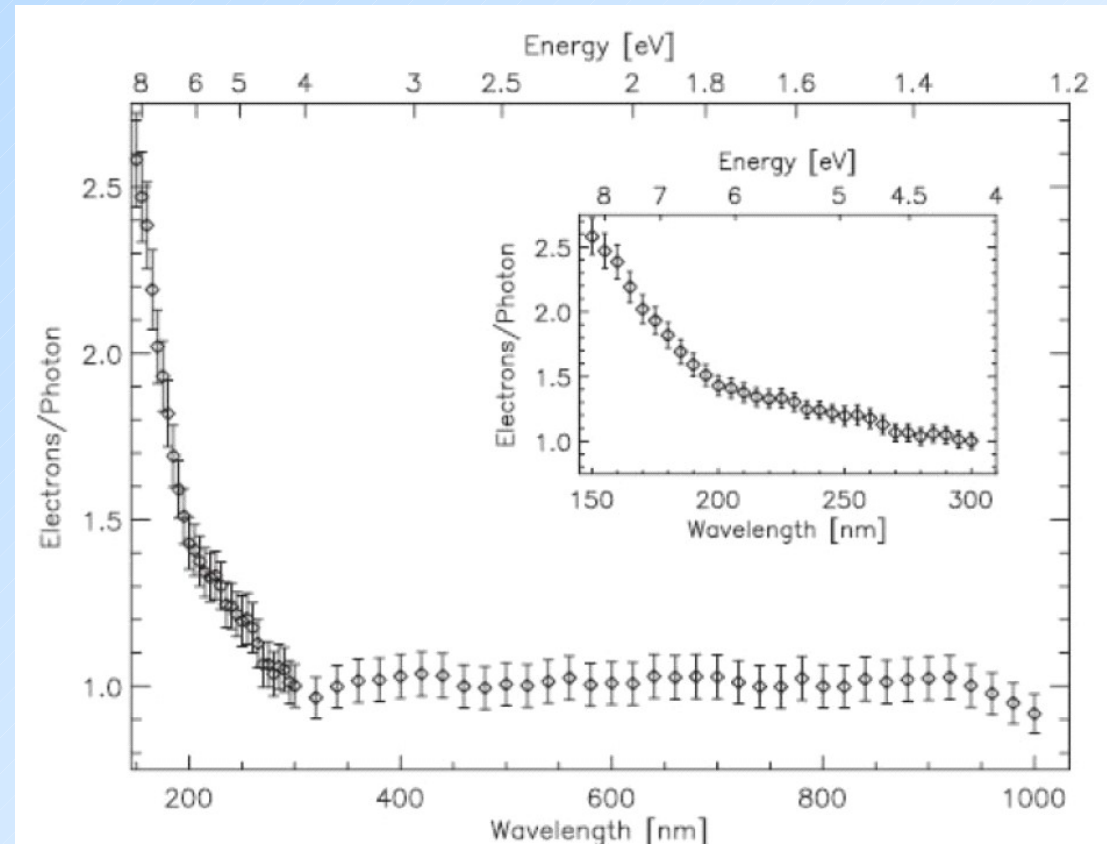
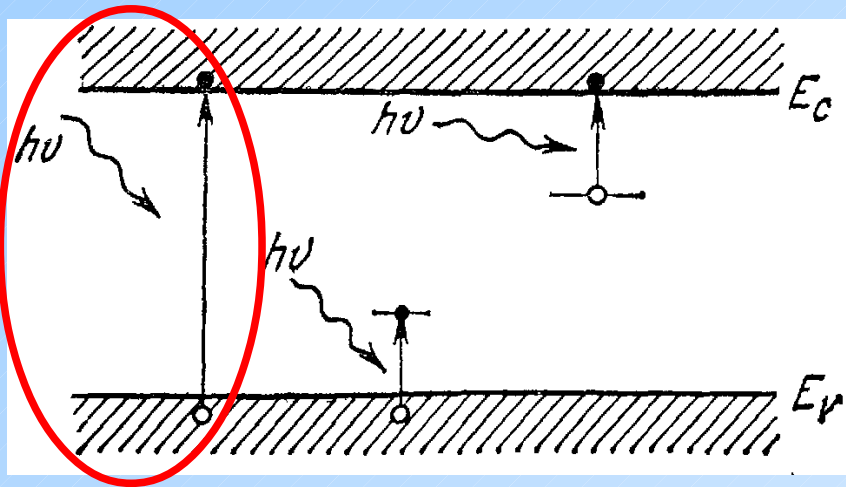
Si optical properties

- large variation of absorption length (10nm-10 μ m) \rightarrow limits QE for short and long wavelengths
- high refractive index \rightarrow high reflectivity \rightarrow anti-reflecting coating is used



Internal photoelectric effect in Si

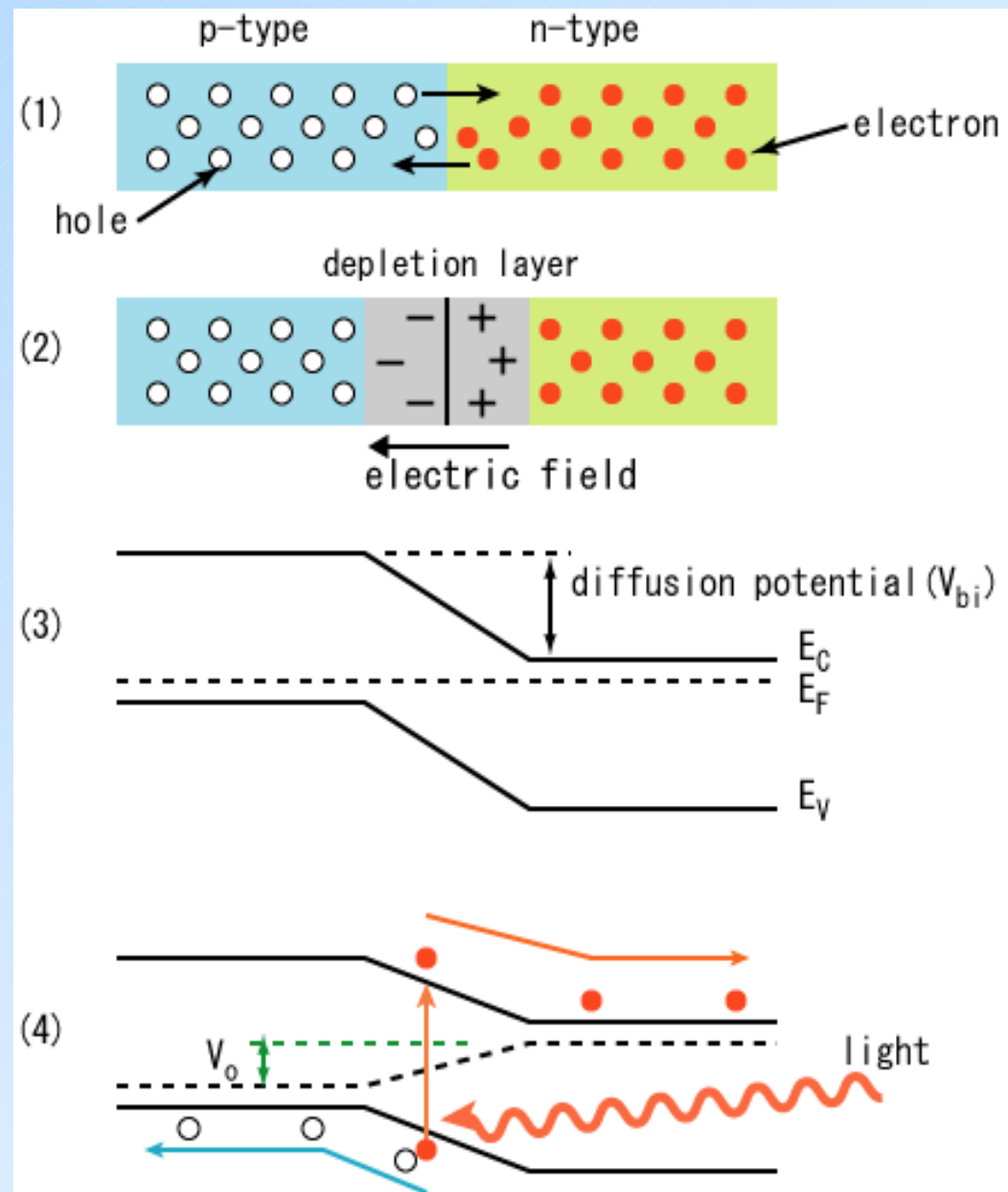
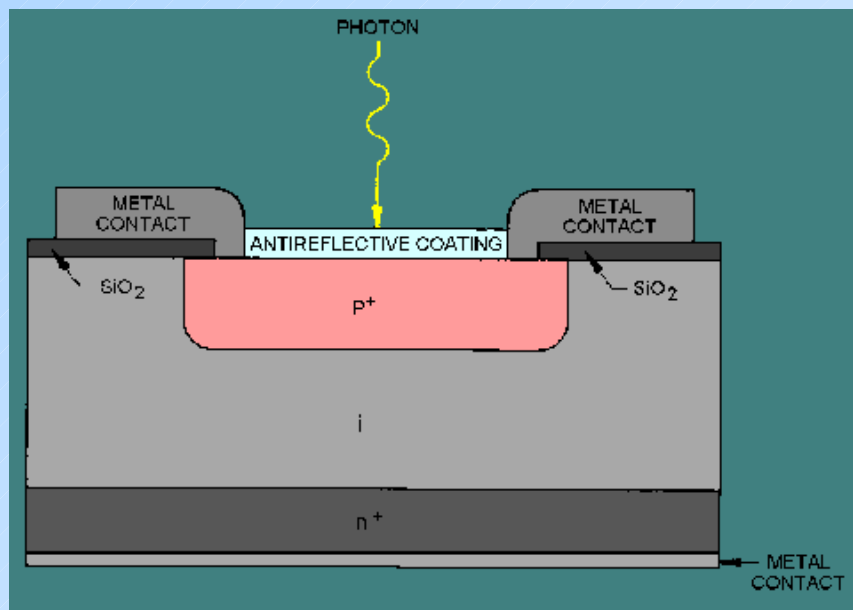
Band gap ($T=300\text{K}$) = 1.12 eV ($\sim 1100\text{ nm}$)



More than 1 electron can be created by light in silicon

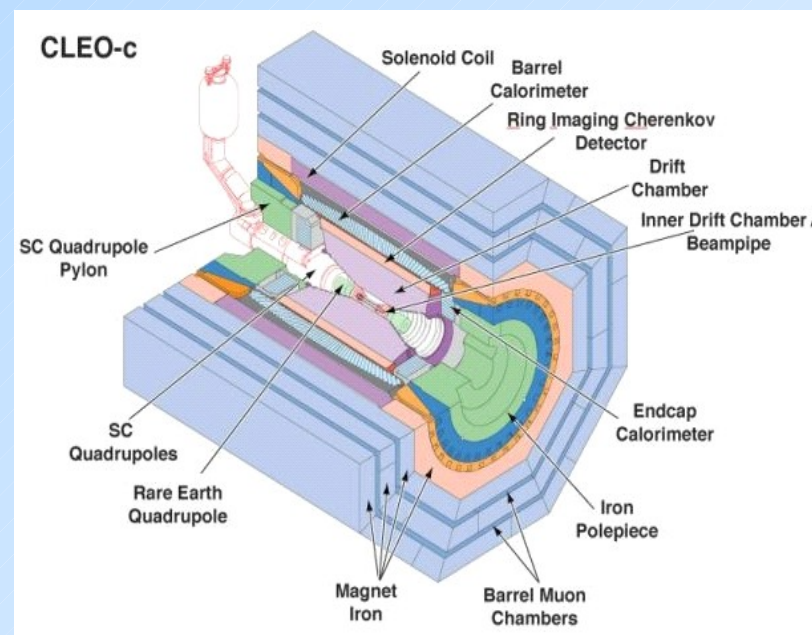
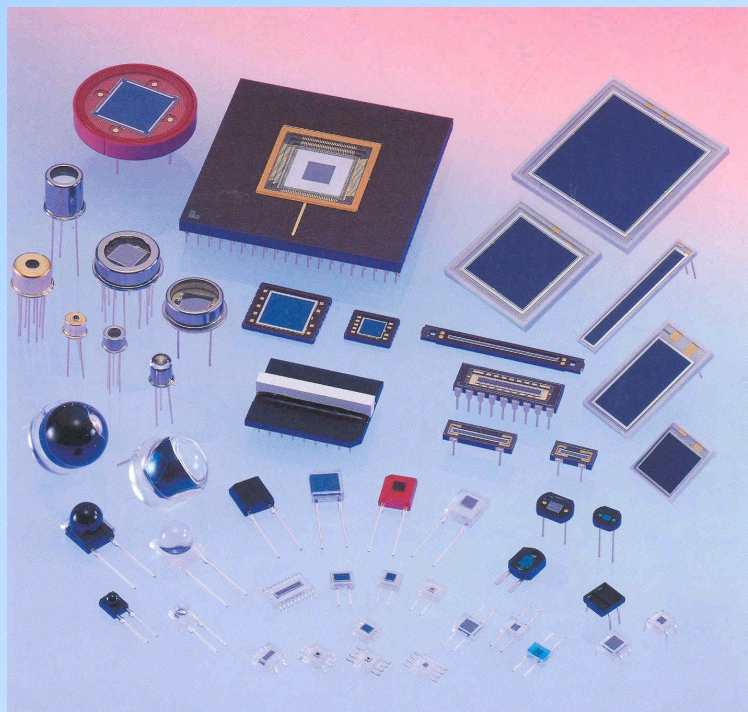
Photo diode (p-n, p-i-n)

- photons absorbed in the depleted region generate photo-current
- no amplification – can detect light pulses with large number of photons ($> \sim 10^4$)
- Si band gap energy 1.12eV (wavelength 1100nm)
- p-i-n \rightarrow lower V_{bias} and C



PIN diodes

The PIN diode is a very successful device. It is used in many big calorimeters in high energy physics (Cleo, L3, Crystal Barrel, Barbar, Belle)

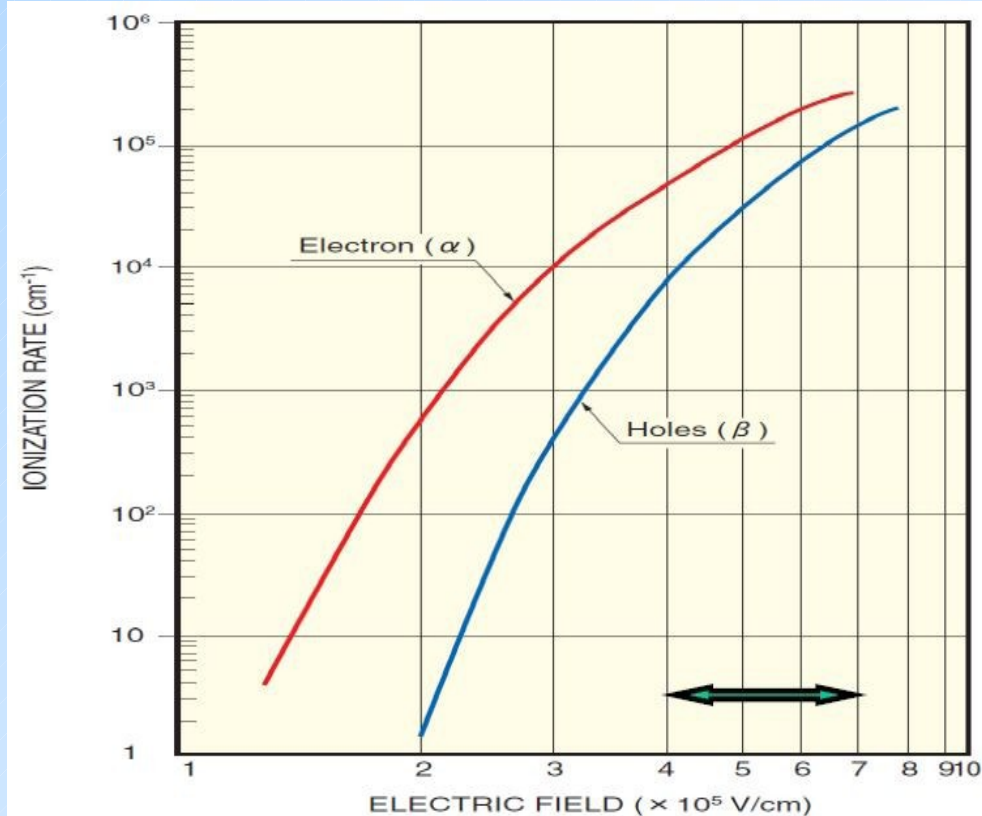


The PIN diode is the simplest, most reliable and cheapest photo sensor. It has high quantum efficiency (80%), very small volume and is insensitive to magnetic fields

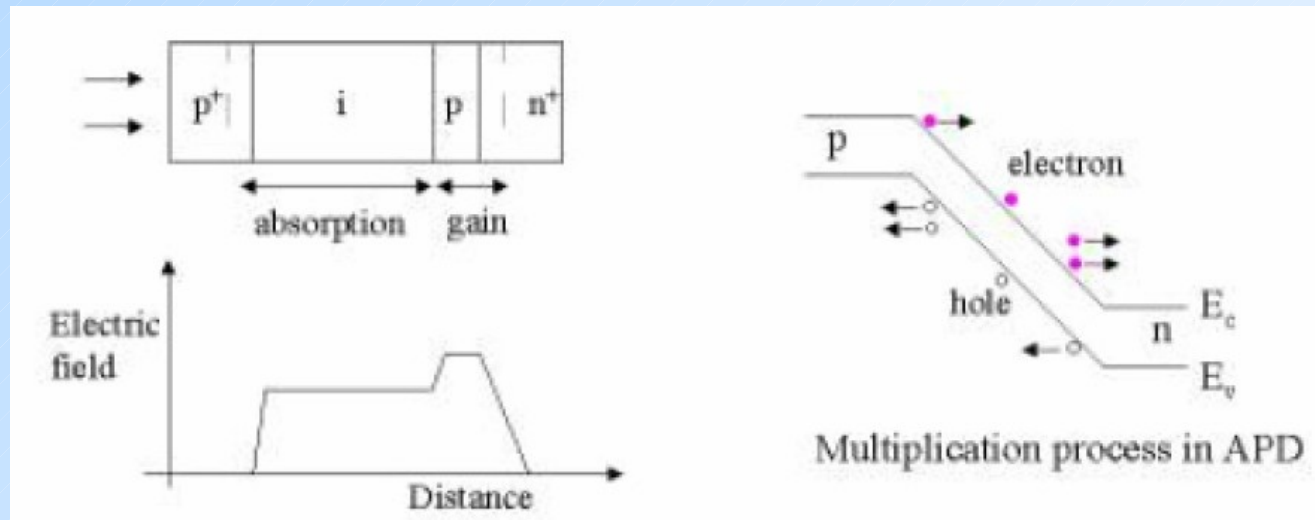
Avalanche photodiode

Photodiode with high field amplification region:

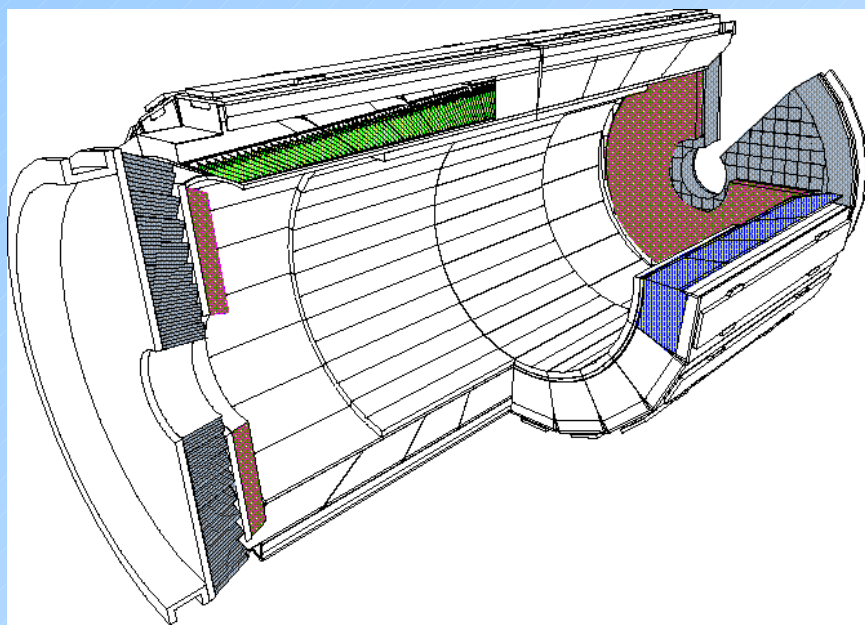
- both carriers can participate in amplification
- modest amplification up to 1000 limited by start of pair production by holes \rightarrow leads to avalanche breakdown.
- not capable of single photon detection



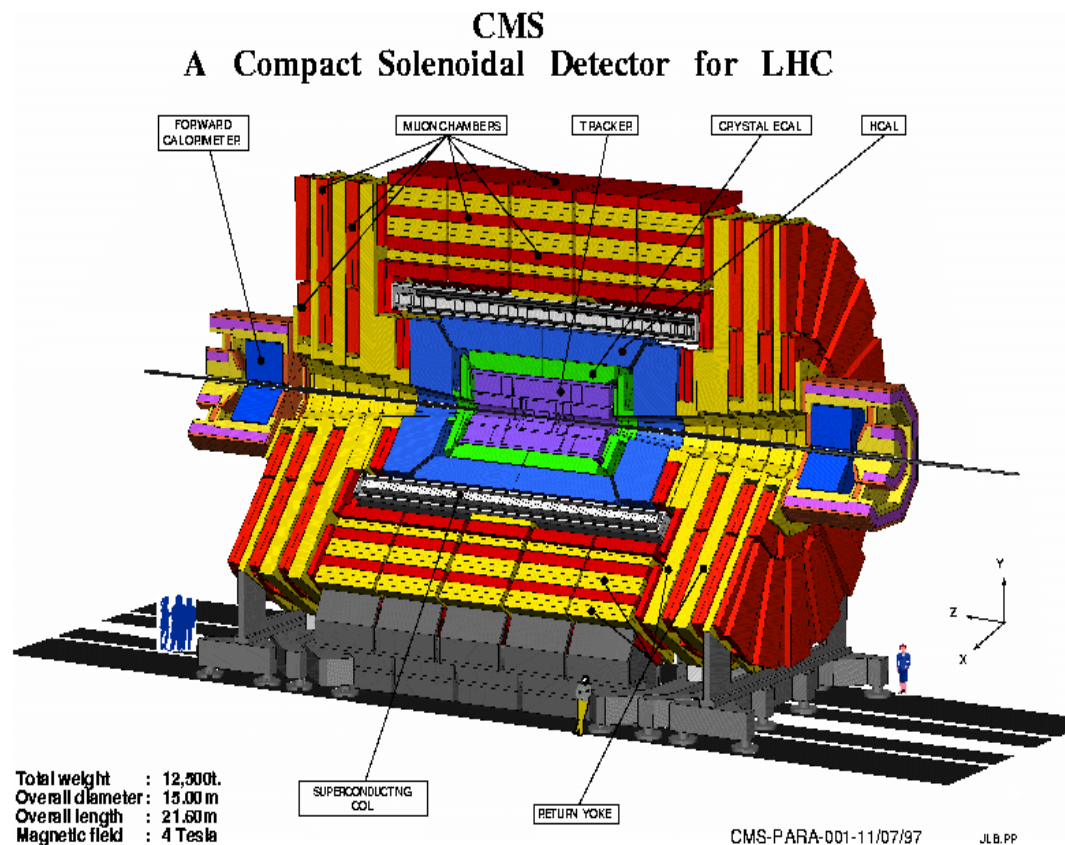
Ionization coefficients α for electrons and β for holes



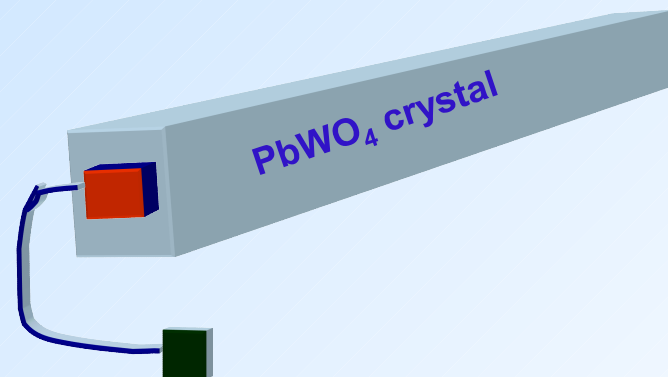
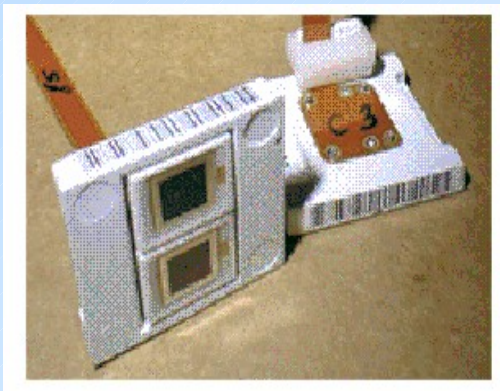
APD: CMS ECAL

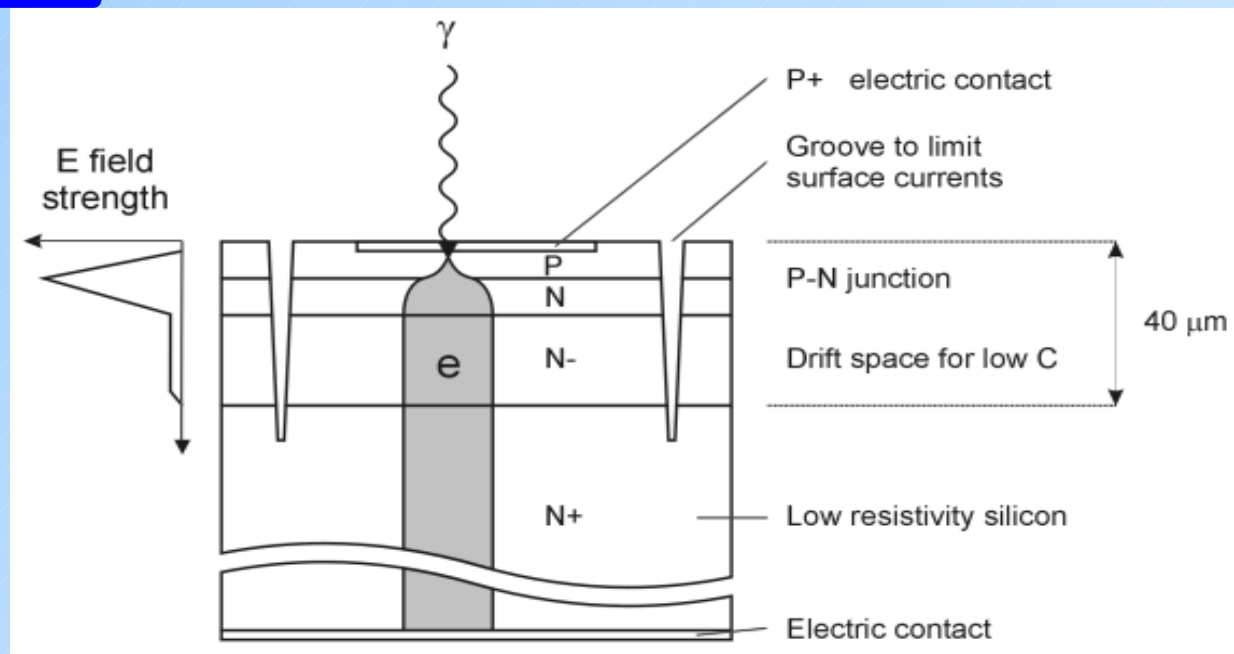


36 supermodules with 1700 crystals each



2 APD's/crystal
→ 122.400 APD's



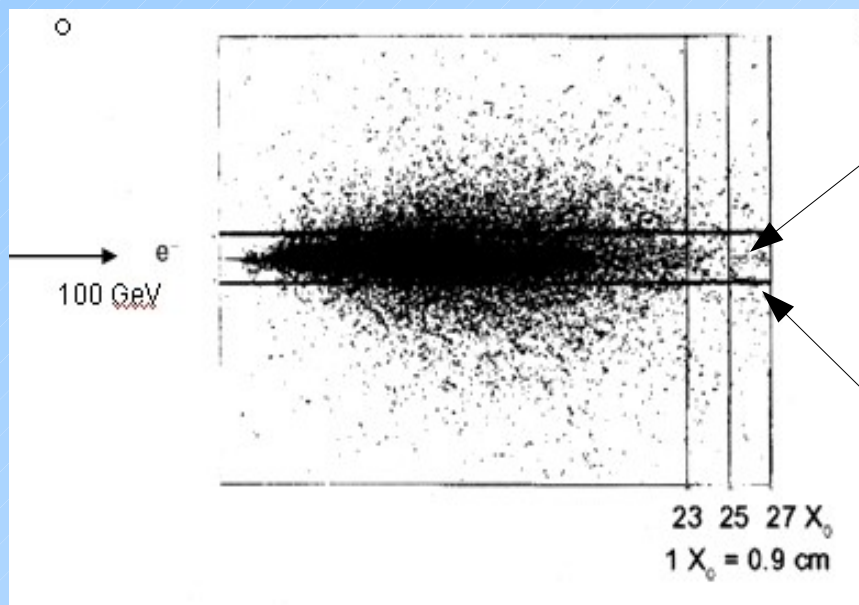


Photons create electron-hole pairs in the thin p-layer on top of the device and the electrons induce avalanche amplification in the high field at the p-n junction. Holes created behind the junction contribute little because of their much smaller ionization coefficient.

Electrons produced by ionizing particles traversing the bulk are not amplified. The effective thickness for the collection and amplification of electrons which have been created by a MIP is therefore about $6 \mu\text{m}$
 $\sim (5 \times 50 + 45 \times 1)/50$.

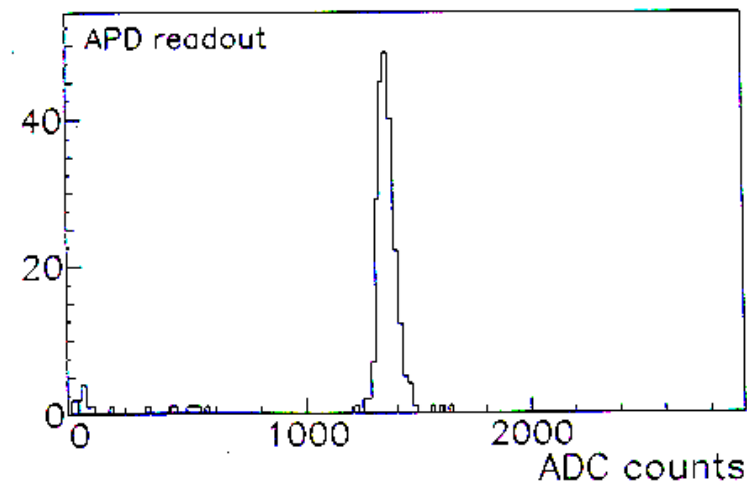
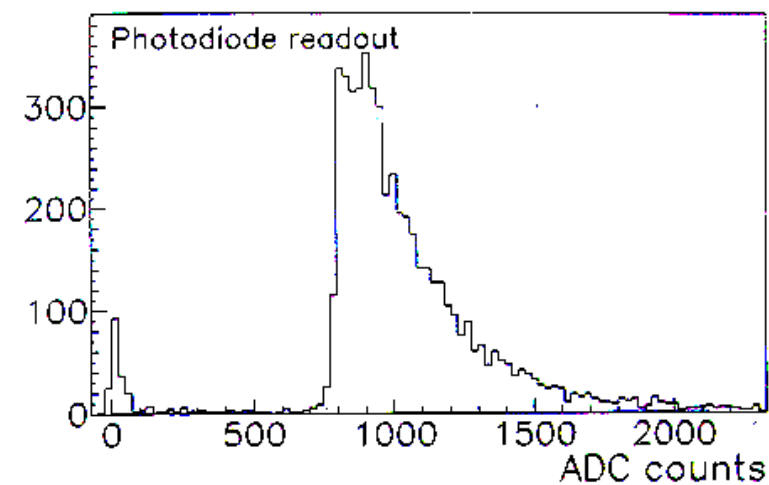
The NCE is 50 times smaller than in a PIN diode.

APD: nuclear counter effect



Geant simulation: each dot stands for an energy deposition of more than 10 keV

A MIP in a PIN diode creates $\sim 30,000$ e-h pairs (the diode thickness of $300 \mu\text{m} \times 100$ pairs/ μm). A photon with an energy of 7 GeV produces in $\text{PbWO}_4 + \text{PIN}$ diode the same number of e-h pairs.



80 GeV e- beam in a 18 cm long PbWO_4 crystal

APD impact on energy resolution

$$\frac{\sigma_E}{E} = \frac{a}{\sqrt{E}} \oplus b \oplus \frac{c}{E}$$

ECAL energy resolution:

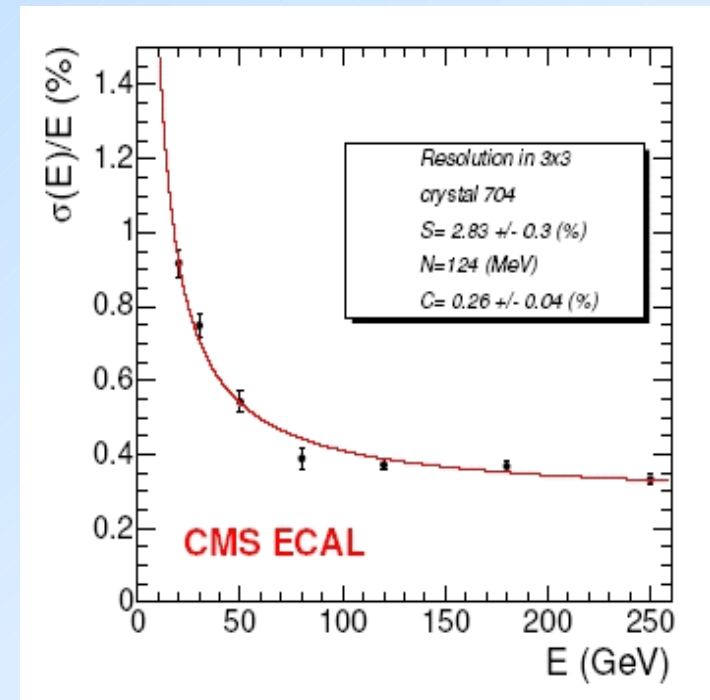
CMS design goal : $a \sim 3\%$, $b \sim 0.5\%$, $c \sim 200 \text{ MeV}$

APD contributions to:

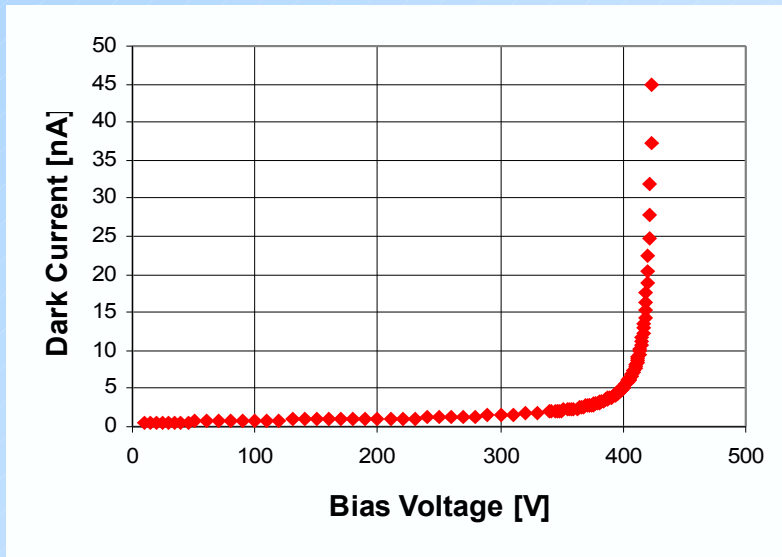
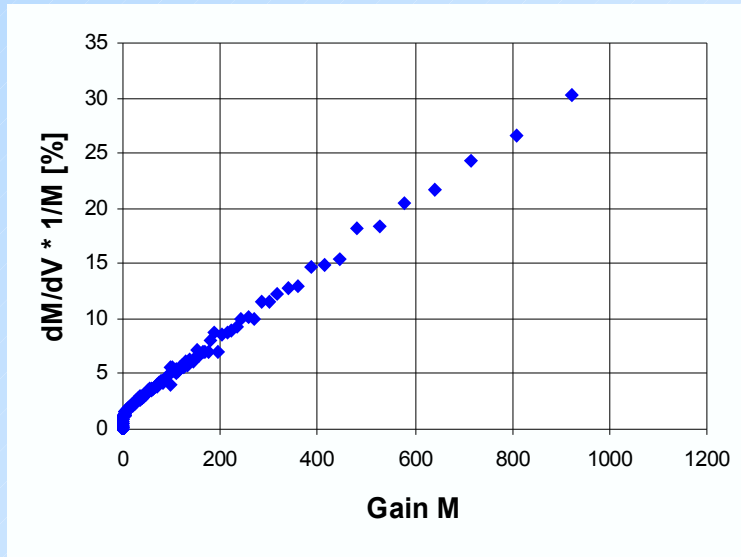
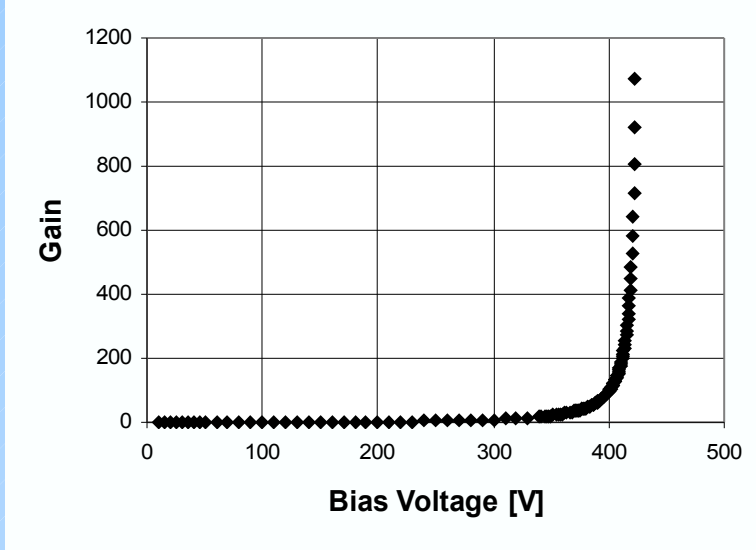
a: photo statistics (area, QE) and avalanche fluctuations (excess noise factor)

b: stability (gain sensitivity to voltage and temperature variation, aging and radiation damage)

c: noise (capacitance, serial resistance and dark current)



APD gain and dark current



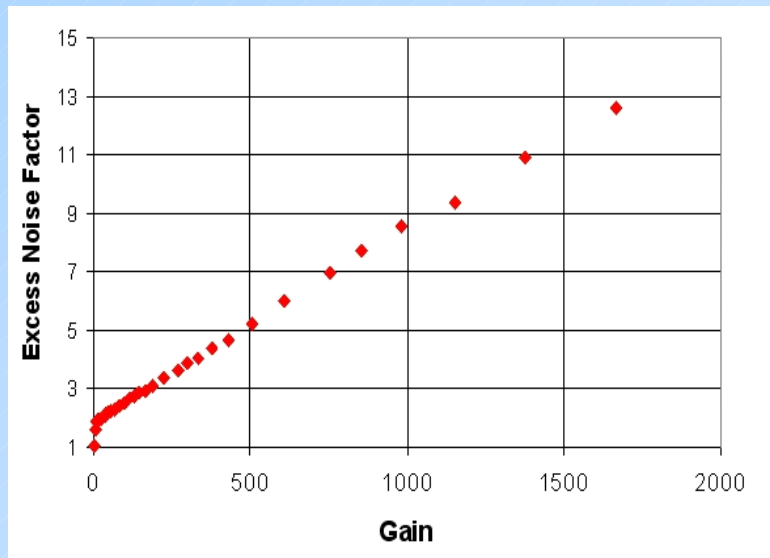
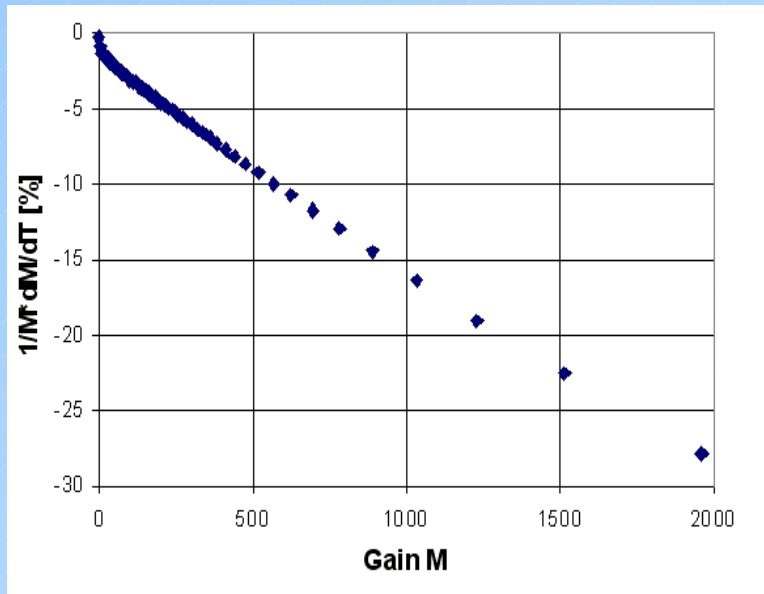
$$dM/dV * 1/M = \text{const} * M$$

$$\rightarrow M \sim 1/(V_{\text{breakdown}} - V)$$

Near the breakdown voltage, where we get noticeable amplification, the gain is a steep function of the bias voltage.

Consequently we need a voltage supply with a stability of few tens of mV.

APD gain



The breakdown voltage depends on the temperature due to energy loss of the electrons in interactions with phonons. Consequently the gain depends on the temperature and the dependence increases with the gain.

At gain 50 the temperature coefficient is - 2.3% per degree C.

Good energy resolution can only be achieved when the temperature is kept stable (in CMS the temperature is regulated with a 0.1 degree C precision).

At high gain the fluctuations of the gain become large and the excess noise factor ENF increases:

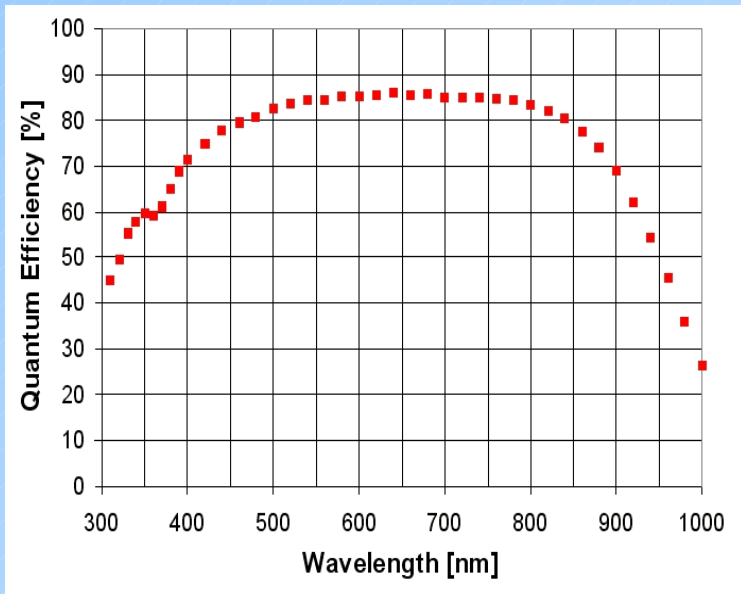
$$\frac{\sigma}{E} = \sqrt{\frac{ENF}{n_{pe} E}}$$

for $M > 10$: $ENF \sim 2 + k_{eff} \cdot M$

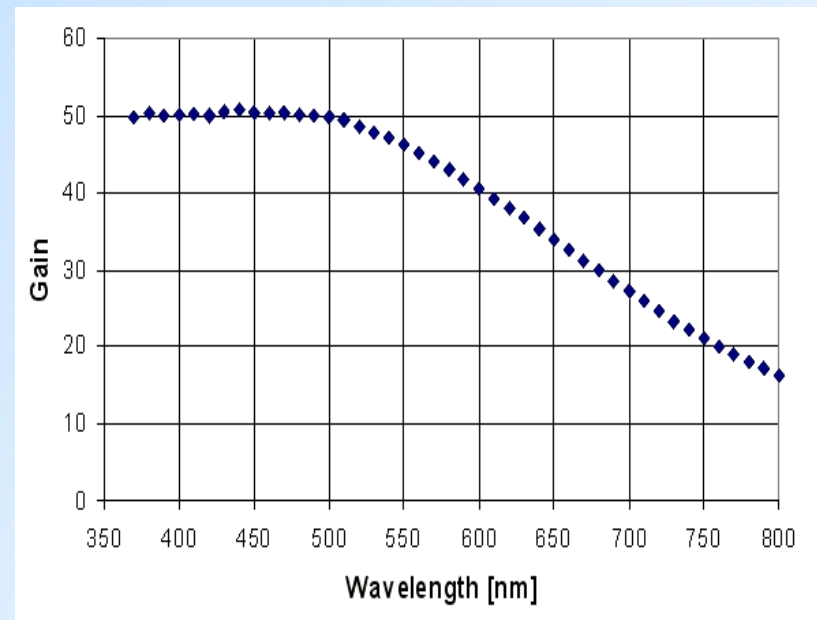
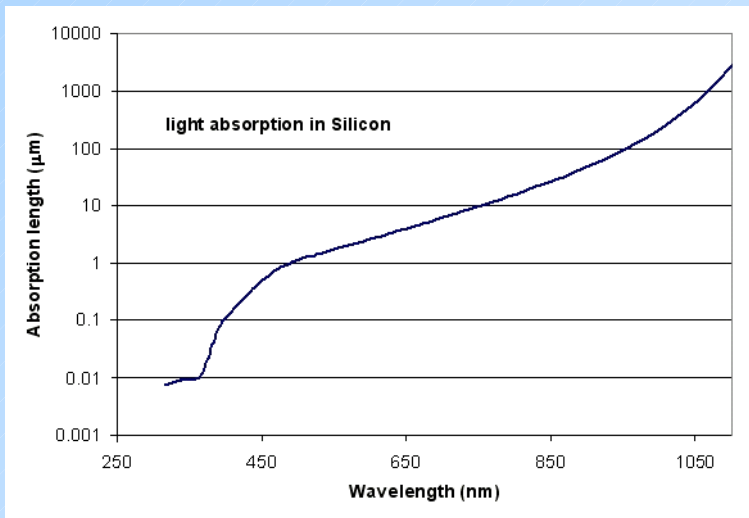
$k_{eff} \approx k = \beta/\alpha$

$$ENF = \frac{M^2 + \sigma_M^2}{M^2}$$

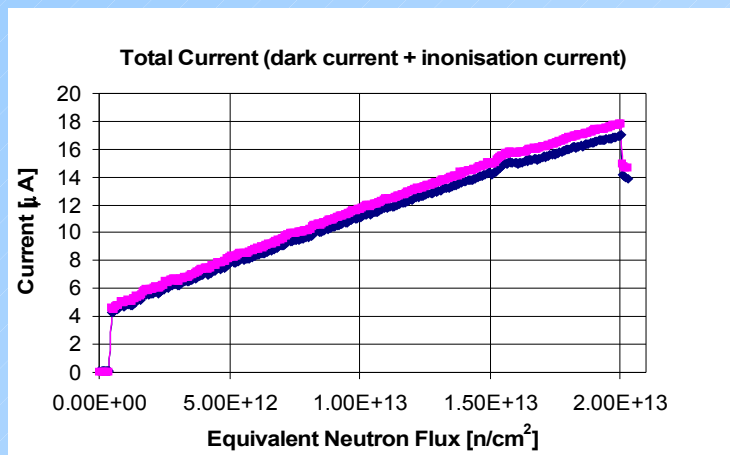
α and β are the ionization coefficients for electrons and holes ($\alpha \gg \beta$)



In the APDs selected for CMS (Hamamatsu S8148) the p-n junction is at a depth of about 5 micron. Behind the junction is a 45 micron thick layer of n-doped silicon. Blue light is absorbed close to the surface. The electrons from the generated e-h pairs drift to the high field of the junction and are amplified. Light with long wavelength penetrates deep into the region behind the p-n junction. Only the generated holes will drift to the junction. They will be much less amplified due to the smaller ionization coefficient.



APD radiation hardness



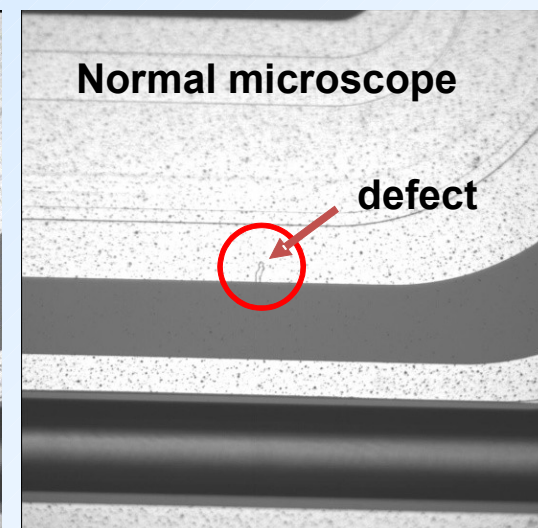
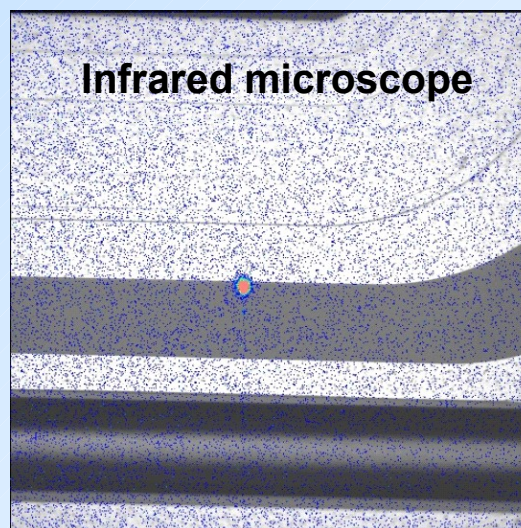
Two APD's have been irradiated at PSI in a 70 MeV proton beam for 10^5 minutes

9×10^{12} protons/cm² corresponds to 2×10^{13} neutrons/cm² with an energy of 1 MeV (10 years fluence expected in CMS barrel)

The mean bulk current after 2×10^{13} neutrons/cm² is $I_d \approx 280$ nA (non-amplified value).

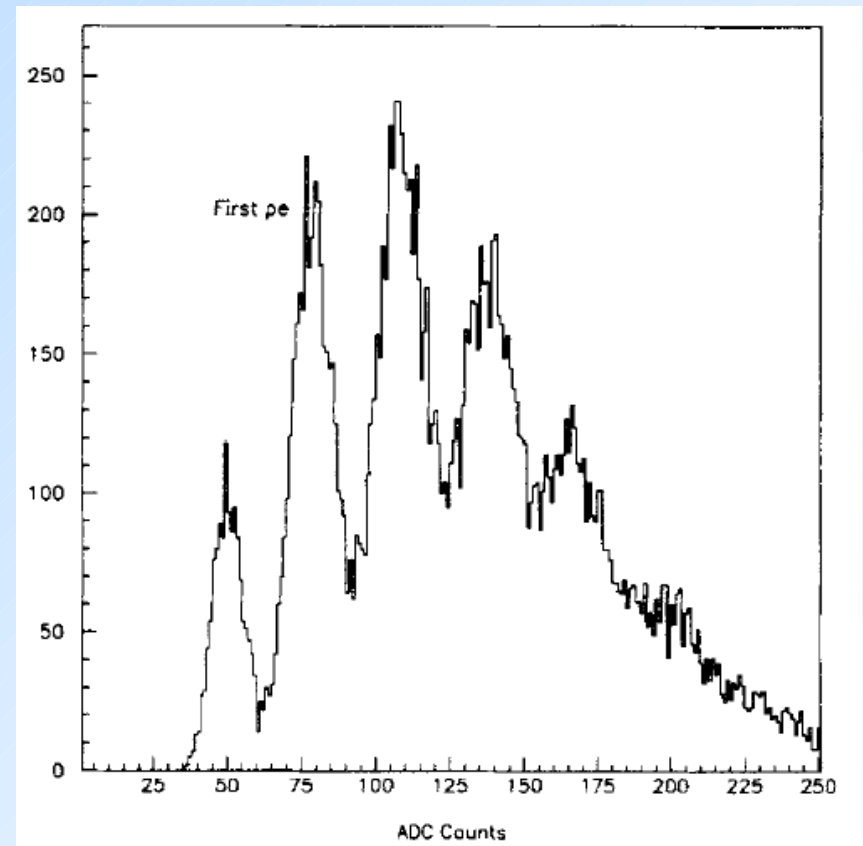
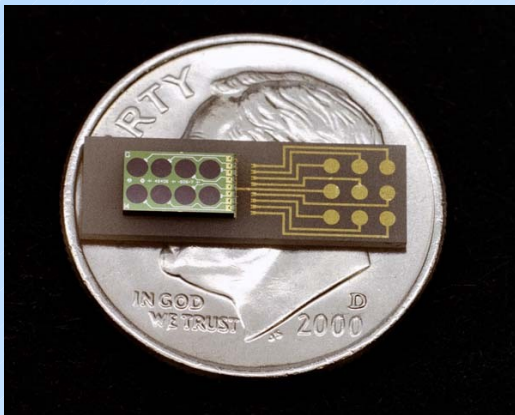
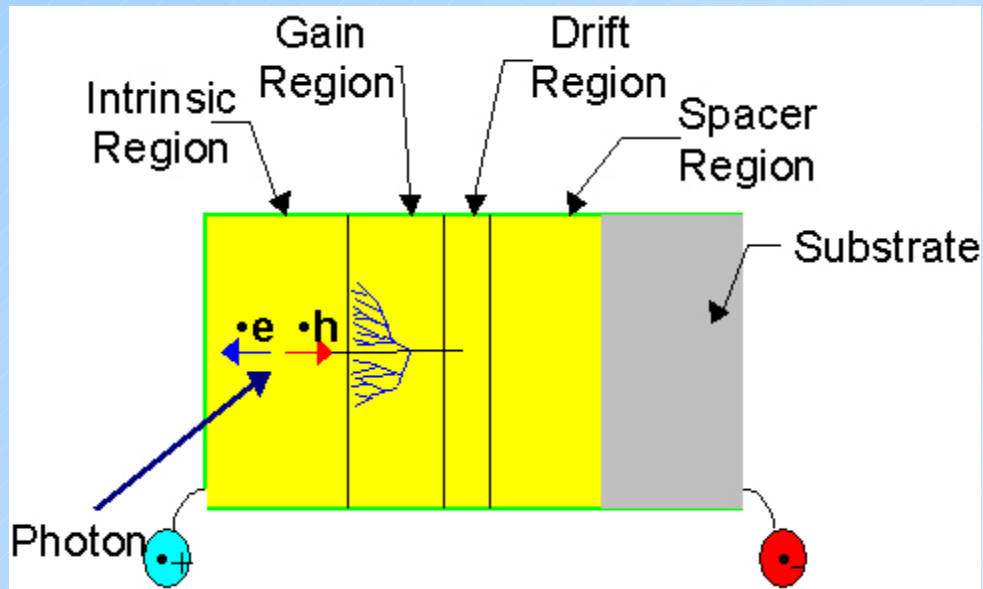
This corresponds to 14 μ A at gain 50 and ~ 80 MeV noise contribution (no recovery considered).

- Neutrons: Displacement of Si atoms => defects in the bulk which generate currents. Slow and never complete recovery at room temperature.
- Ionizing radiation (γ): breakup of the SiO₂ molecules and very little effect in the bulk (10^{-4}) => the surface currents increase. Fast and almost complete recovery for good APD's. There can be a strong reduction of the breakdown voltage if there is a weakness on the surface due to an imperfection in the production process (dust particles, mask misalignment ...).



Visual Light Photon Counter - VLPC

VLPC (Visual Light Photon Counter) is impurity band conduction silicon diode capable of detecting single photons. Band gap energy $\sim 50\text{meV}$ \rightarrow operation at cryogenic temperature (6.5K). Gain few times 10^4 . Used for D0 fiber tracker.

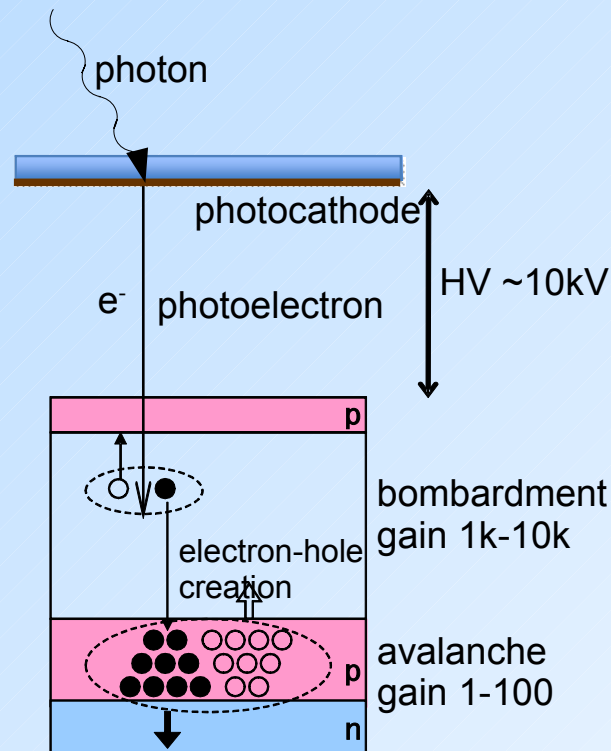


M.R. Wayne, NIM A387 (1997) 278

Hybrid photo detectors: HPD, HAPD

Single photon detection can be achieved by using PD or APD in vacuum device (replacing diode structure):

- photon interacts in photocathode and produces photoelectron
- high electric field accelerates photoelectron
- on impact electron-hole pairs are generated (bombardment gain)
- in APD signal is further amplified \rightarrow lower HV and higher gain



- Photo-emission from photo-cathode;
- Photo-electron acceleration to $\Delta V \approx 10\text{-}20\text{kV}$;
- Energy dissipation through ionization and phonon excitation ($W_{\text{Si}} = 3.6\text{eV}$ to generate 1 e-h pair in Si) with low fluctuations (Fano factor $F \approx 0.12$ in Si);

$$M = \frac{e(\Delta V - V_{th})}{W_{\text{Si}}}$$

- Gain M:

- Intrinsic gain fluctuations σ_M : $\sigma_M = \sqrt{F \cdot M}$

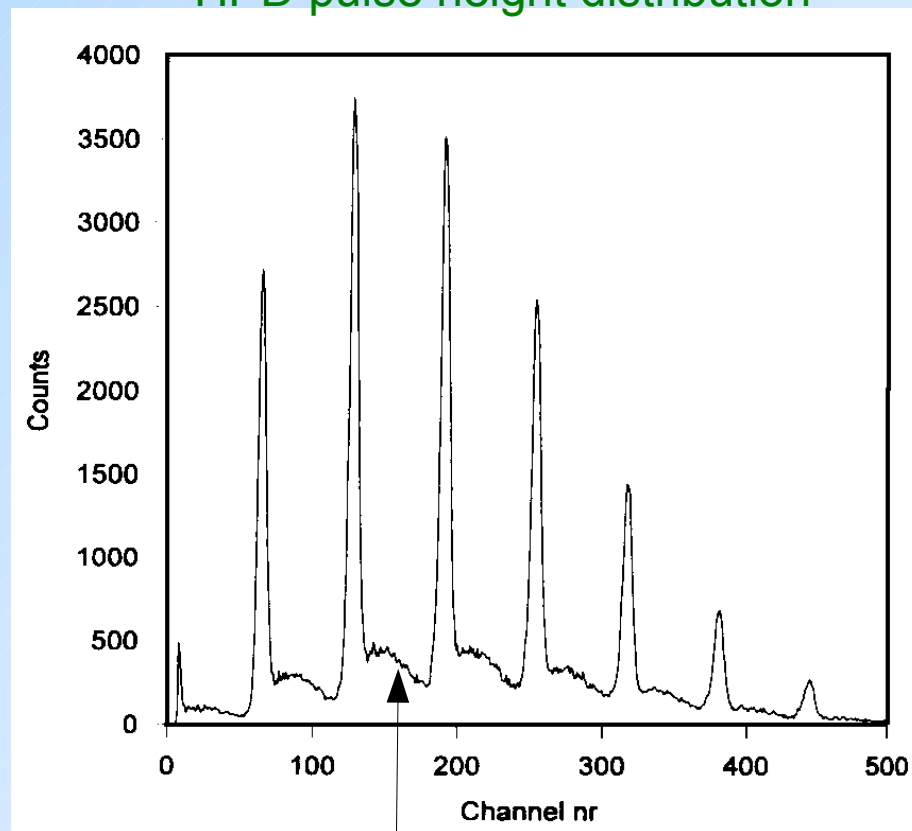
→ overall noise dominated by electronics

- Example: $\Delta V = 20\text{kV}$

→ $M \approx 5000$ and $\sigma_M \approx 25$

- Suited for photon counting with high resolution

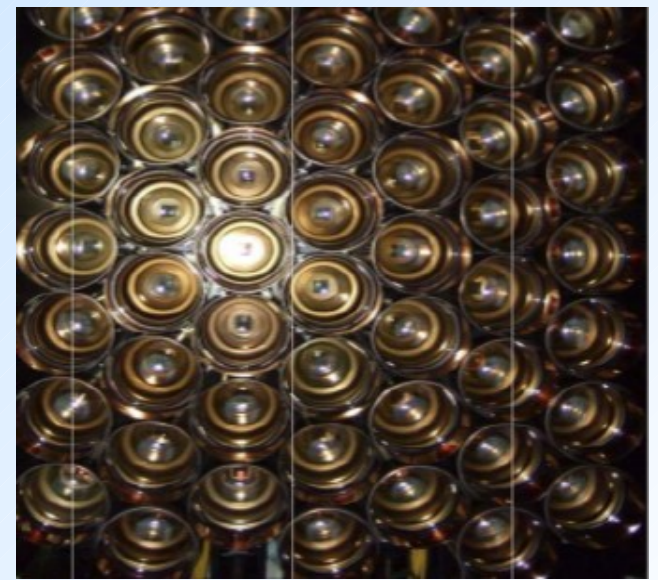
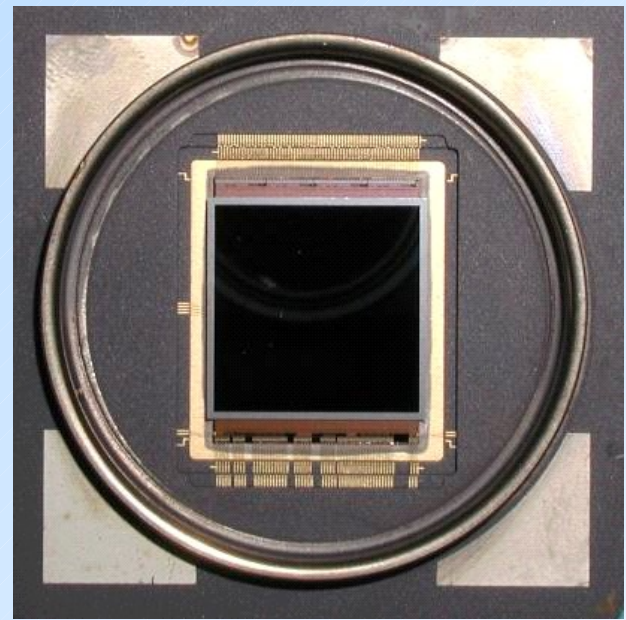
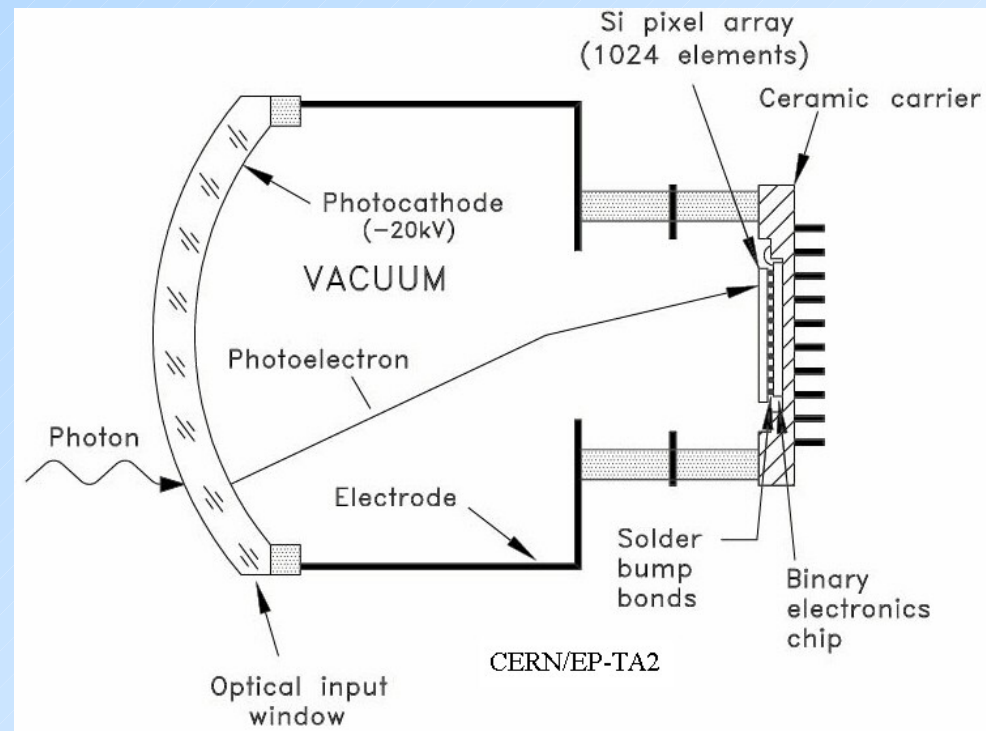
HPD pulse height distribution



- Continuum from photo-electron back-scattering effects at Si surface

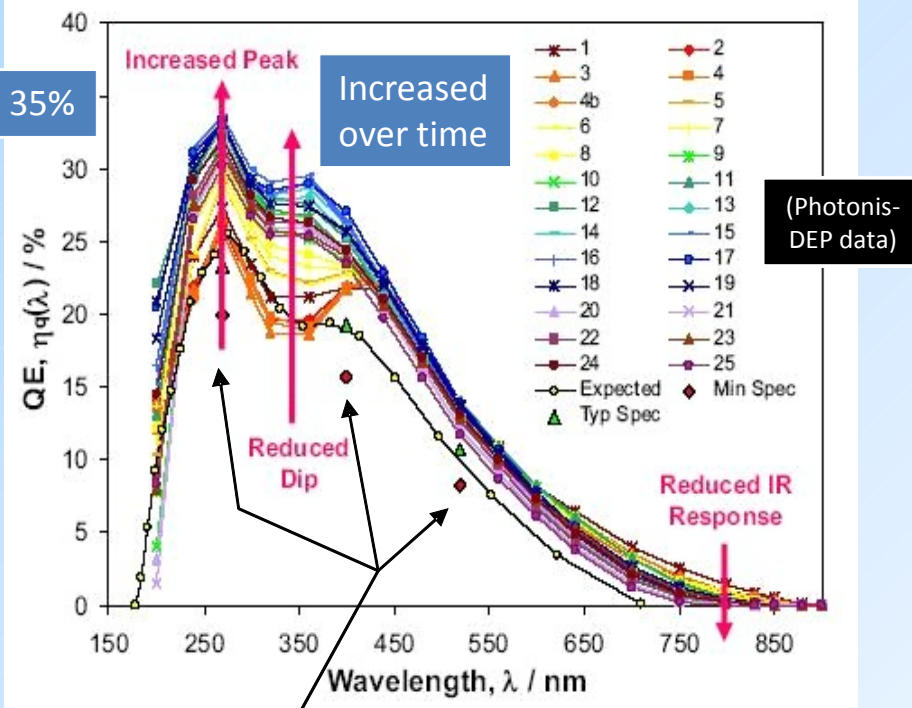
HPD - LHCb RICH

- electron optics → 5x demagnification
- sensitive to magnetic field
- HV ~20kV, gain ~5k
- detector in operation
- CERN+DEP-Photonis

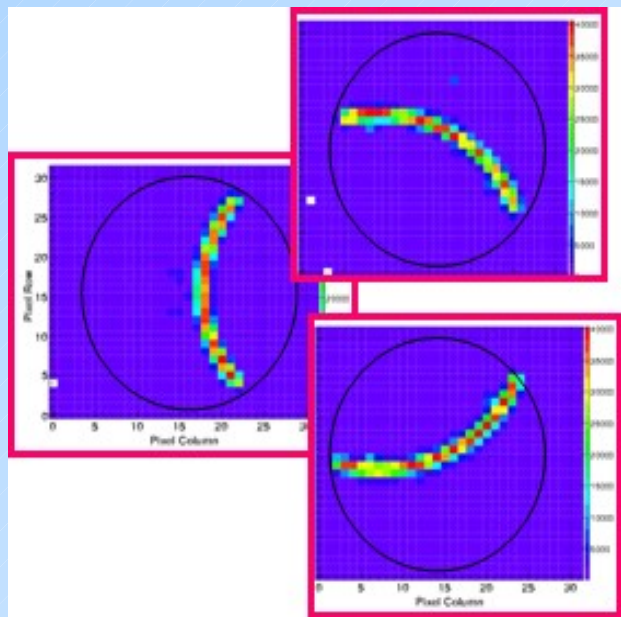


HPD: LHCb RICH

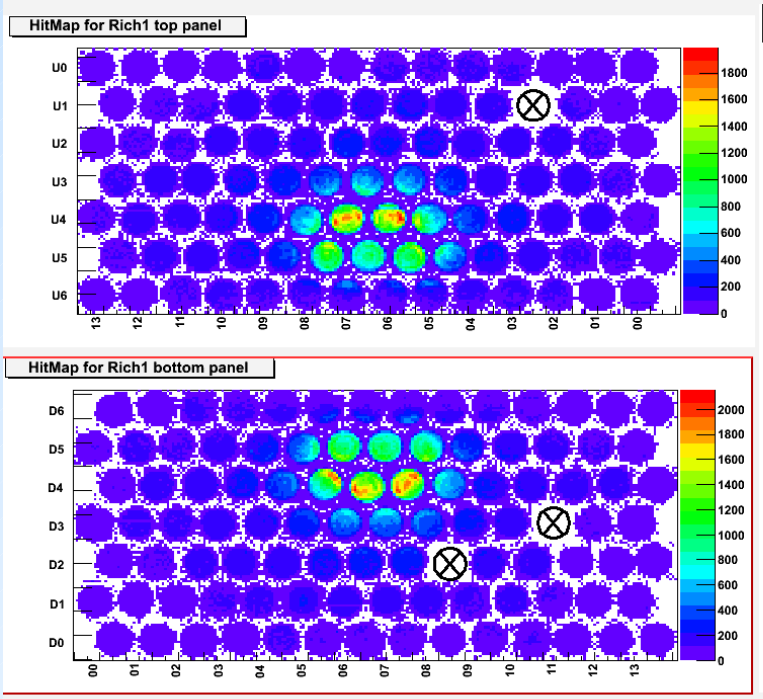
- Must cover 200-600nm wavelength range
- Multi-alkali S20 (KCsSbNa2)
- Improved over production
- Resulted in a $\int QE d\lambda$ increased by 27% wrt the original specifications



Cherenkov rings from 80 GeV/c π^- through C_4F_{10}



M Adinolfi et al., NIM A 603 (2009) 287



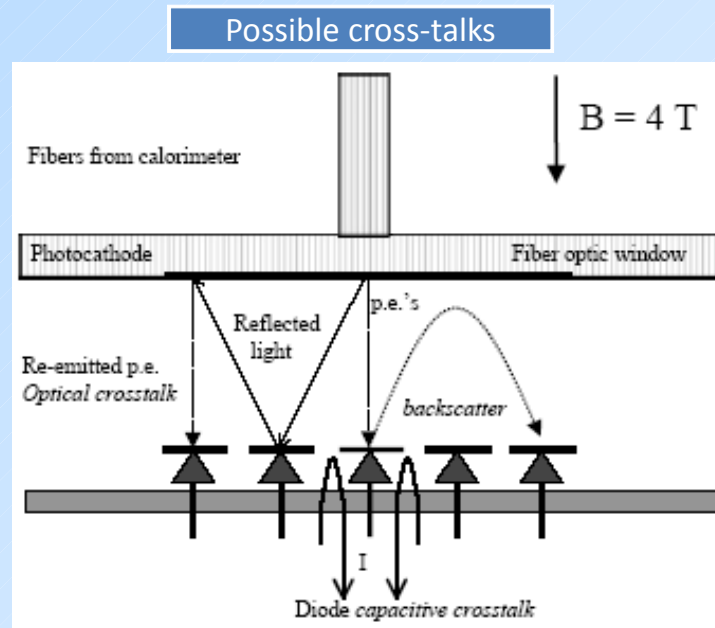
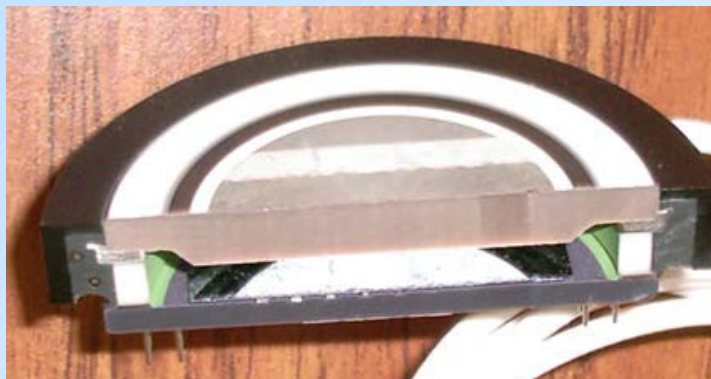
HPD: CMS HCAL

$B=4T \rightarrow$ proximity-focussing with 3.35 mm gap and $HV=10kV$;

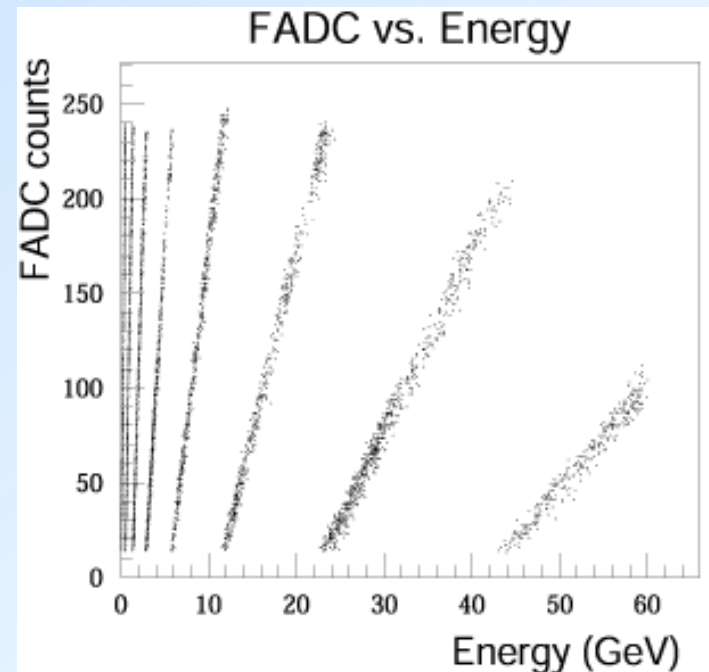
Minimize cross-talks:

- photo-electron back-scattering: align with B ;
- capacitive: Al layer coating;
- internal light reflections: a-Si:H AR coating optimized @ $\lambda = 520nm$ (WLS fibres);

Results in linear response over a large dynamic range from minimum ionizing particles (muons) up to 3 TeV hadron showers;



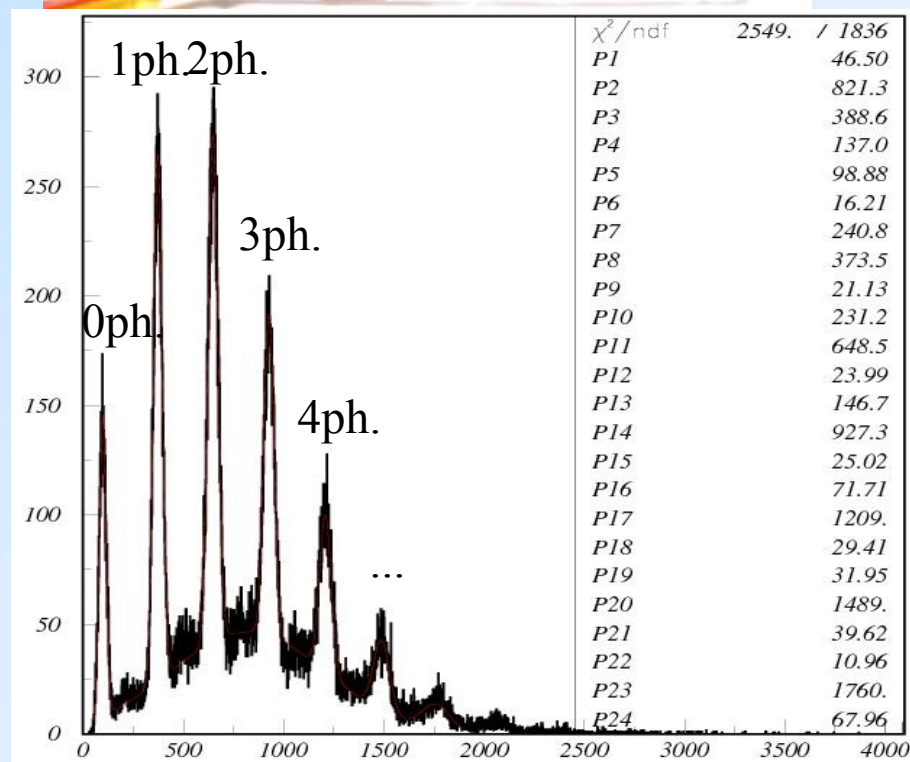
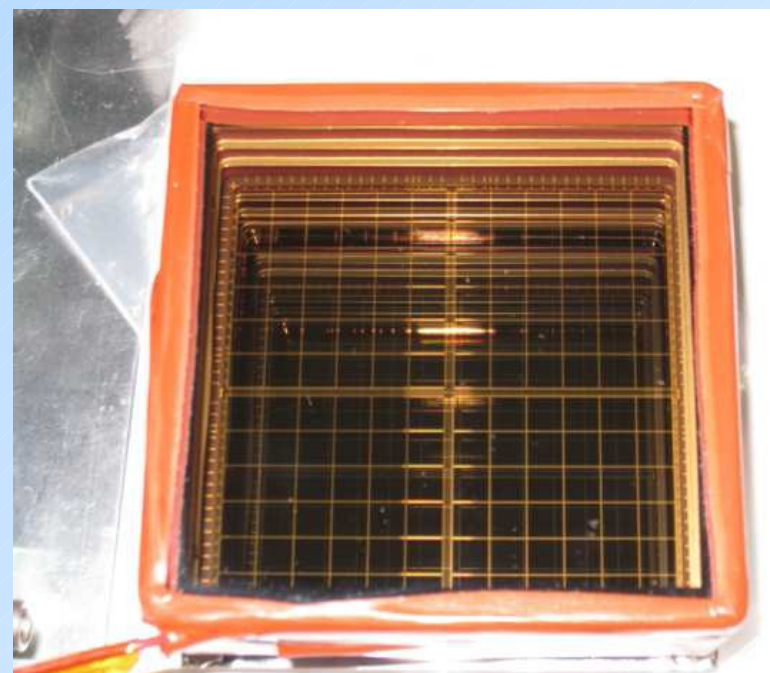
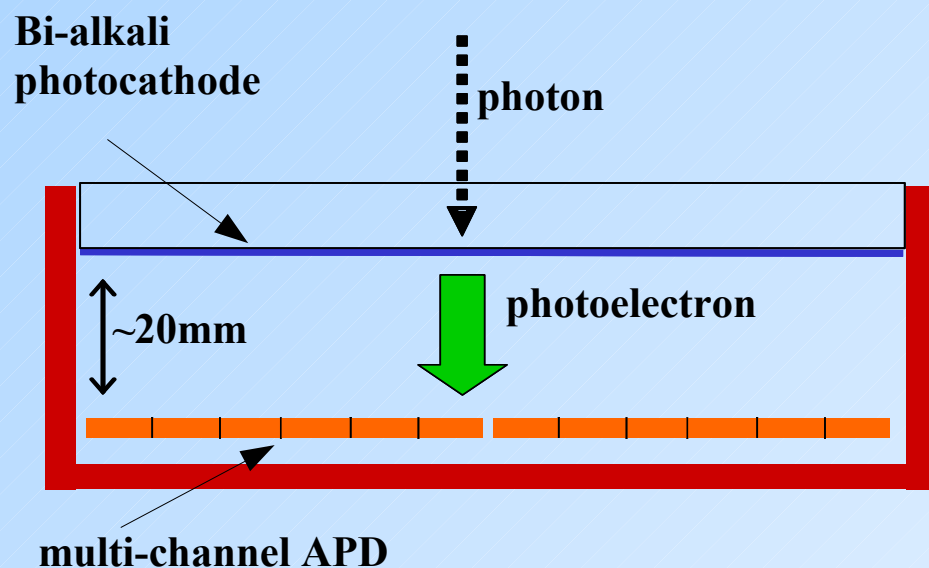
P. Cushman et al., NIM A 504 (2003) 62



HAPD: Belle II

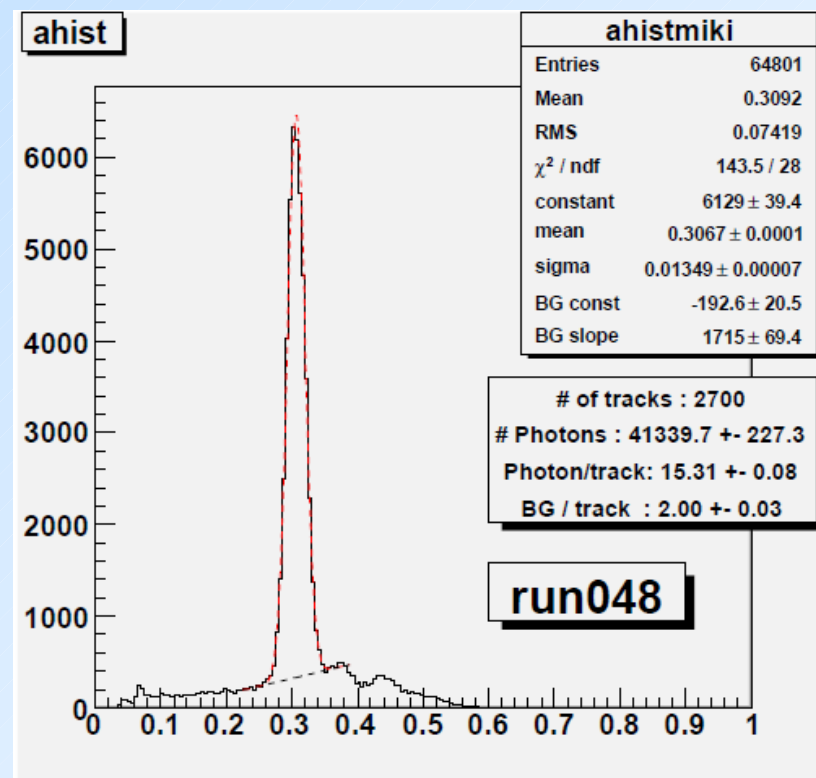
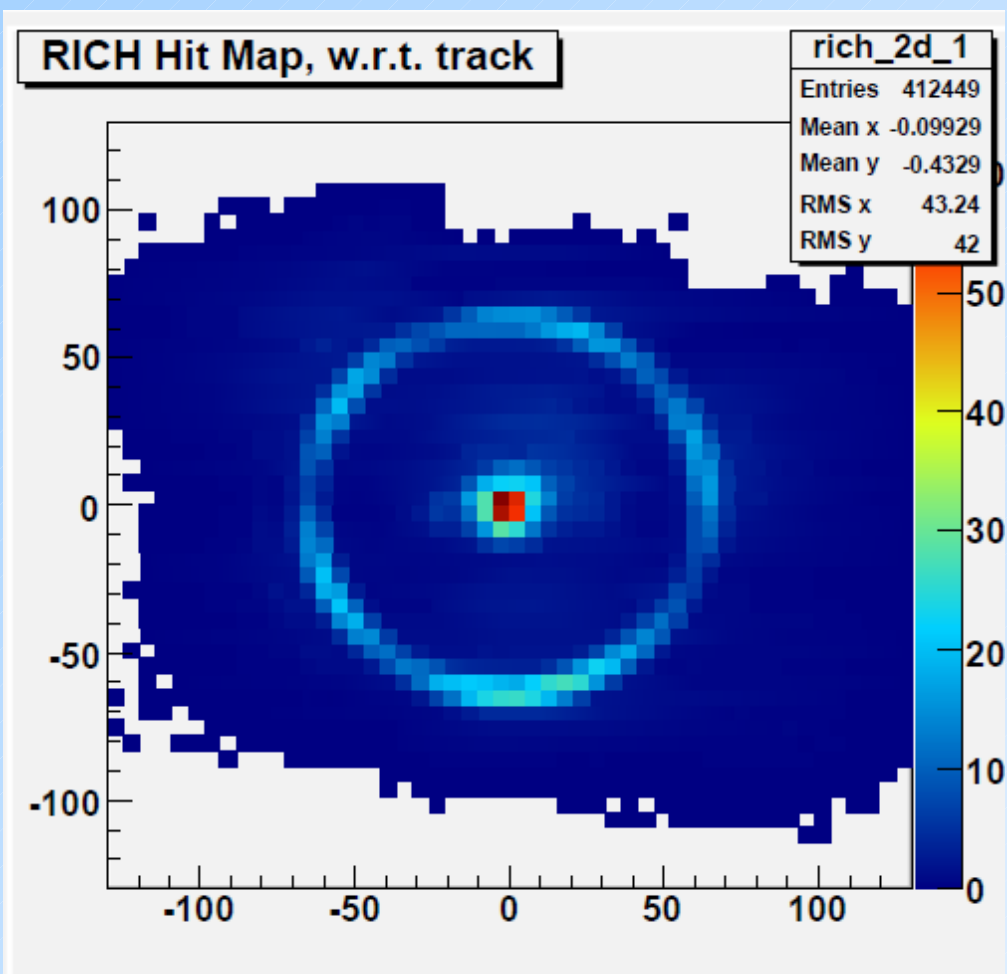
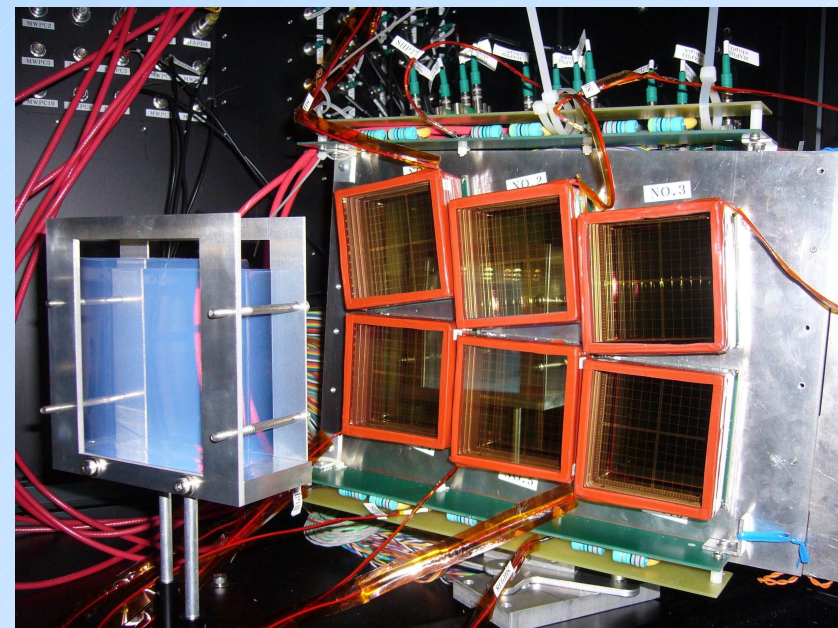
Belle II aerogel RICH HAPD

- proximity focusing configuration
- operation in magnetic field
- HV $\sim 8\text{kV}$, gain $\sim 100\text{k}$
- Belle + Hamamatsu



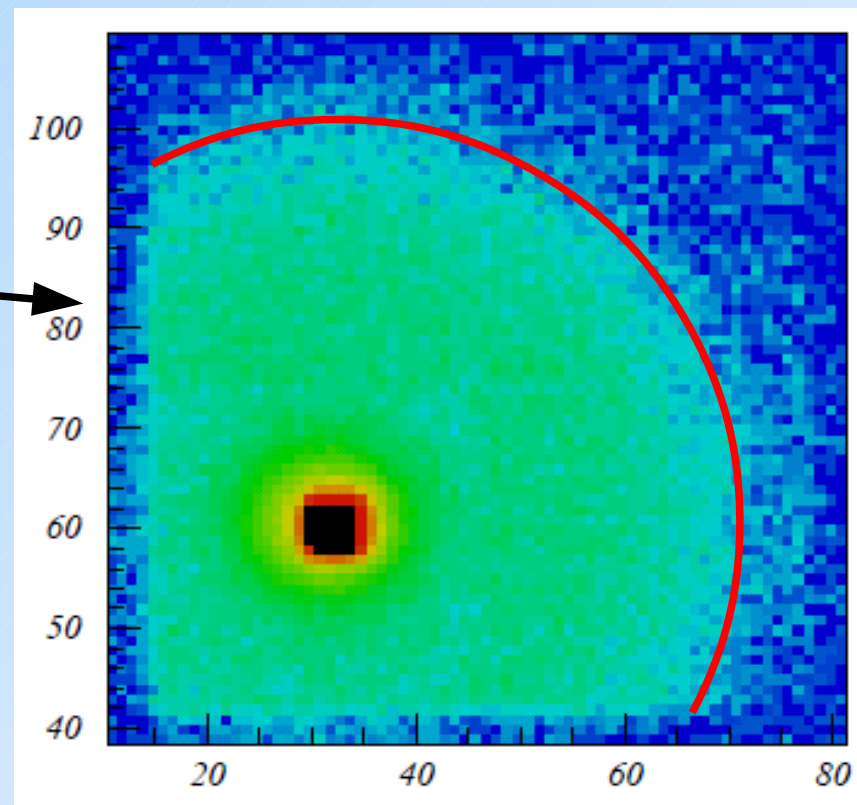
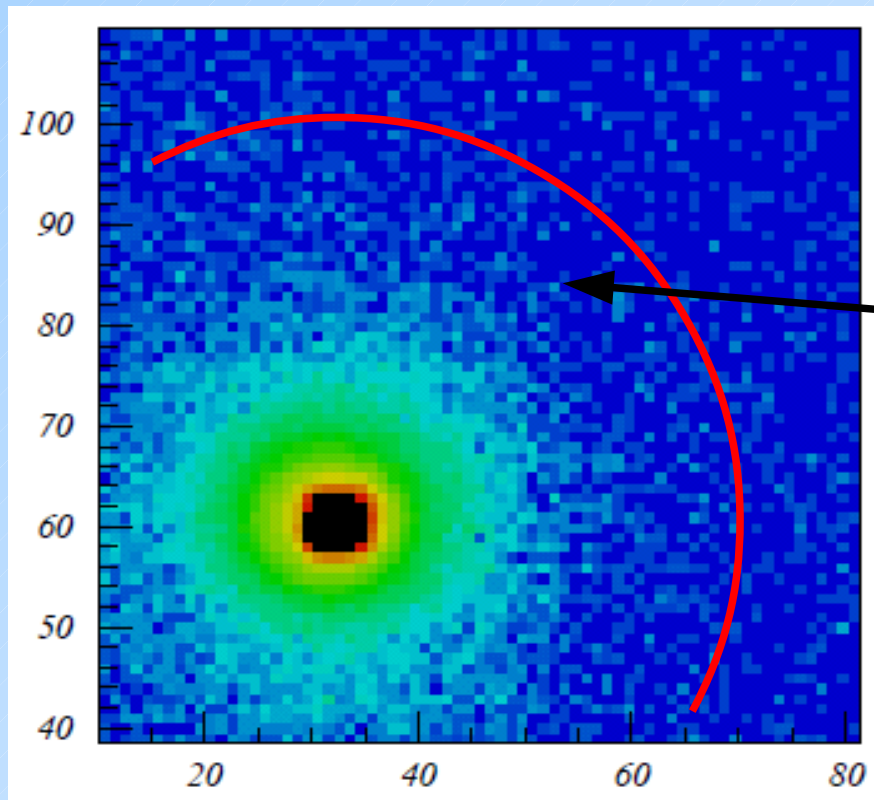
HAPD: Belle II

Beam test of prototype aerogel RICH with 2 GeV electrons.



HAPD: Test in magnetic field 1.5 T

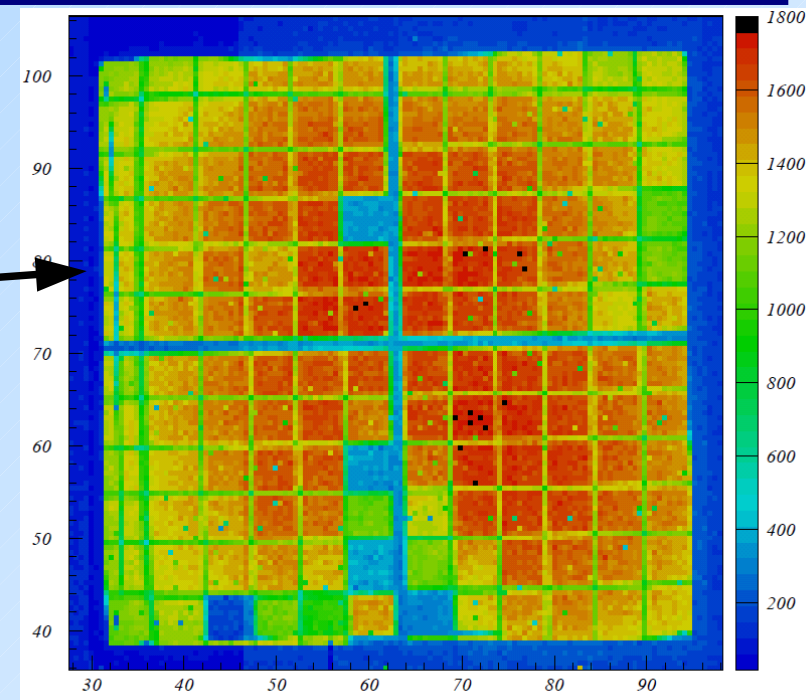
- around 20% of photoelectrons back-scatter and the maximum range is twice the distance from photocathode to APD ~40mm



- in magnetic field these photoelectrons follow magnetic field lines and fall back on the same place

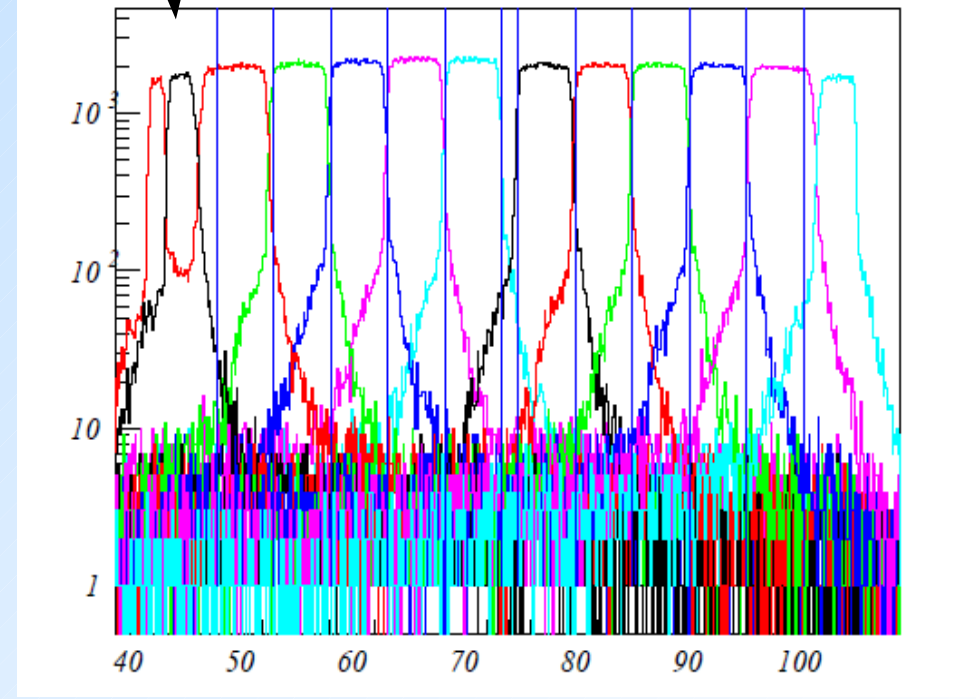
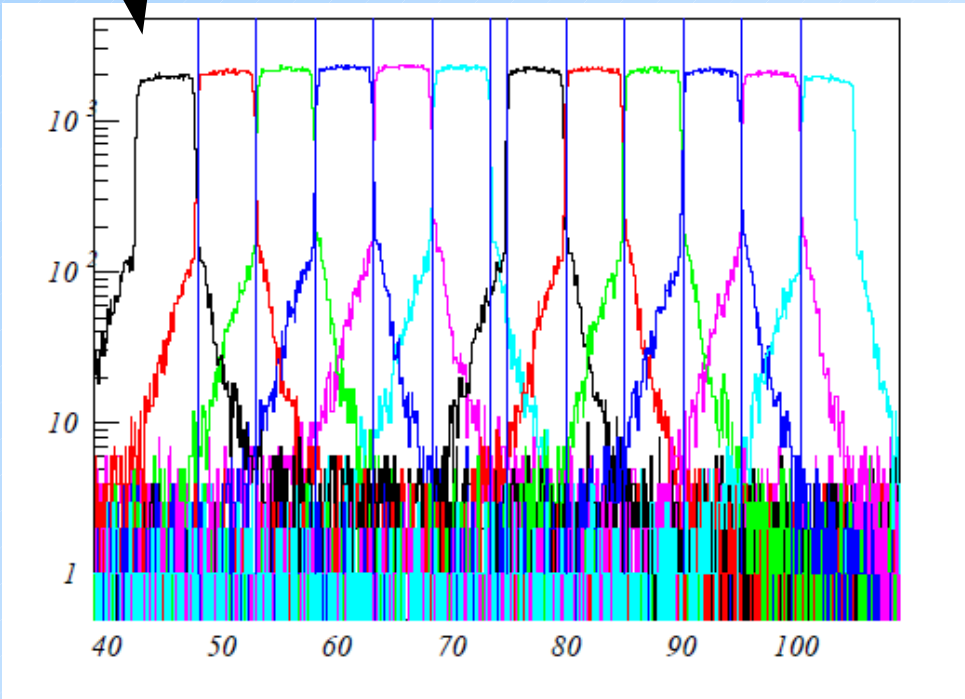
HAPD: Test in magnetic field 1.5 T

- distortion of electric field lines at HAPD edge produces irregular shapes of areas covered by each channel
- in magnetic field photoelectrons circulate along the magnetic field lines and distortion disappears



no magnetic field

magnetic field 1.5 T

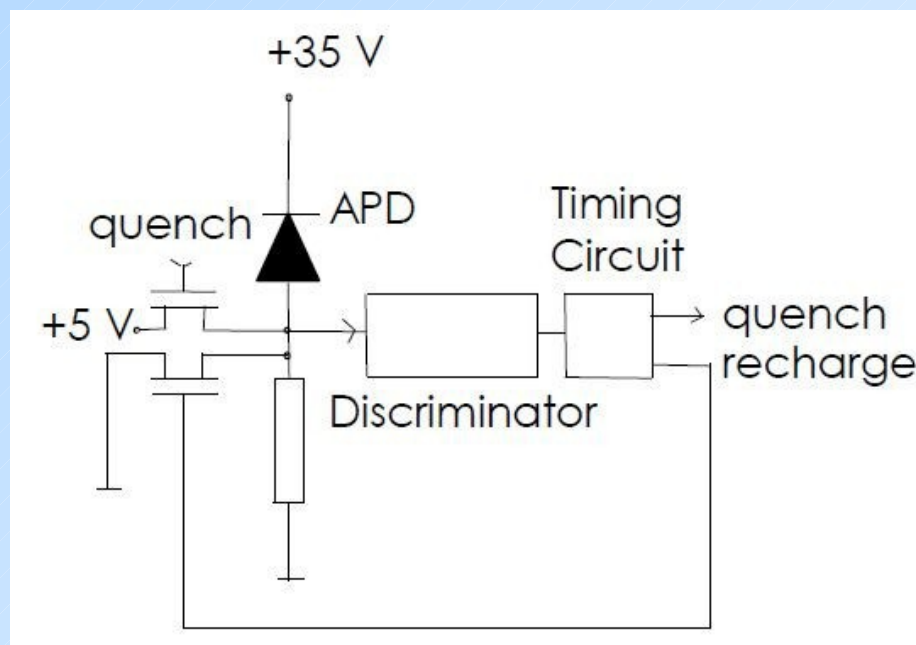


APDs operated in Geiger mode

Another option is to operate the APD in Geiger mode.

Bias voltage is increased above the breakdown voltage and avalanche must be stopped by:

- active bias control or
- quenching resistor



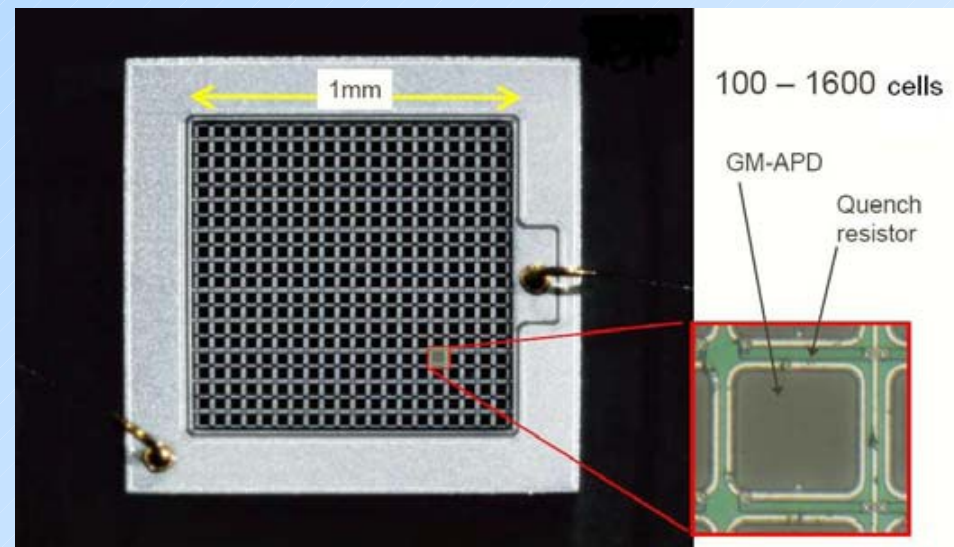
Large area APD operating in Geiger mode would be most of the time in the recovery state due to the large number of dark counts.

Solution: localization of quenching, division of large area APD in an array of smaller ones → SiPM (1990's: Golovin, Sadygov)

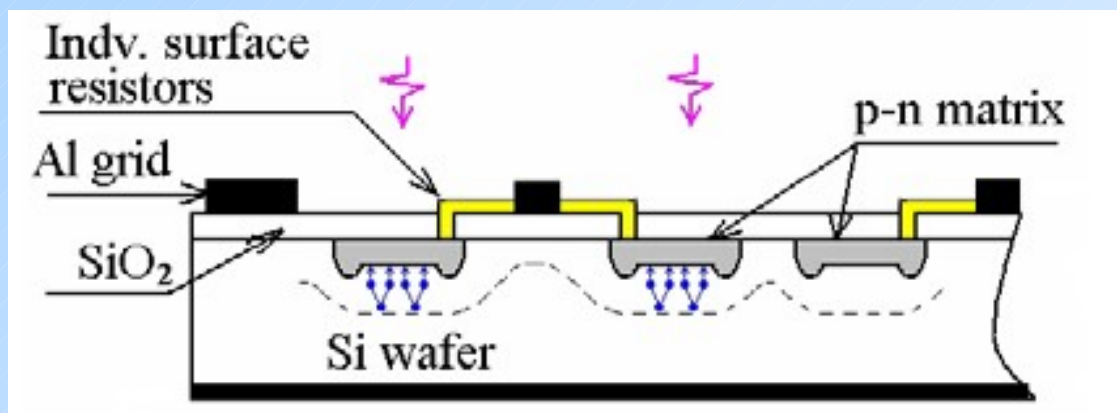
SiPM - Structure

SiPM is an array of Geiger mode APDs (micro cells) each consisting of:

- p-n structure with high field region
- quenching resistor connected to common electrode by metal strips



Hamamatsu MPPC with 50um cells

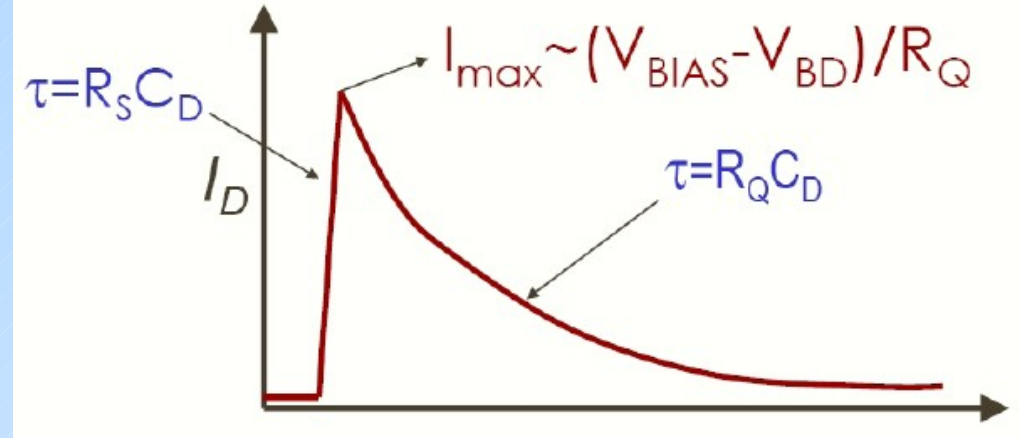


Manny producers: Photonique/CPTA, MEPhi/PULSAR, Hamamatsu, MPI, FBK-irst, STMicroelectronics, SensL, Philips (dSiPM), Zecotec ...
using different names: SiPM, MRS APD, MAPD, SSPM, MPPC, PPD ...

SiPM - Signal

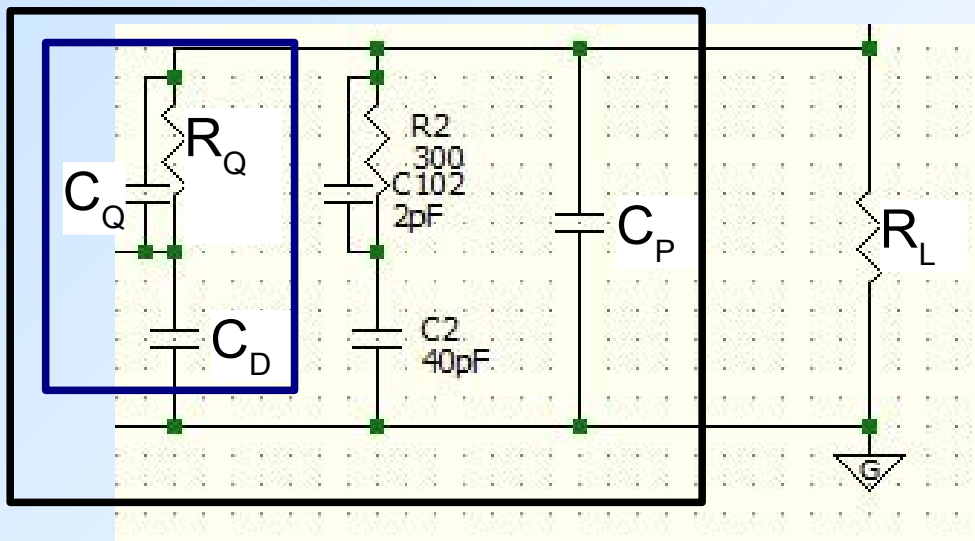
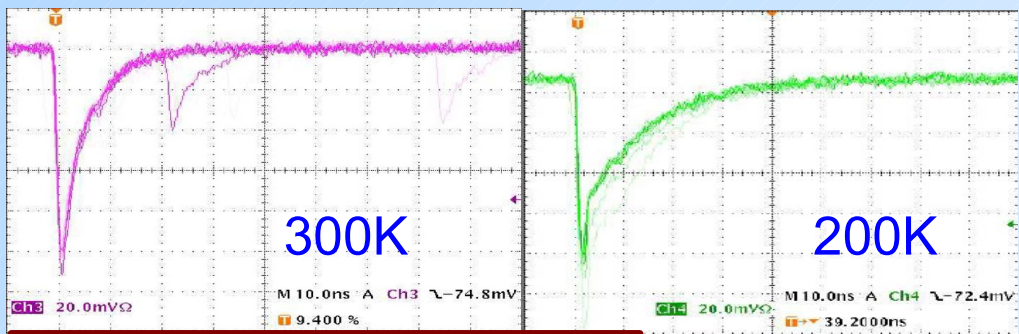
SiPM signal sequence:

- charged to V_{bias}
- carrier enters breakdown region and initiates the avalanche
- micro cell is discharged to $V_{breakdown}$ and avalanche process stops
- micro cell is recharged to V_{bias} – during this time a new avalanche process in the same micro cell will result in a reduced signal



Simplified explanation of output signal ($C_D \sim 20\text{fF}$, $R_S \sim 1\text{k}\Omega$, $R_Q \sim 100\text{k}\Omega$).

Parasitic capacitances C_Q and C_P also influence the output signal.

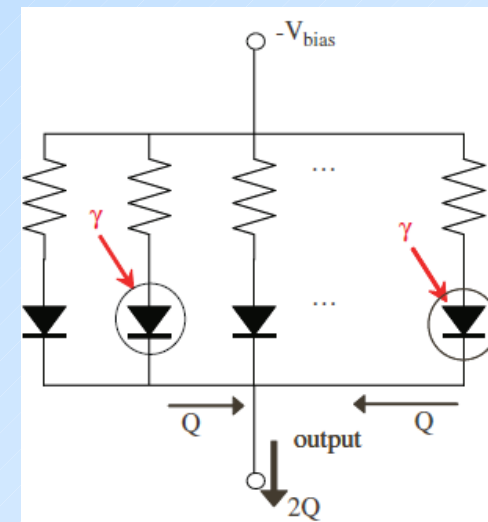


H. Otono (U. of Tokyo)@PD07

SiPM - Gain

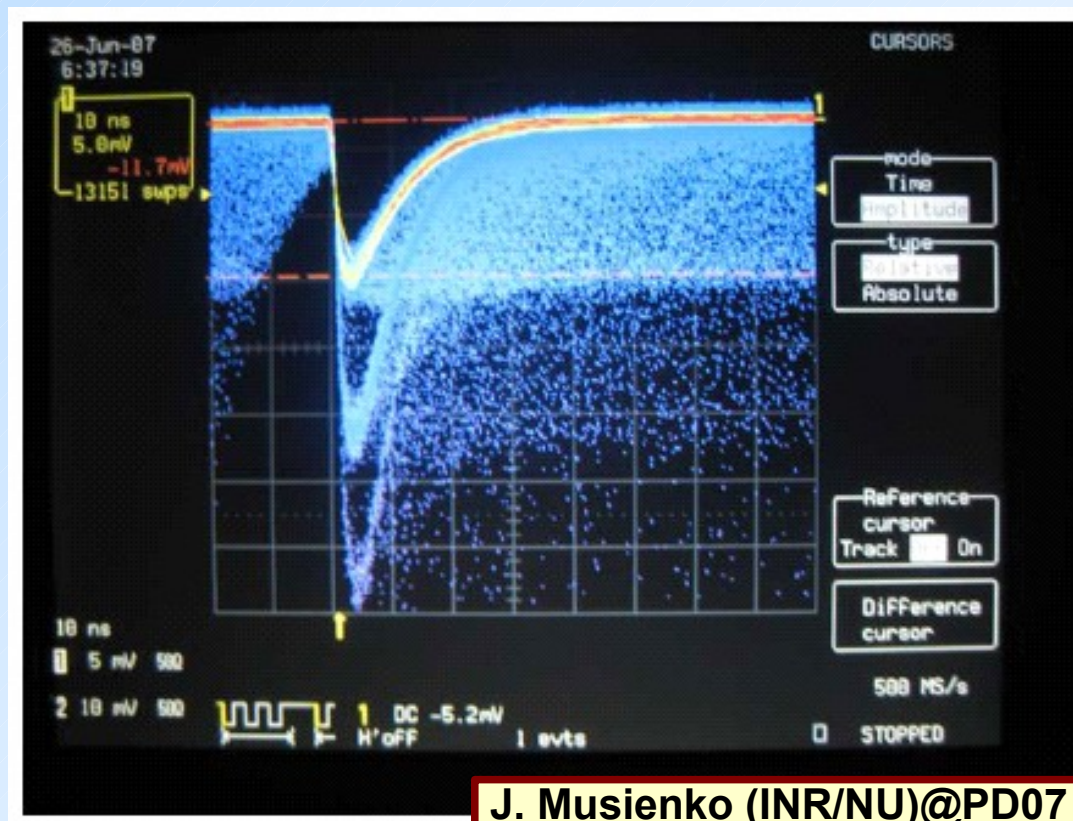
Gain is determined by micro cell capacitance ($\sim 10 - 100$ fF) and over-voltage \rightarrow the difference between bias and breakdown voltage (typically few volts).

$$G = C_{m.c.} \times (V_{bias} - V_{breakdown}) / e_0$$



- large gains, typically $10^5 - 10^7$
- short signals (~ 10 ns) produce several mV on 50 Ohm
- total signal is the sum of signals from individual micro cells
- afterpulses and optical crosstalk also contribute to total charge produced by single photon

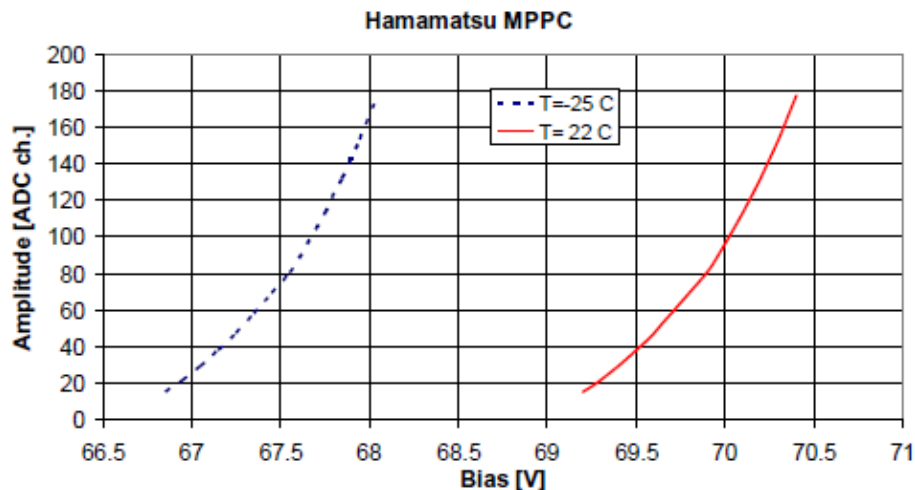
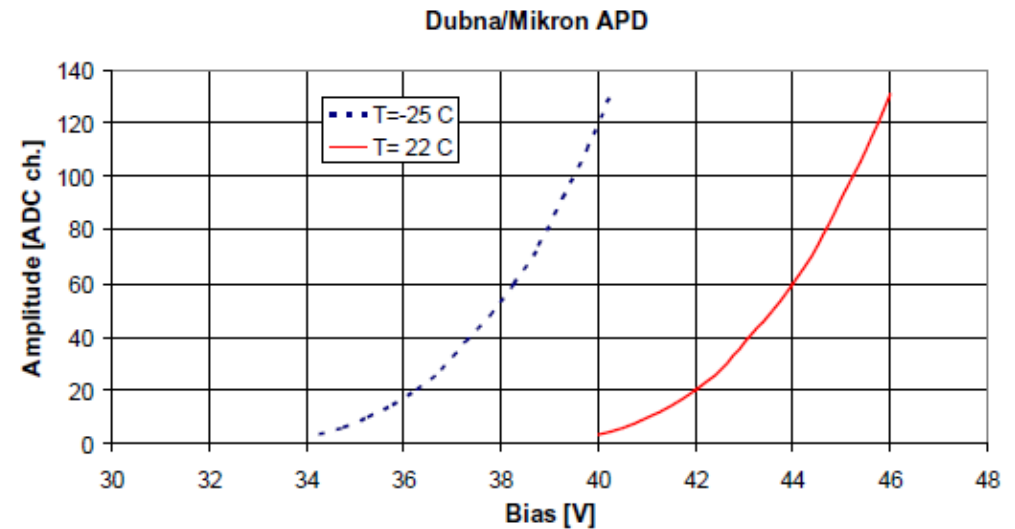
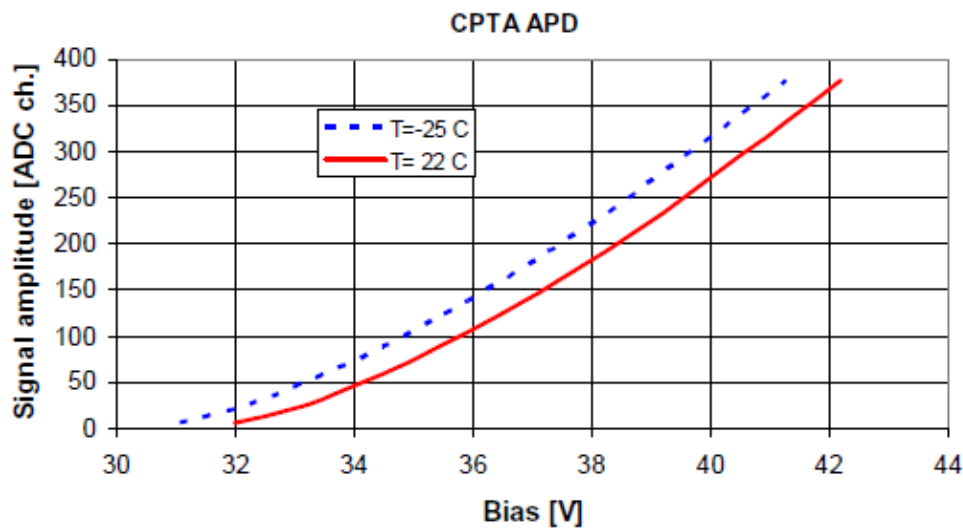
Photon counting(?)



J. Musienko (INR/NU)@PD07

SiPM - Gain vs. temperature

Breakdown voltage changes with temperature → gain variation.
Not critical for single photon detection.



CPTA/Photnique:
 $dVB/dT = -20 \text{ mV/C}$
Dubna/Micron:
 $dVB/dT = -122 \text{ mV/C}$
Hamamatsu:
 $dVB/dT = -50 \text{ mV/C}$

J. Musienko (INR/NU)@PD07

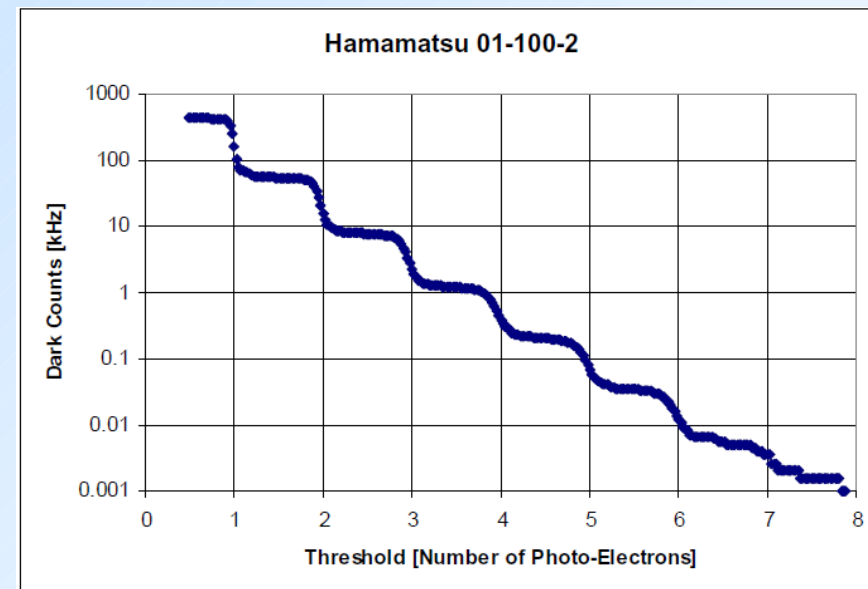
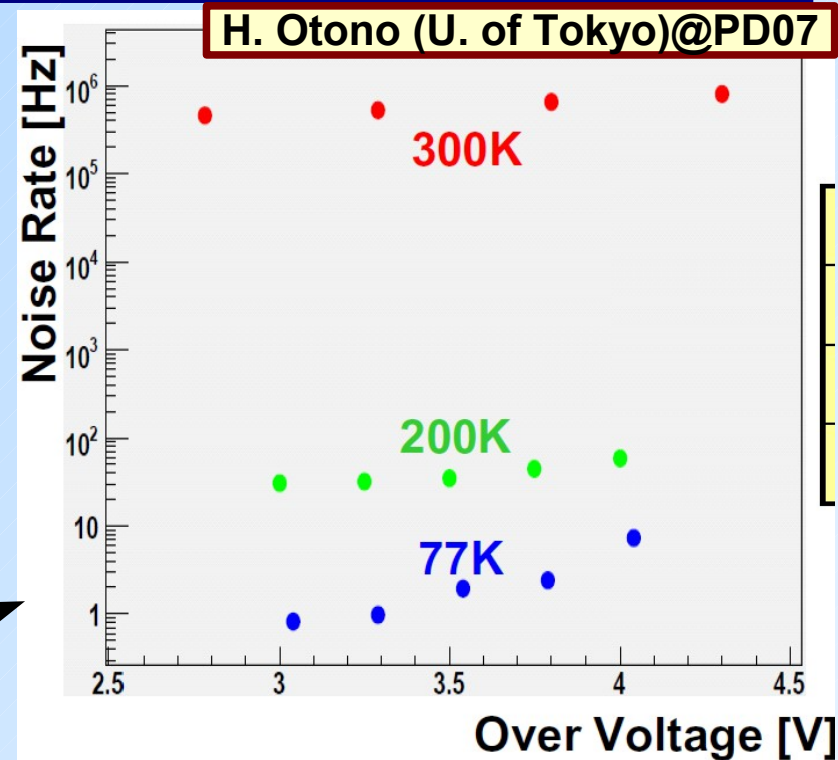
SiPM-Dark noise

Any free carrier entering breakdown region produces the same signal as single photon. The rate of breakdowns initiated by thermally generated carriers is in the range of 100 kHz to several MHz per mm² at room temperature.

Thermal generation can be reduced by:

- cooling → roughly factor 2 every 8°C
- smaller electric field (also reduces gain and PDE)
- small active volume (charge collection region)

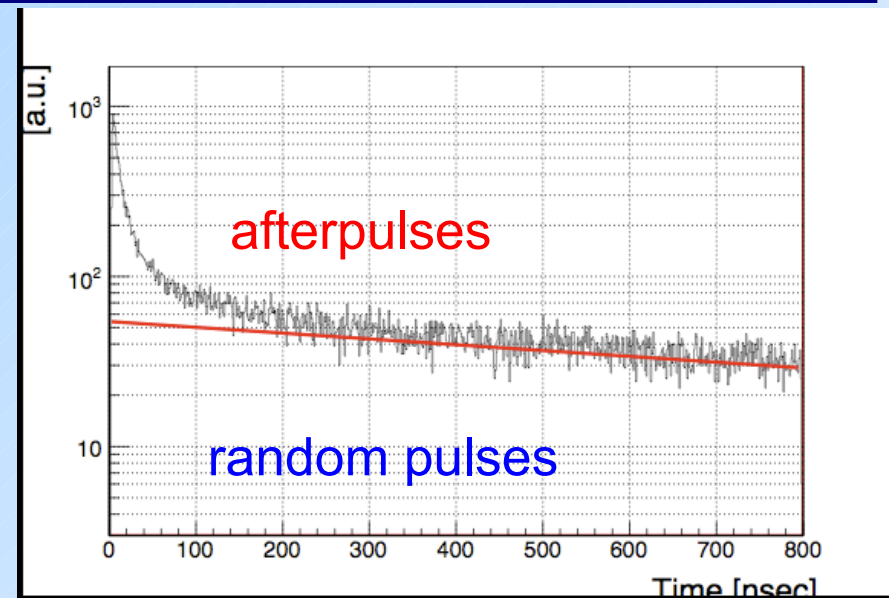
Signals are at the single micro cell level and can be effectively suppressed by threshold level at the signal of few micro cells (depends on optical cross talk level).



SiPM-Afterpulses

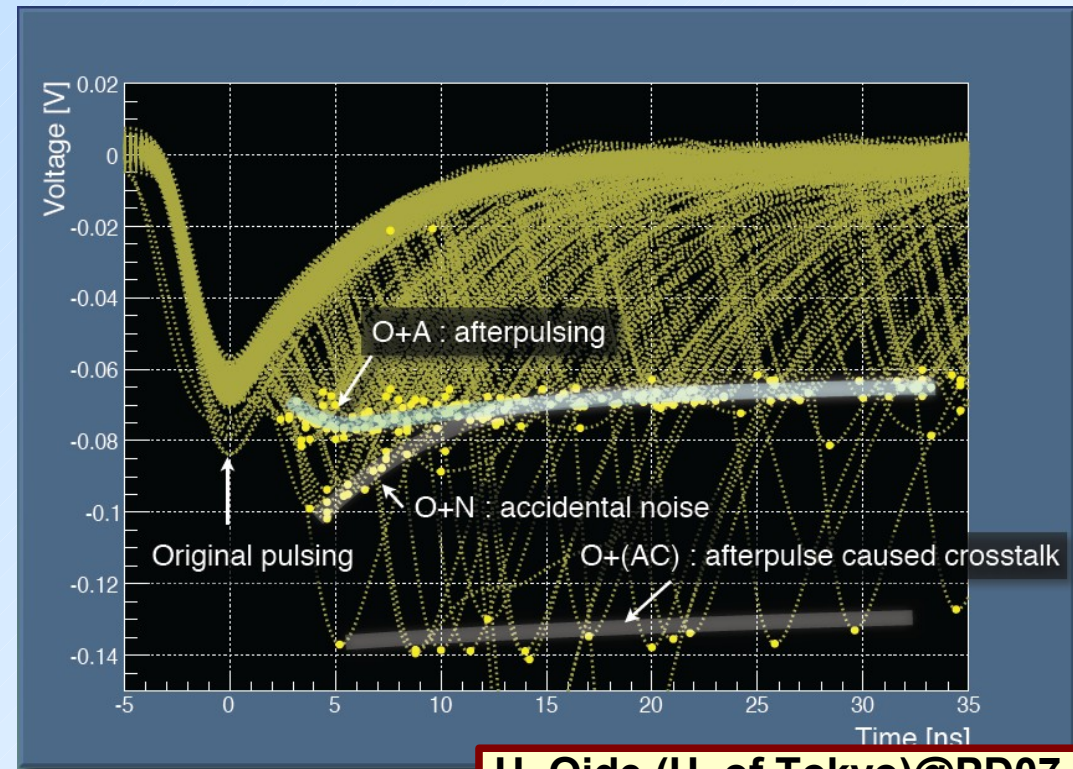
Deep traps are loaded during the avalanche processes and carriers that are subsequently released trigger after-pulses:

- after-pulses can occur several hundred ns after the primary pulse
- probability for afterpulses increases with overvoltage – higher gain



T. Murase (U. of Tokyo)@PD09

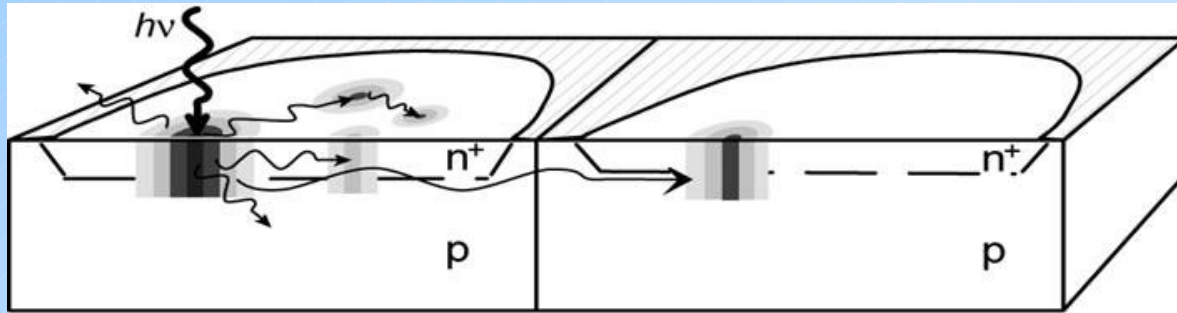
	40x40 px	20x20 px	10x10 px
Afterpulsing 1-1/e Recovery	~ 4 [ns]	~ 9 [ns]	~ 33 [ns]
Pulse Shape returning time (RC Time Const.)	~ 5 [ns]	~ 11 [ns]	~ 35 [ns]



H. Oide (U. of Tokyo)@PD07

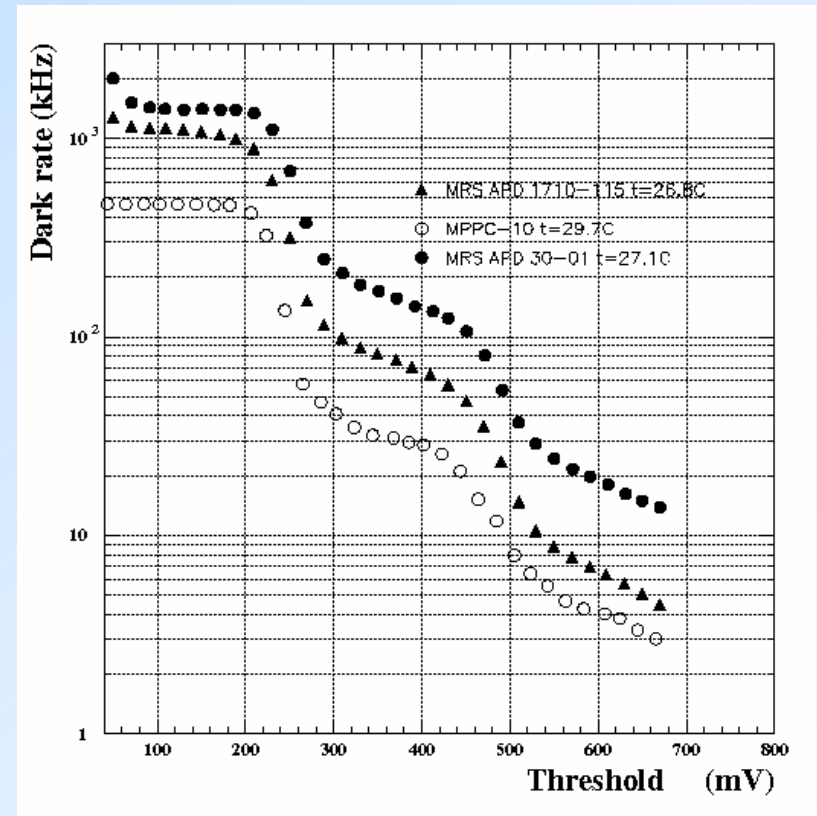
SiPM-Optical cross-talk

Optical cross-talk is generated when photon produced in the avalanche process escapes to the neighboring cell and initiates Geiger discharge → large excess noise factor.



It is the main cause of the larger number of fired micro cells in dark pulses than expected from accidental coincidences (Poisson probability).

Increases with overvoltage – higher gain.

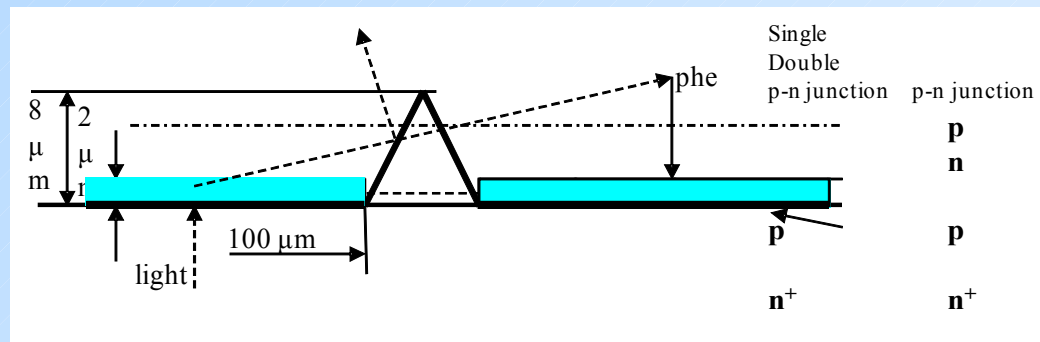


Y. Kudenko (INR Moscow)@PD07

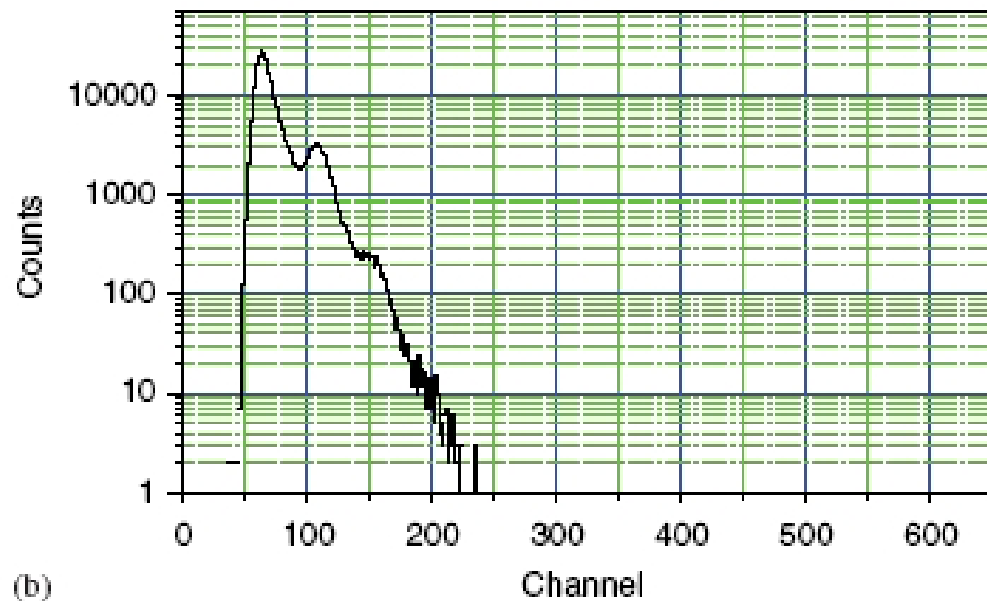
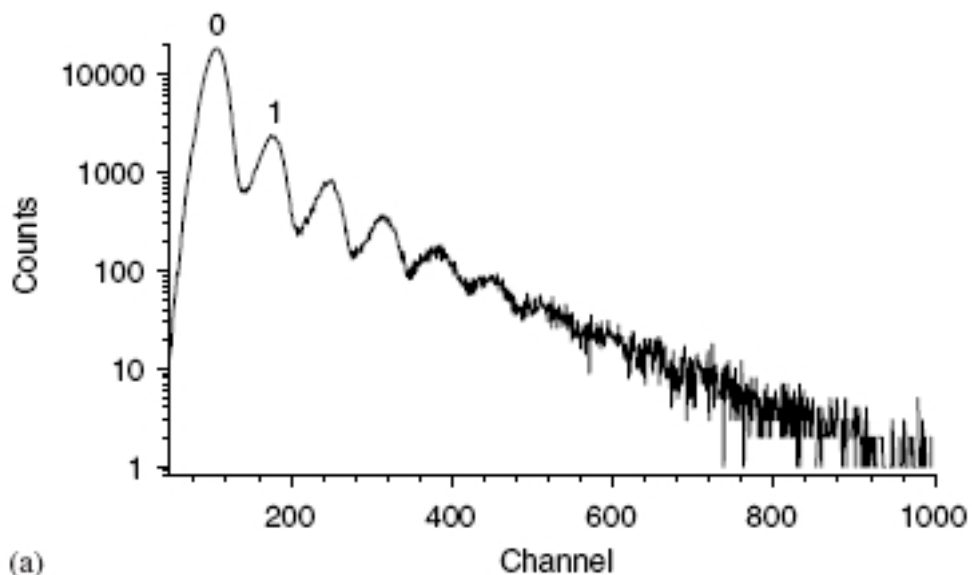
SiPM - Optical cross-talk suppression

Optical crosstalk can be suppressed by shielding one micro cell from the other:

- tranches are introduced between the cells
- typically lower photon detection efficiency – more dead space



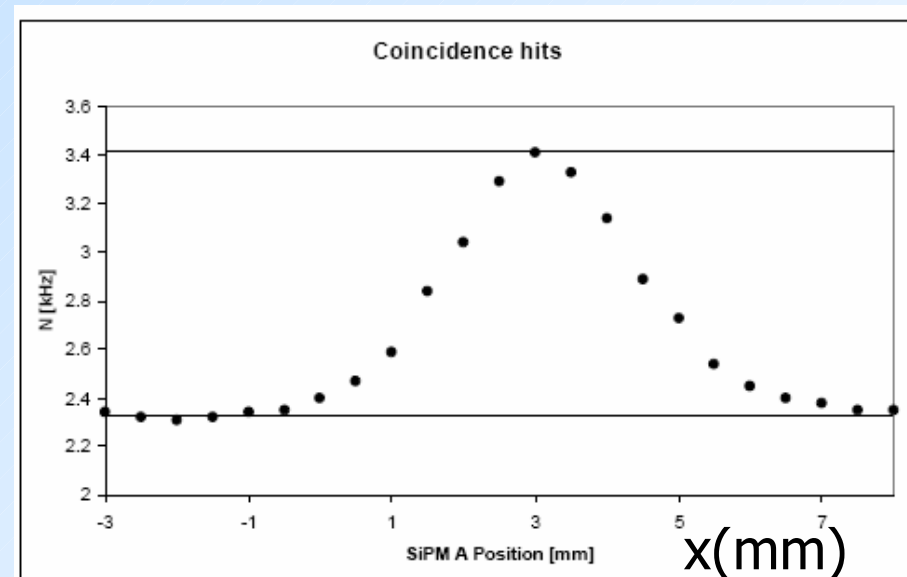
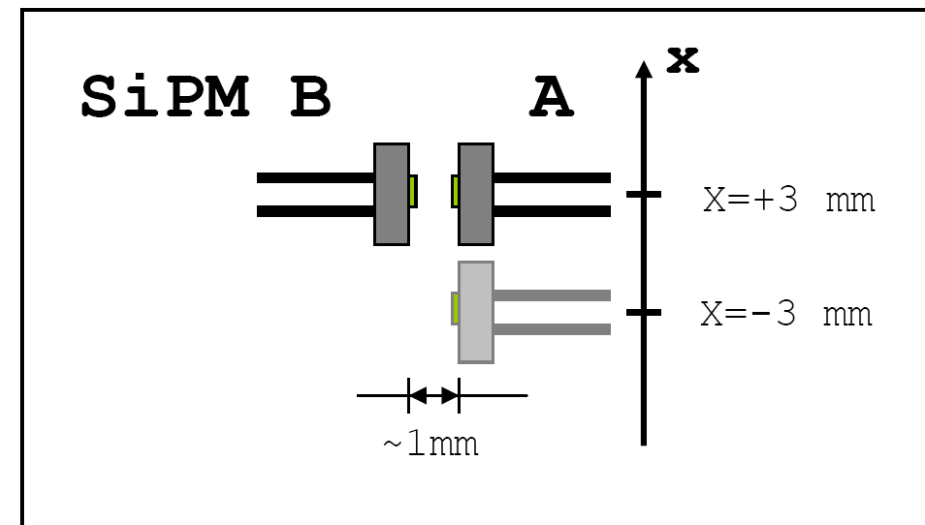
NIM A567 (2006) 78



External secondary photon cross talk

Will SiPMs “communicate”?
Scan one SiPM in front of a second one and observe coincidence rate

- single sensor dark rate ~ 200 kHz
- coincidence background rate ~ 2.4 kHz
- coincidence rate increase when face to face ~ 1 kHz
- 1 mm active area 1 mm away
→ $\sim 15\%$ of 2π solid angle
- full (2π) solid angle:
 $1\text{kHz}/(2 \times 200\text{kHz})/15\% \sim 2\%$
→ OK, increase of background at % level

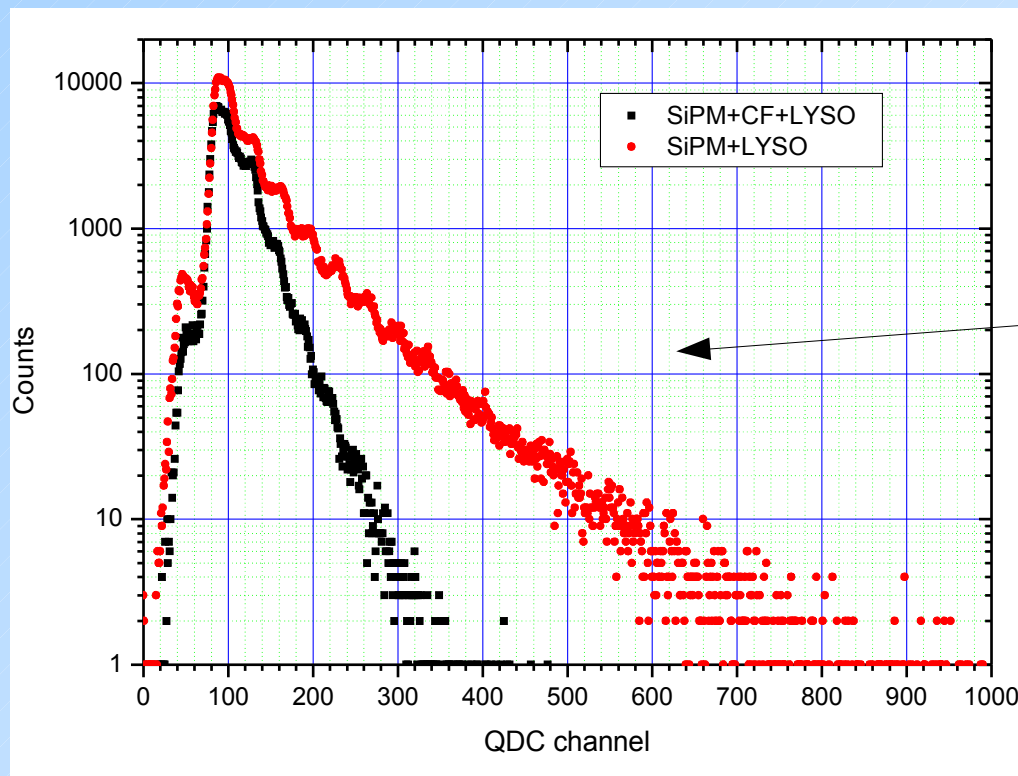
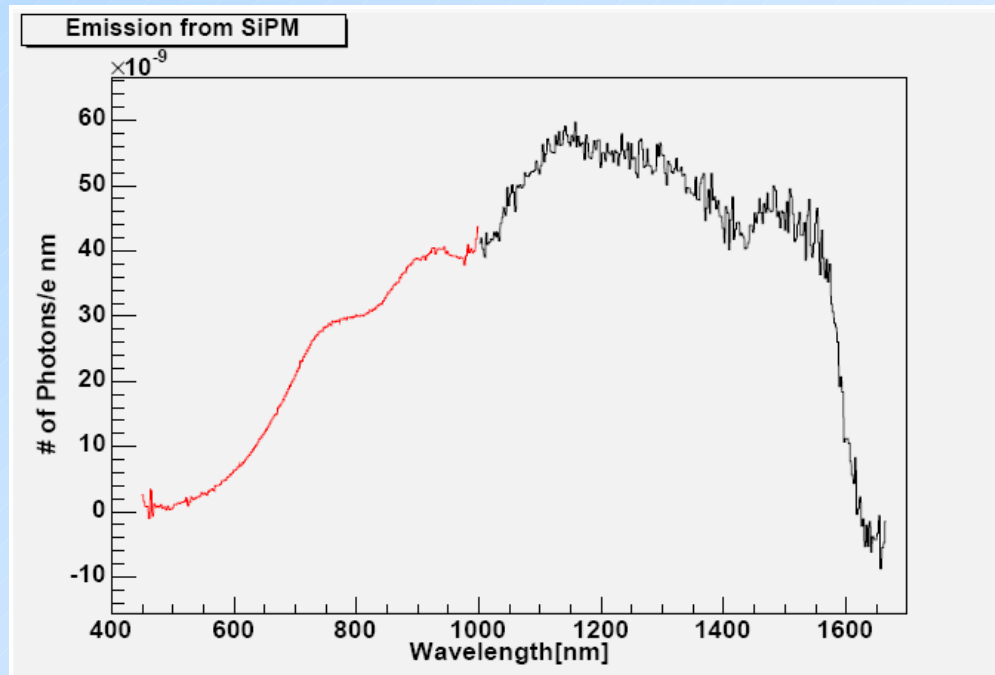


P. Križan (IJS)@LIGHT07

External secondary photon cross talk

Photons escaping SiPM can be reflected back when SiPM is coupled to crystal.

Wavelength distribution of light escaping from SiPM



Effect can be suppressed by use of color filter:

- 5x5 mm² SiPM with OC suppr.
- operated at gain 107
- LYSO 4x4x20 mm³
- BGC20 color filter

R. Mirzoyan (MPI Munich) @ PD09

SiPM-Signal saturation

Output of SiPM is saturated if number of photons in the pulse is comparable to number of micro cells:

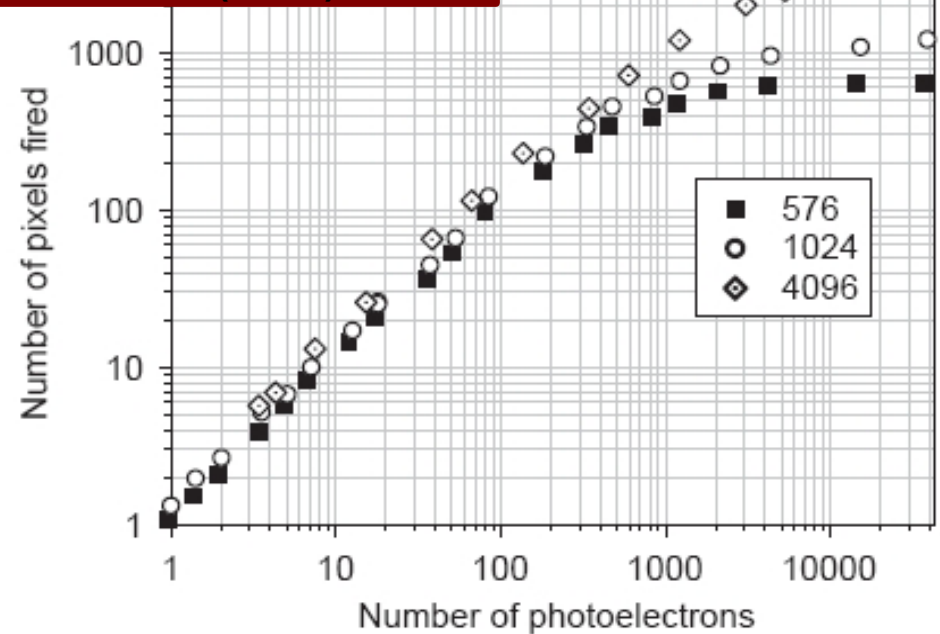
- photons hitting the same micro cell count as one for signal charge
- if photons are simultaneous (Cherenkov light) signal limit is number of pixels (disregarding after-pulse contribution)

- saturation can be approximated by

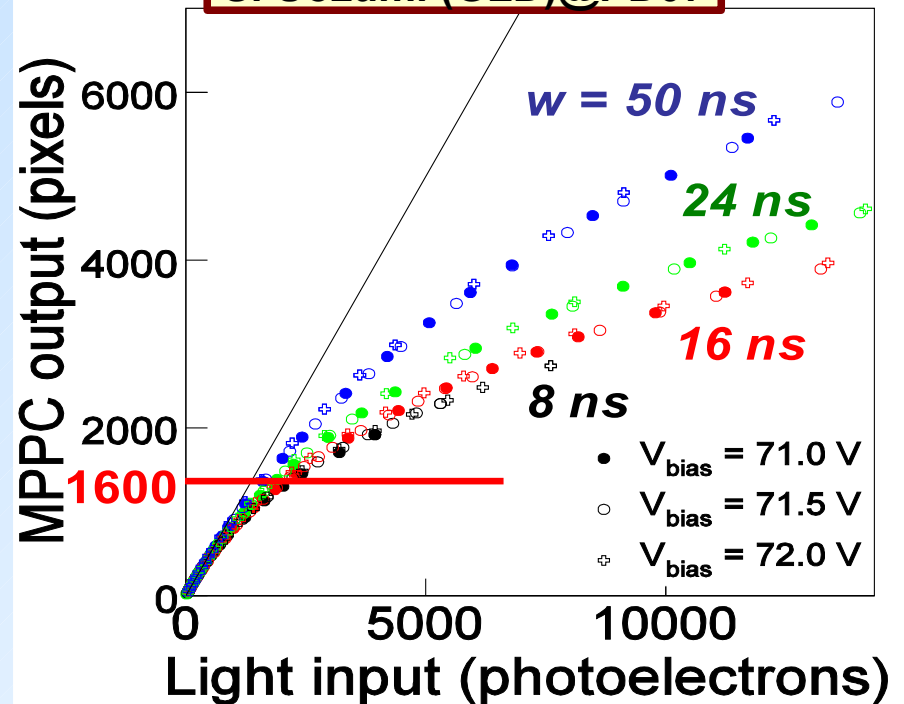
$$N_{sig.} = N_{all} \cdot \left(1 - e^{-\frac{PDE \cdot N_{ph.}}{N_{all}}} \right)$$

- pulses from scintillators with decay times longer than pixel recovery time can produce signals significantly exceeding number of micro cells

NIM A540 (2005) 368

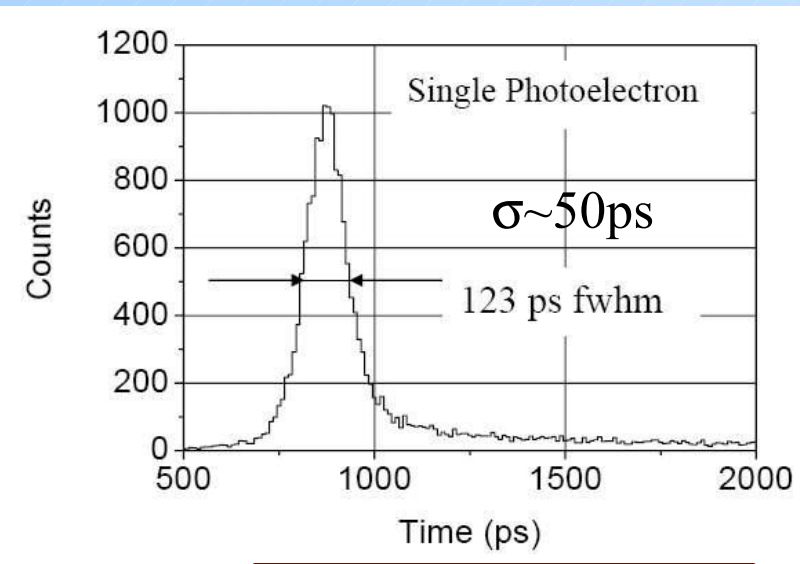


S. Uozumi (GLD)@PD07

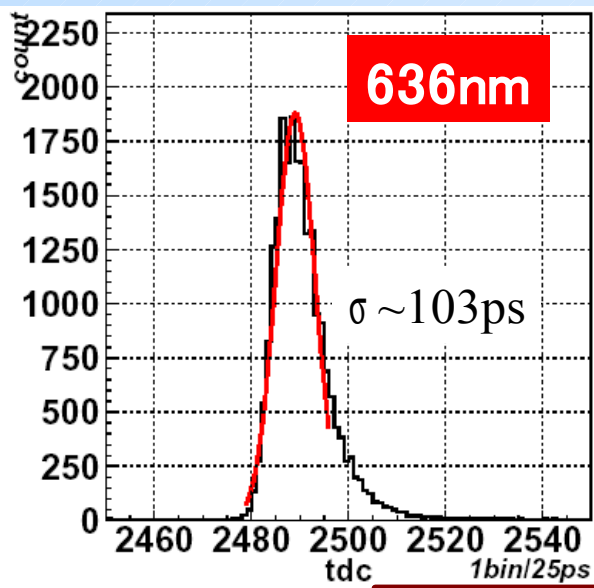


SiPM-Timing

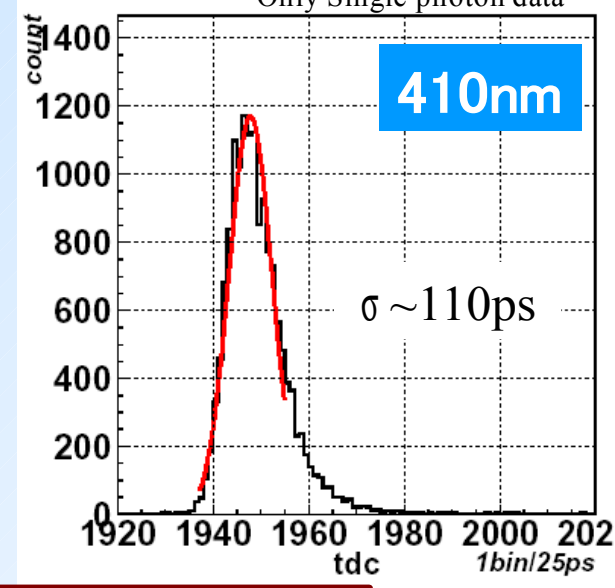
Fast rise time of the signal and high gain result in an excellent timing properties of SiPMs. Single photon timing resolution is on the order of 100ps. Applications to TOF, PET-TOF etc. are being investigated.



NIM A504 (2003) 48



T. Iijima (Nagoya U.) @ PD07



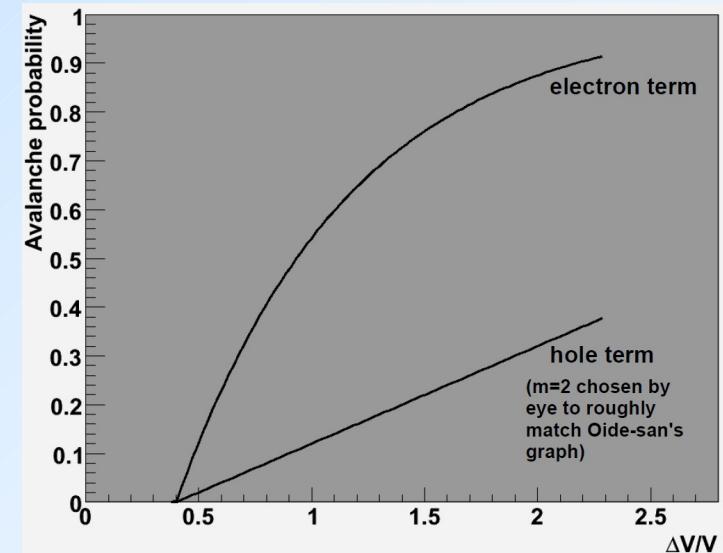
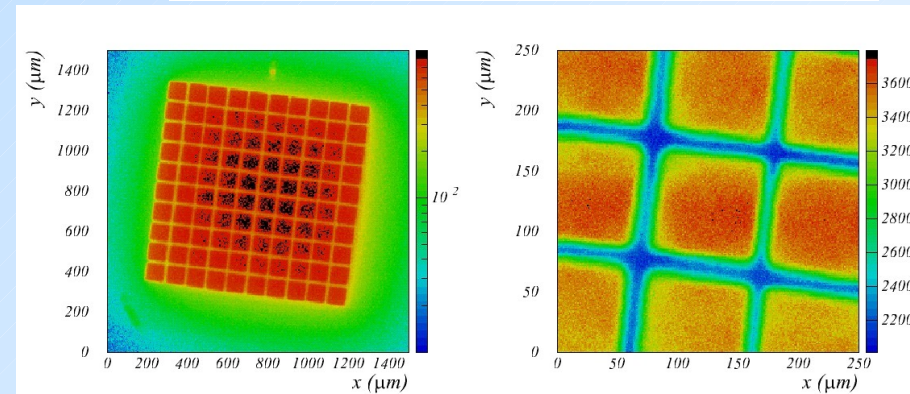
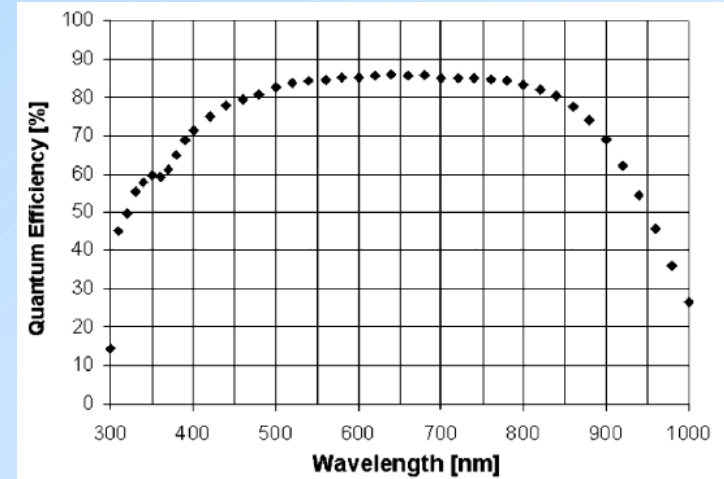
Sample MPPC
Bias -71.5V
Threshold 0.5pe
Only Single photon data

SiPM - Photon detection efficiency

Photon detection efficiency (PDE) depends on three factors:

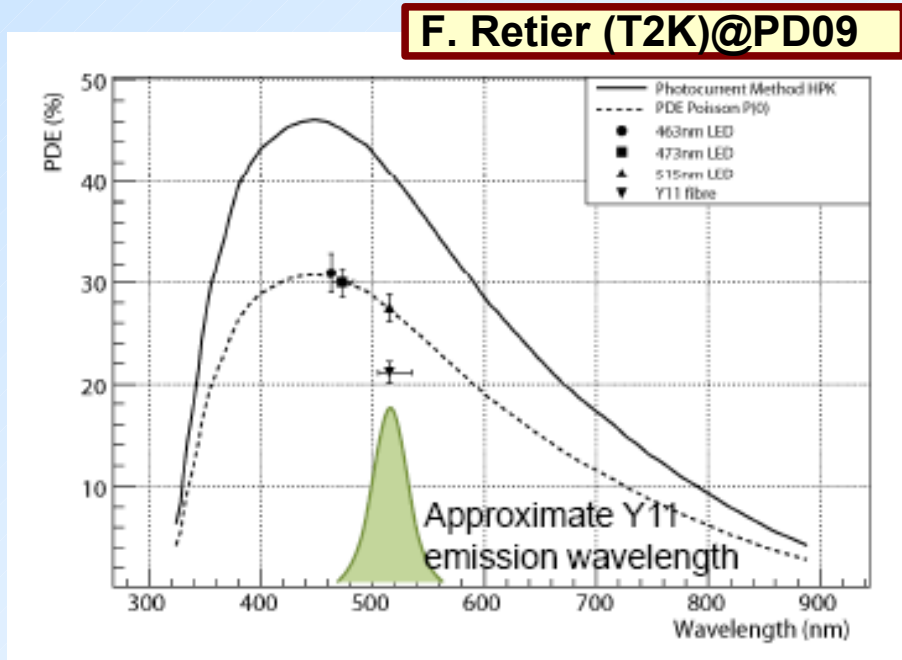
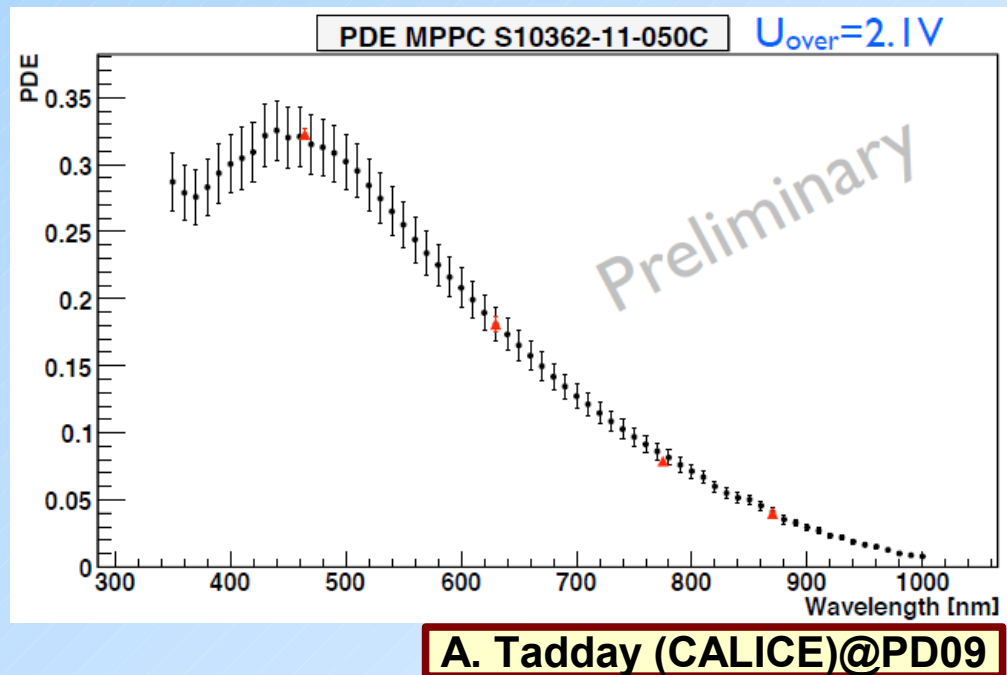
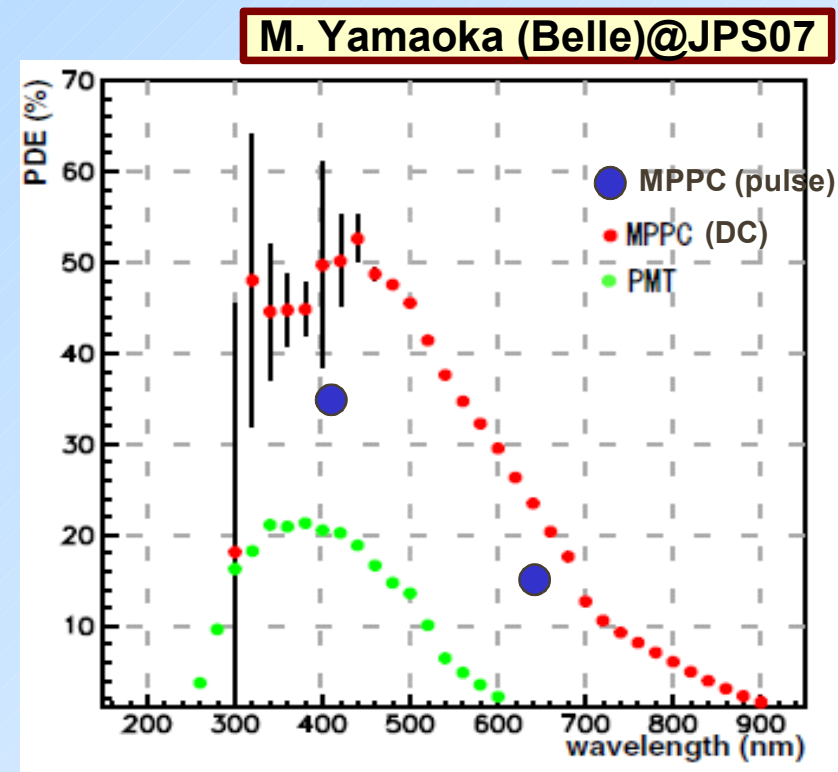
$$PDE = Q.E. \times \epsilon_{geom.} \times \epsilon_{Geiger}$$

- quantum efficiency (mainly absorption of photons in active volume)
- geometrical efficiency – ratio of active to total area
- probability for a carrier to initiate avalanche
 - depends on electric field
 - higher for electrons than holes→ increases with overvoltage



SiPM - PDE measurements

Standard measurement of QE by measuring photo current overestimates PDE by up to 30% due to the underestimation of the gain measured without including afterpulses. More accurate results are obtained by pulse counting method. Current measurement is renormalized to points measured by pulse counting.



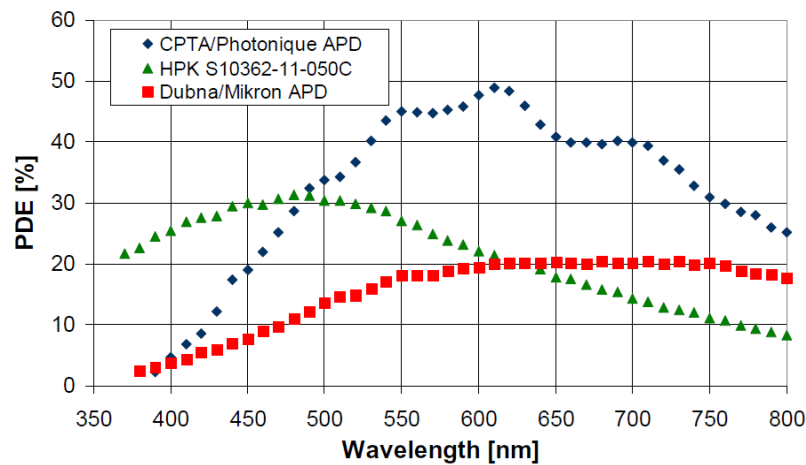
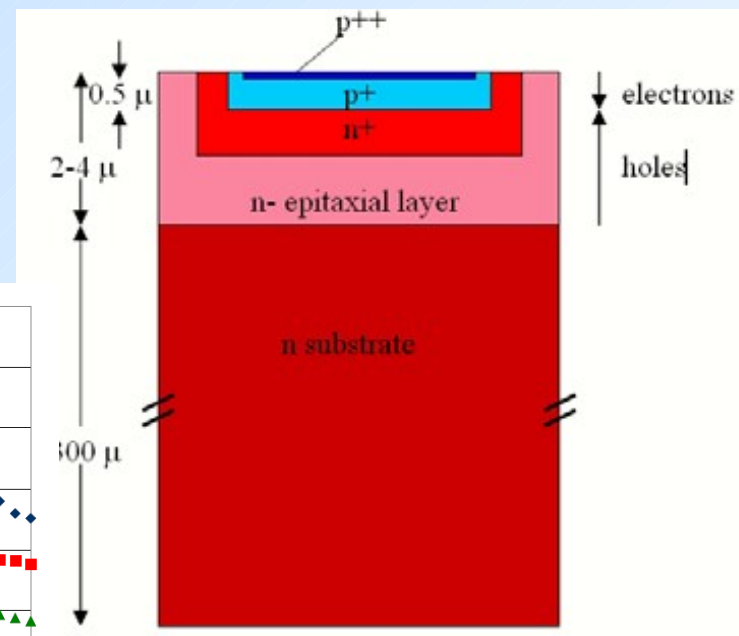
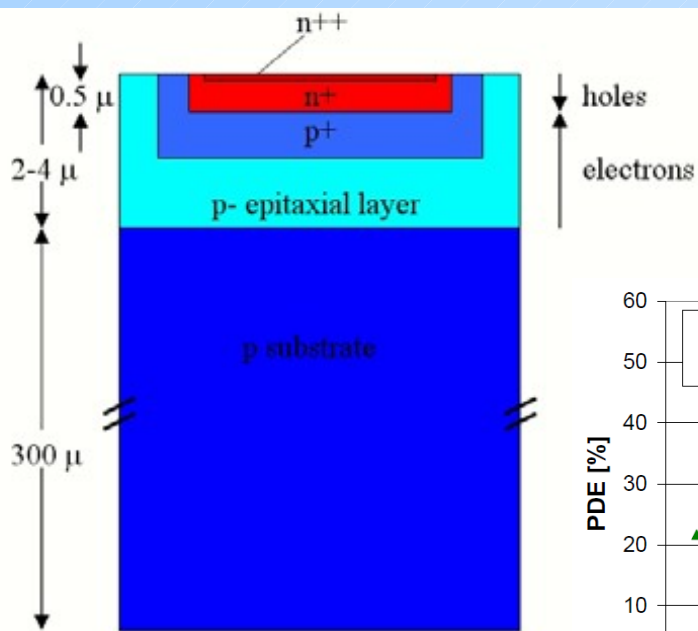
SiPM - p on n vs. n on p

n on p - green/red light sensitive:

- electrons drift to Geiger region from substrate and holes from surface side
- higher dark count rate – most of the thermally generated carriers arriving to Geiger region are electrons

p on n - green/blue light sensitive:

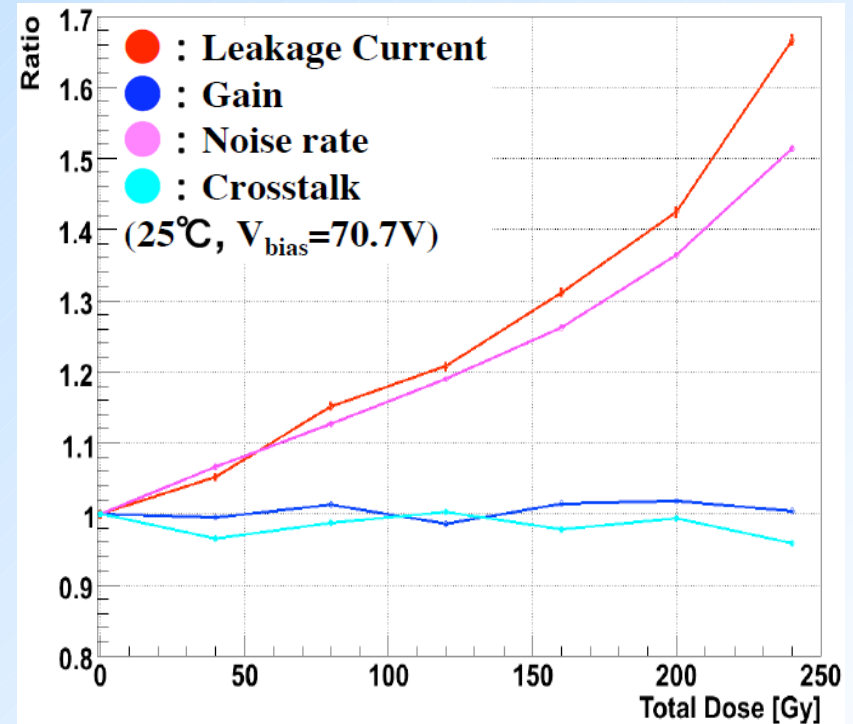
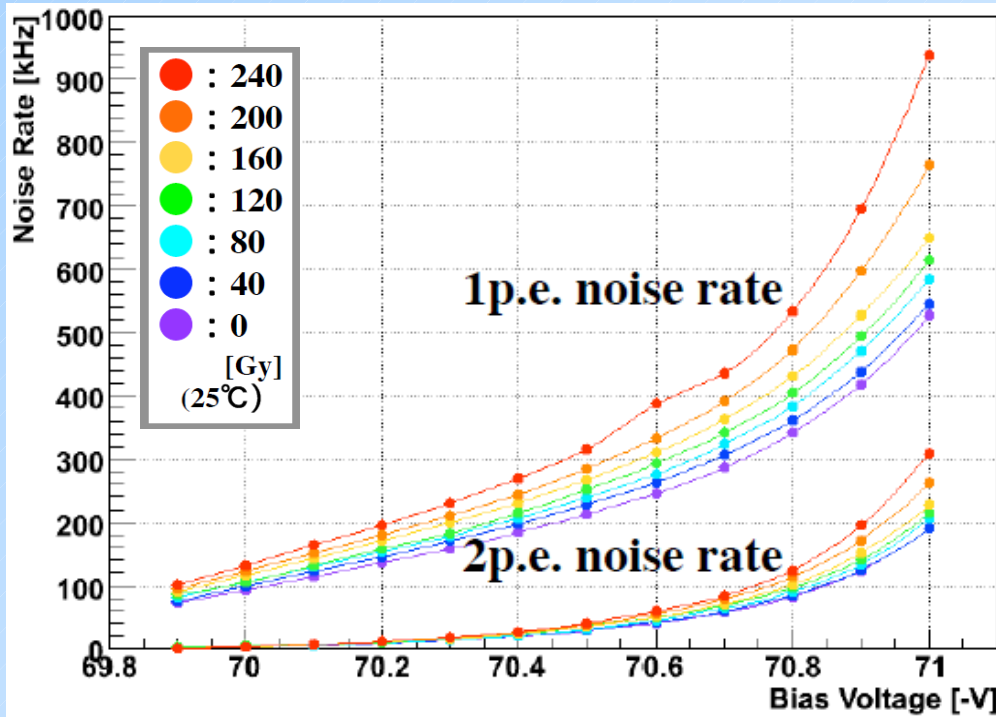
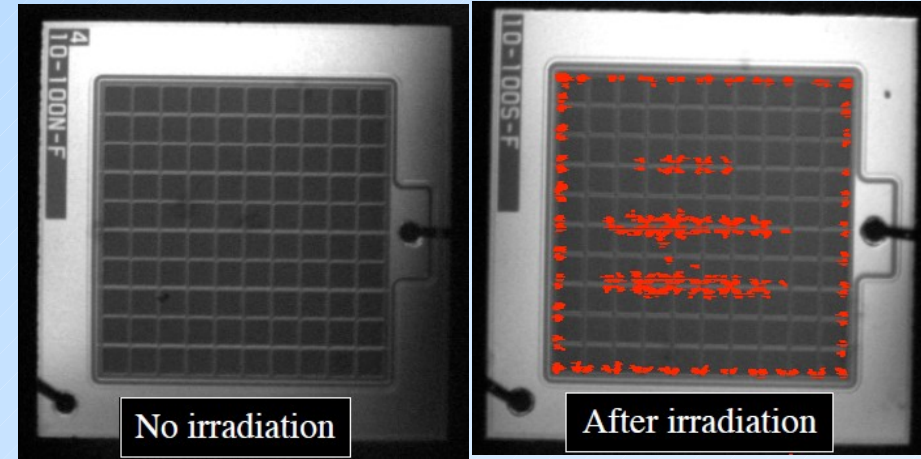
- electrons drift to Geiger region from surface and holes from substrate side
- lower dark count rate – most of the thermally generated carriers arriving to Geiger region are electrons



J. Musienko (INR/NU)@PD07

SiPM - Irradiation by γ rays from ^{60}Co

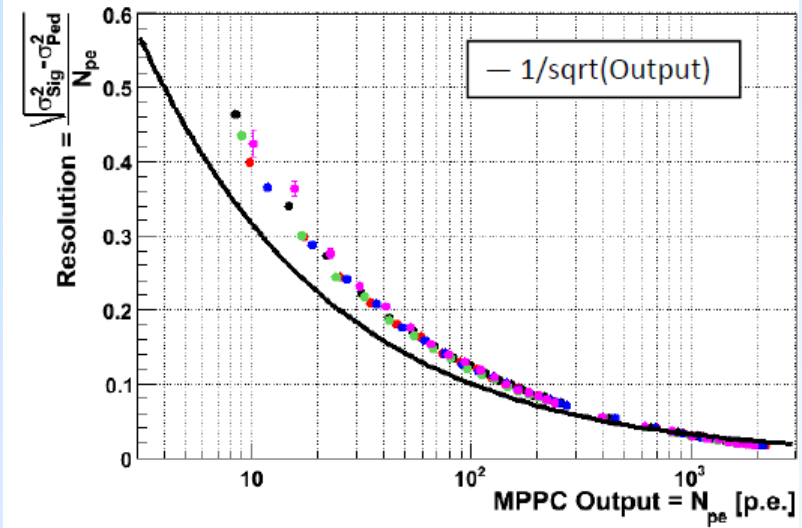
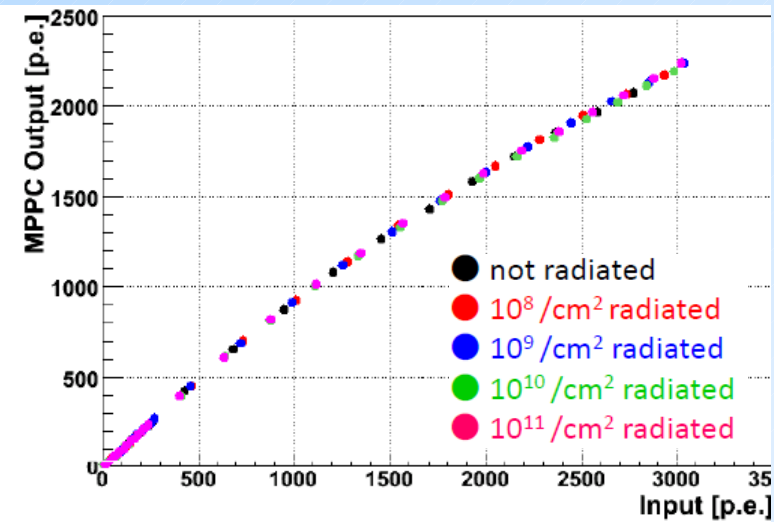
- moderate leakage current is observed and corresponding increase of dark counts
- functionality still OK after 240 Gy
- damage is produced mainly in SiO_2 layer – along the metal traces



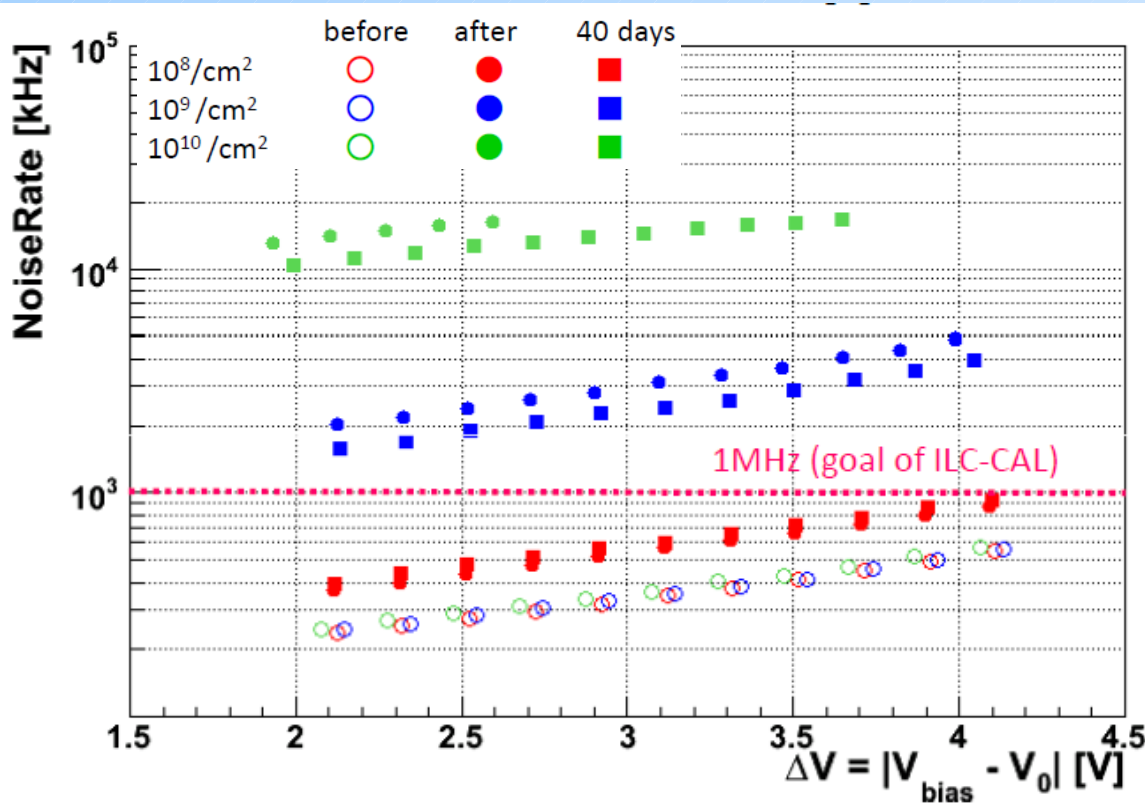
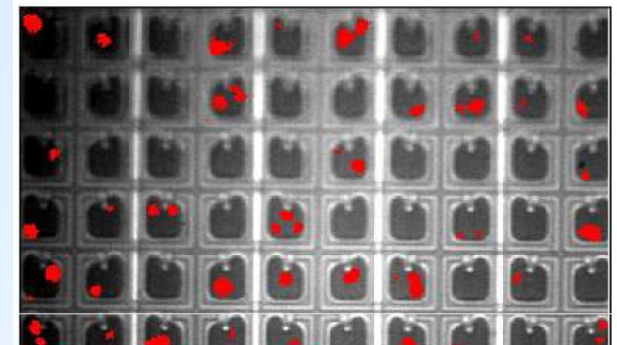
T. Matsubara (TIT)@PD07

SiPM - p,n irradiation

- non ionizing energy loss introduces lattice defects where carriers are thermally generated
→ dark count rate increases as expected
- increase of after-pulses
- detection of many photon pulses still OK

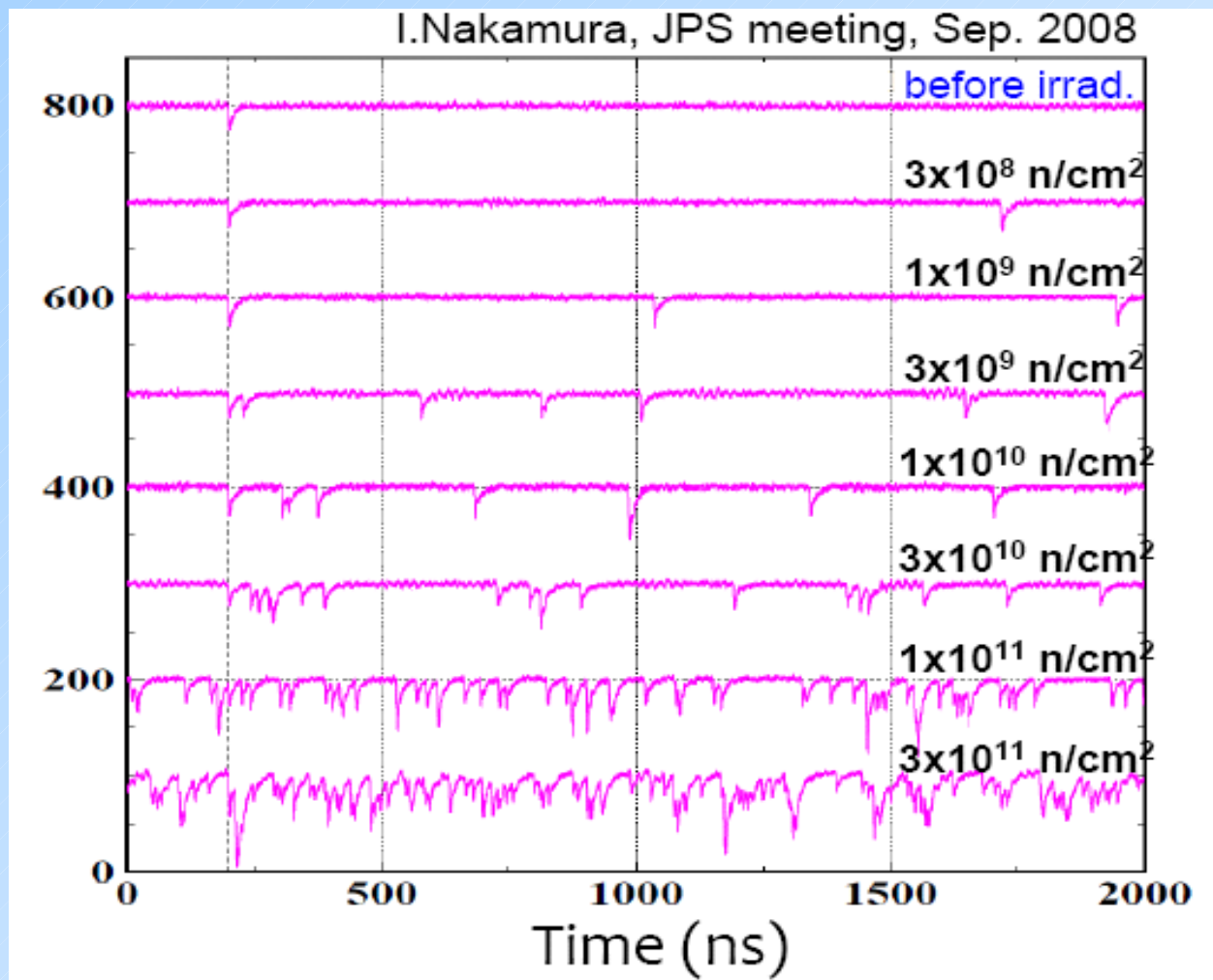


$10^{11}/\text{cm}^2$ irradiated (zoomed)



Y. Sudo (Tsukuba)@PD09

SiPM - p,n irradiation



→ Very hard to use present SiPMs as single photon detectors after fluence of 10^{11} n/cm² 1MeV neutrons

SiPM - Summary of characteristics

In many ways SiPM behaves like an ordinary PMT and is a very promising photon detector for Cherenkov applications.

Advantages:

- high PDE
- low bias voltage (less than 100V)
- high gain – single photon detection
- excellent timing
- operation in magnetic field
- (potentially low cost?)

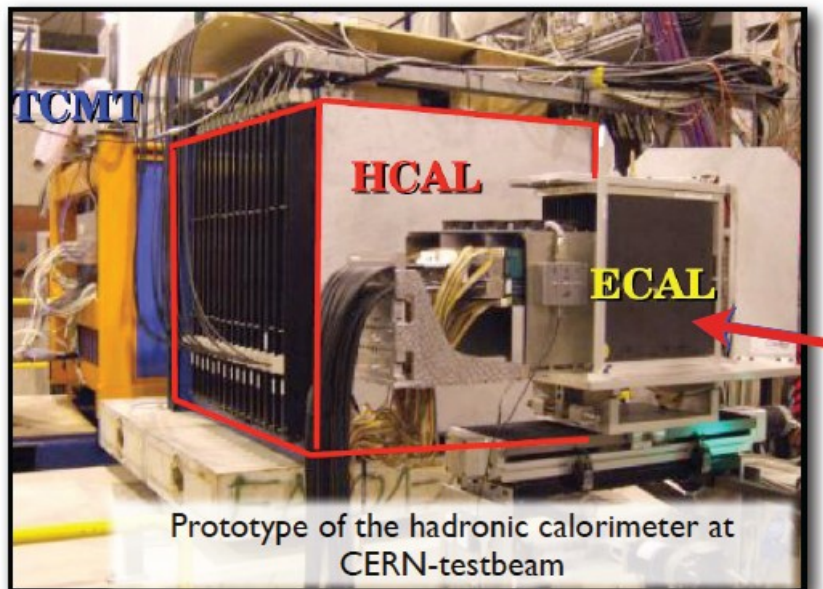
Disadvantages (low light intensity):

- high dark count rate
- sensitive to radiation damage (n,p)

CALICE - first large system experience

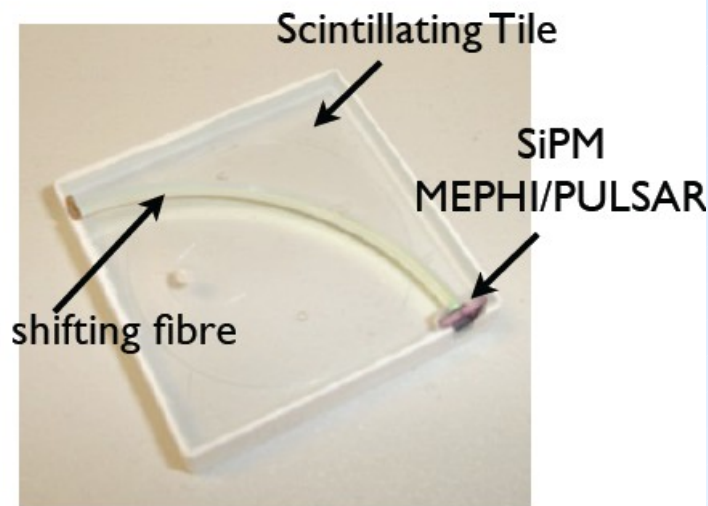
- only 8 bad channels in 3 years of testing – mostly mechanical problems

CALICE: Calorimeter for the Linear Collider Experiment



Prototype of the hadronic calorimeter at CERN-testbeam

~ 7600 SiPMs



Wavelength shifting fibre
blue → green (highest sensitivity of sensor)

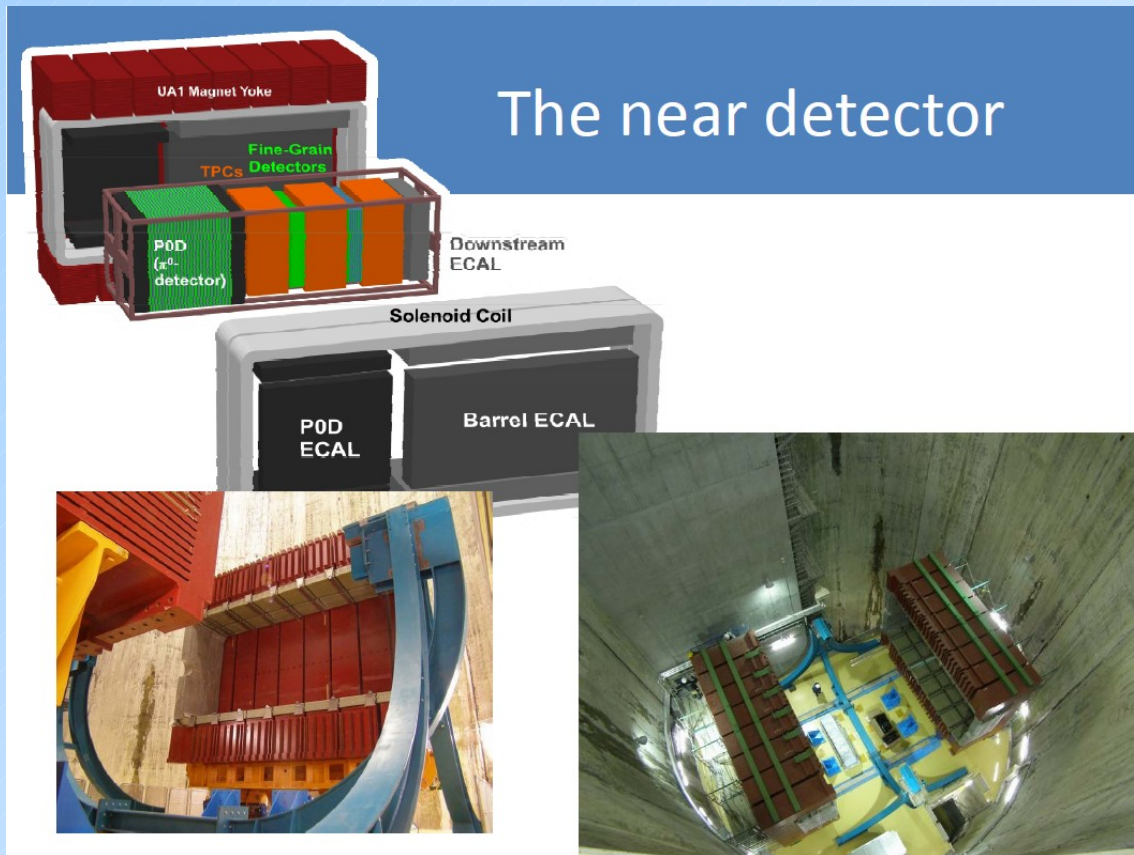
+ response uniformity

- Several producers/sensor types
- Which sensor is best for the application?
- Characterisation is needed

A. Tadday (CALICE)@PD09

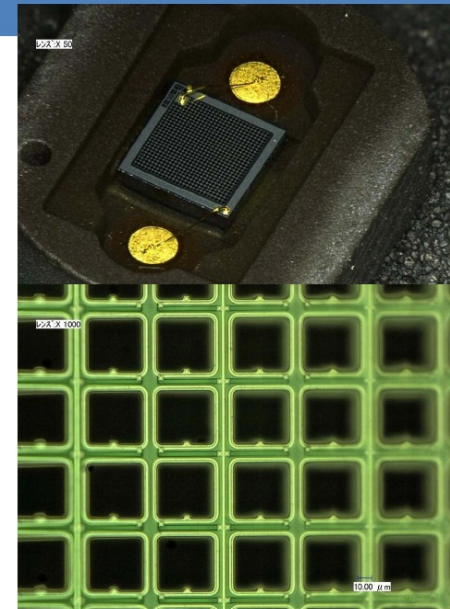
T2K - first experiment with SiPMs

- same type of SiPM used in many detectors in total more than 60000
- all have been tested → very low number of bad samples



Using the same MPPC

- 1.3x1.3 mm² specifically designed for T2K
 - Well suited for 1 mm diameter fiber
- 667 pixels
 - 26x26 50 μm pixels minus 9 in the corner for lead
- Dark noise < 1.2 MHz at nominal voltage (7.5 10⁵ gain at 25C)



	Institution	tested	bad
FGD	Kyoto	9,559	5
ECAL	Imperial/warwick	4,000	0
INGRID	Kyoto	8,235	4
INGRID	Ecole Polytechnique	3,194	?
POD	Colorado State	11,500	80*
SMRD	Louisiana State	1,717	11*
SMRD	INR Moscow	600	1
SMRD	Warsaw University of Technology	1,202	4

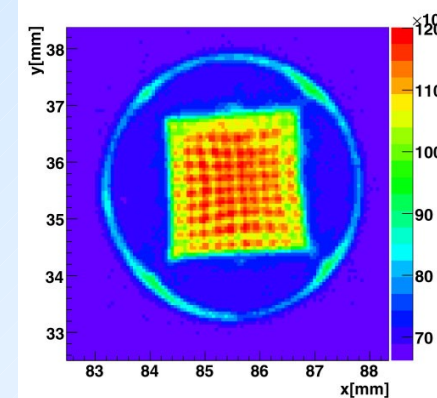
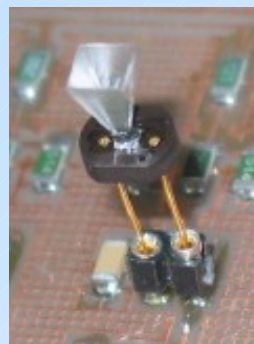
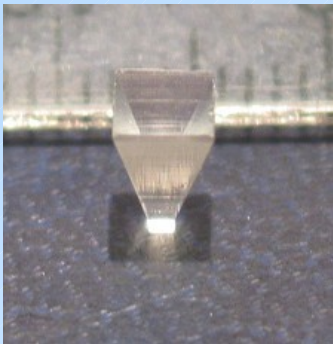
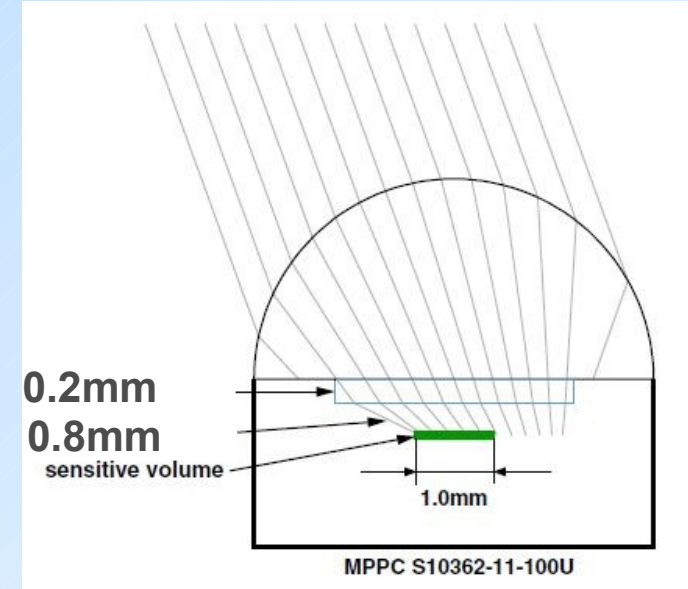
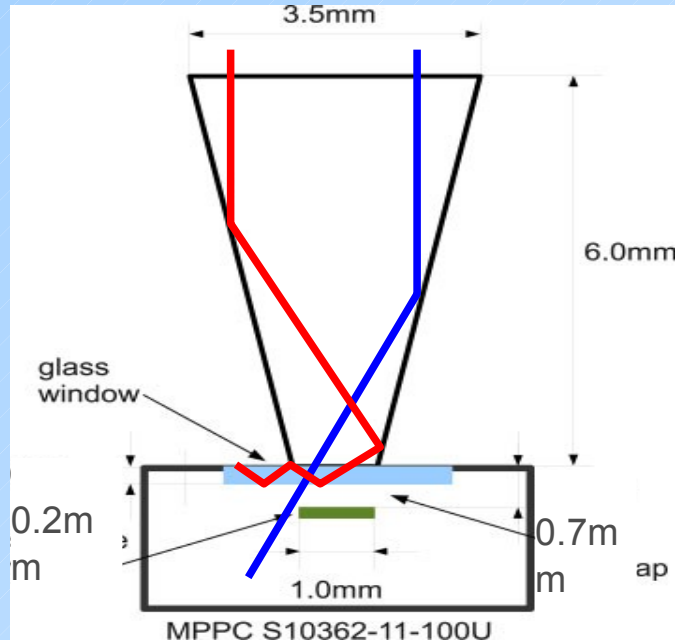
* Conservatively removed

F. Retier (T2K)@PD09

Light concentration

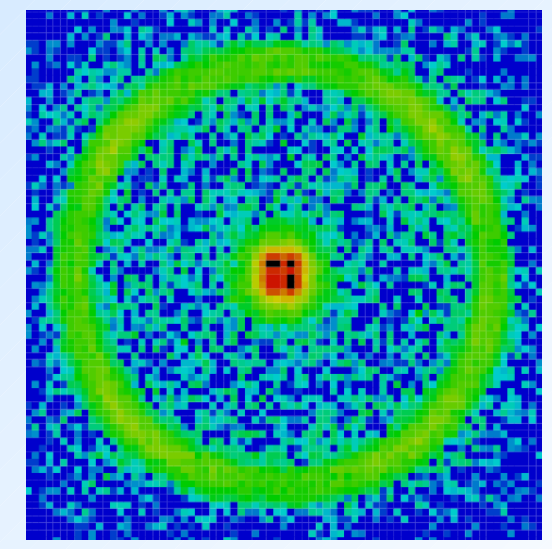
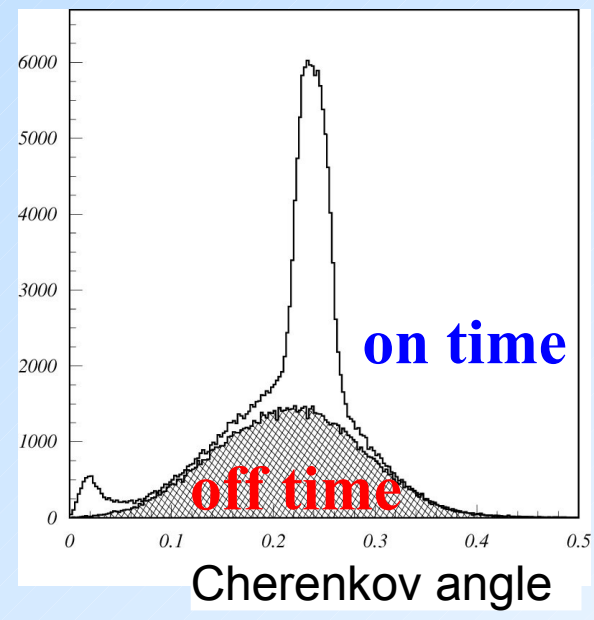
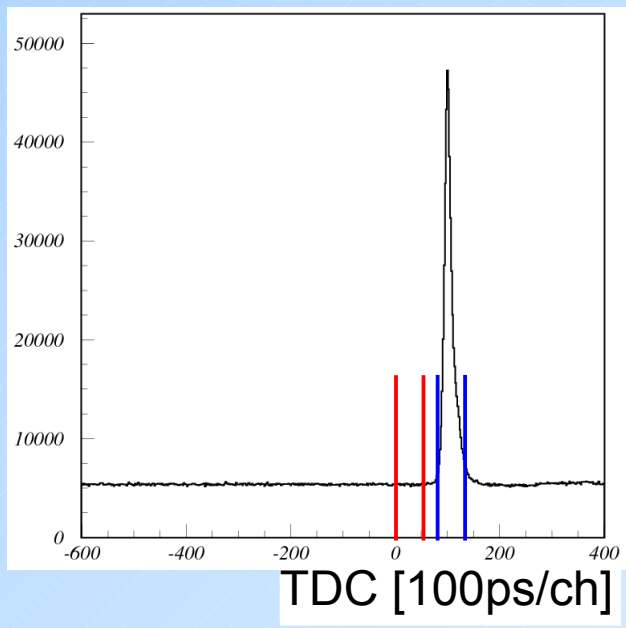
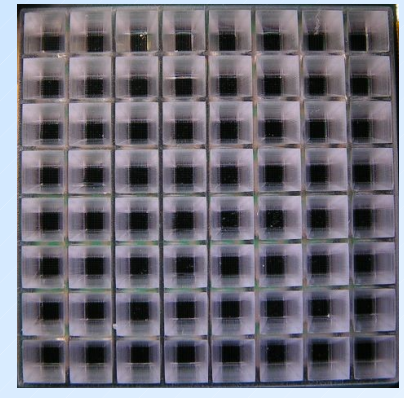
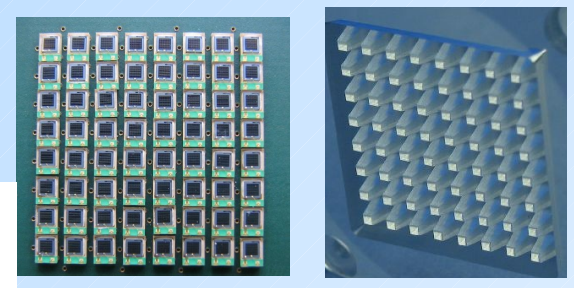
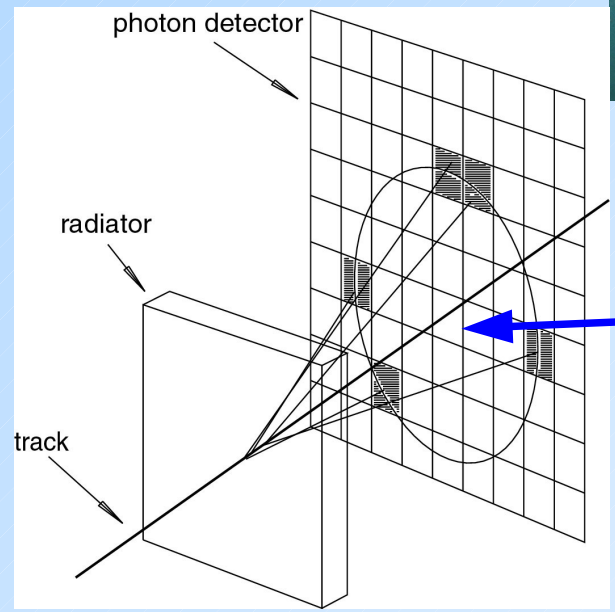
Can be used if light comes within the limited solid angle

- Winston cones produce large angular spread at the exit surface – photons can miss the active area
- hemispherical light concentrators give better results with large spacing between concentrator and SiPM



Belle II aerogel RICH development

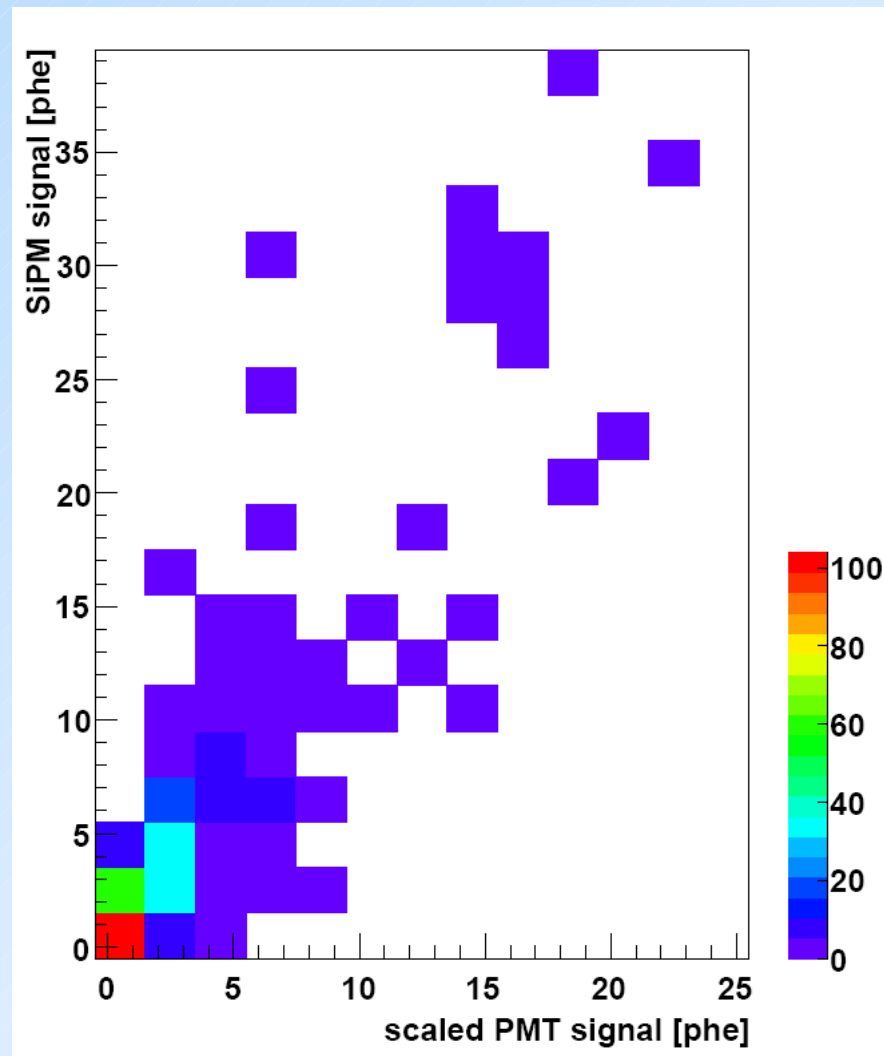
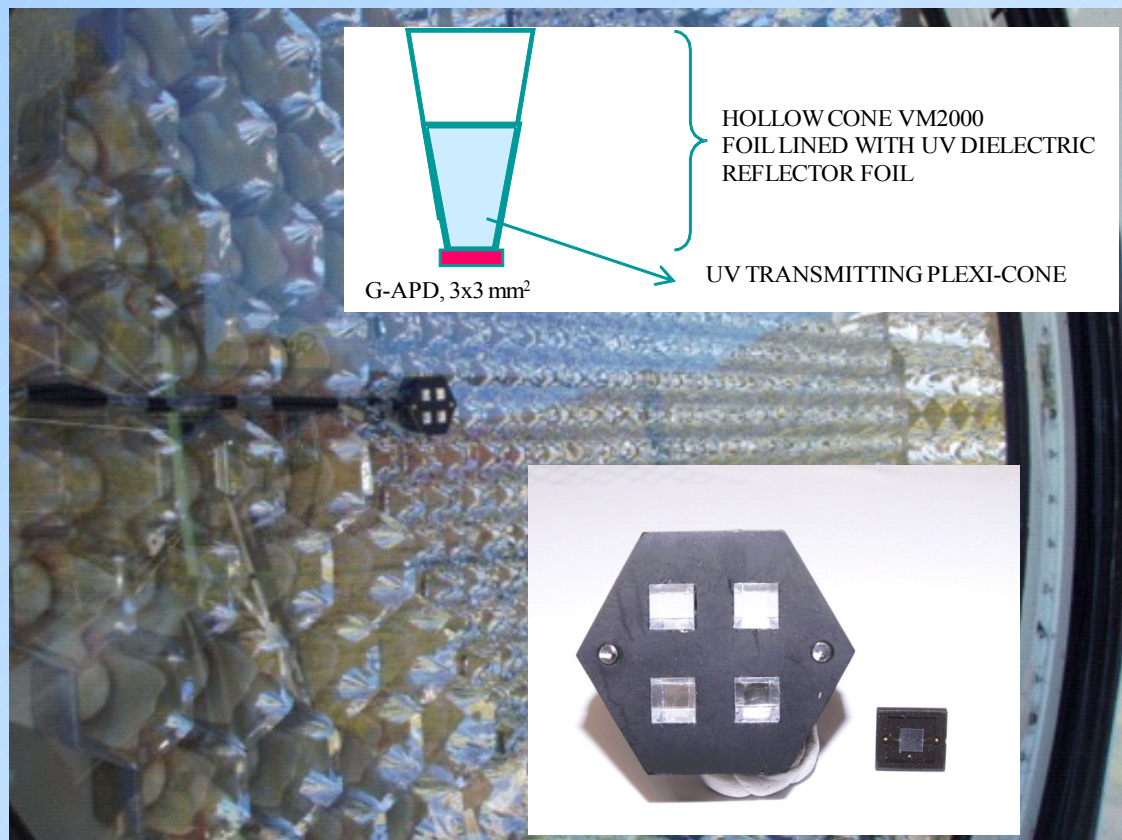
- SiPM based photon detector was considered for aerogel RICH.
- 8x8 array of MPPCs + light guides was produced
 - module was tested in the test beam with 1cm thick aerogel radiator and performed well



MAGIC project

First detection of air-shower Cherenkov light presented at RICH 2007.

On average larger signal in SiPM modules than in PMT modules.



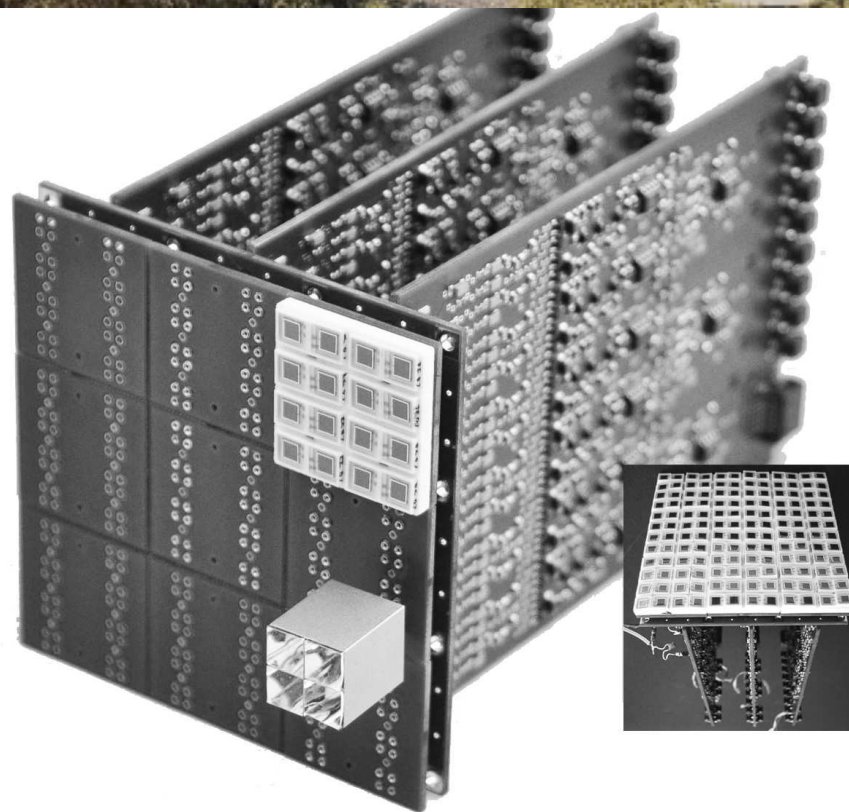
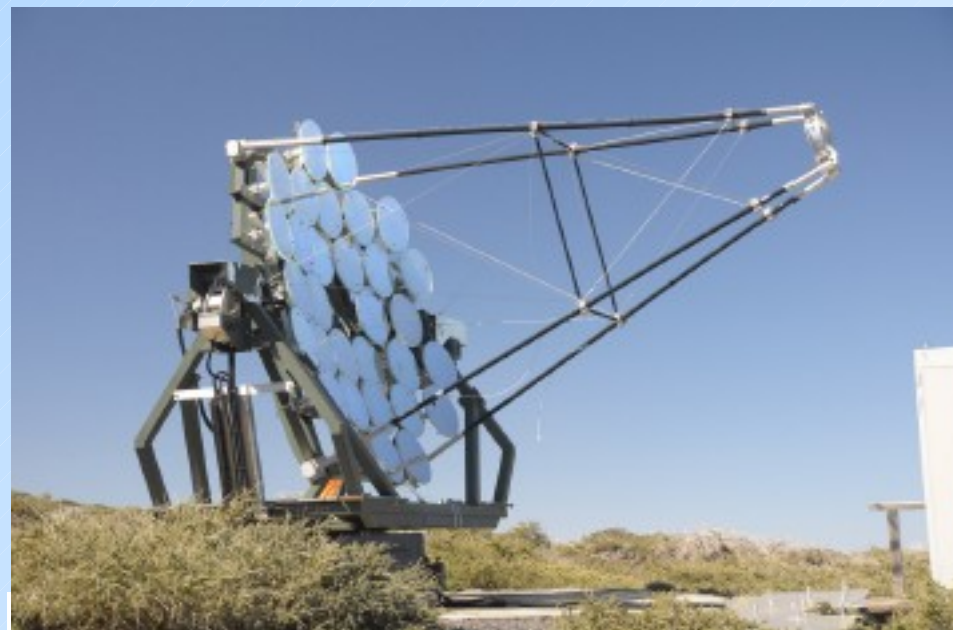
E. Lorenz (MPI,ETH) @ RICH2007

FACT project

- SiPM based module for camera for a Cherenkov telescope (DWARF: Dedicated multi Wavelength AGN Research Facility)
- 144 SiPMs + Winston cones
- 36 electronic channels



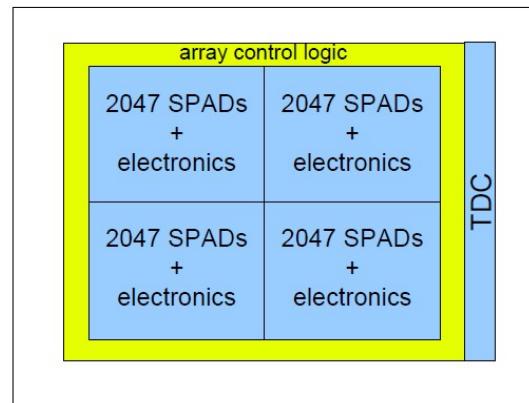
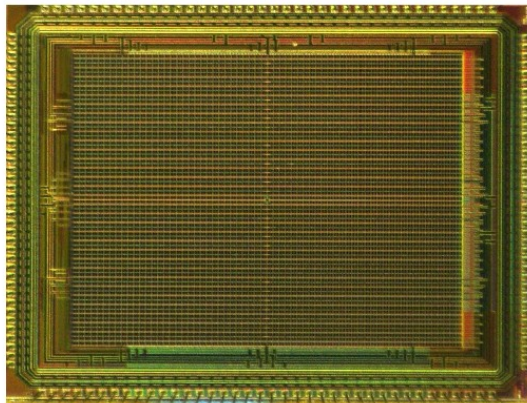
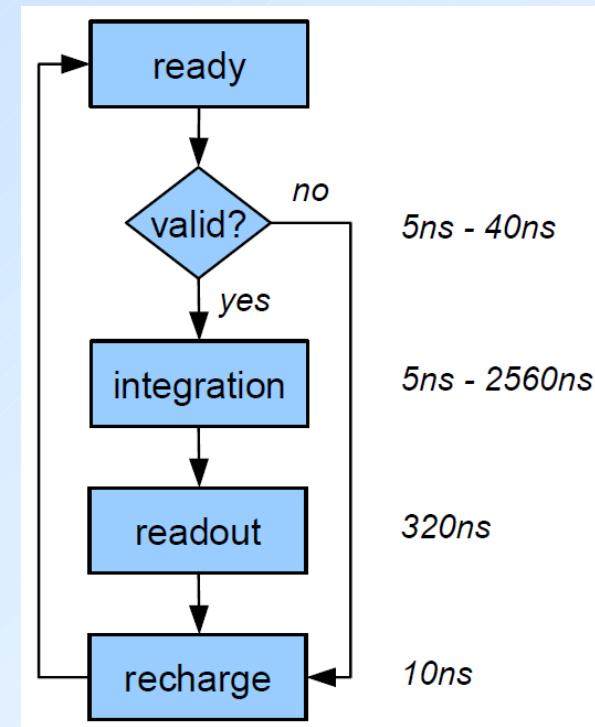
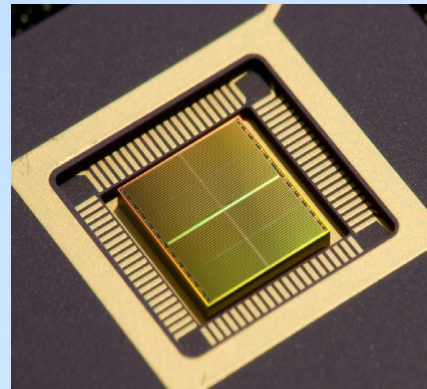
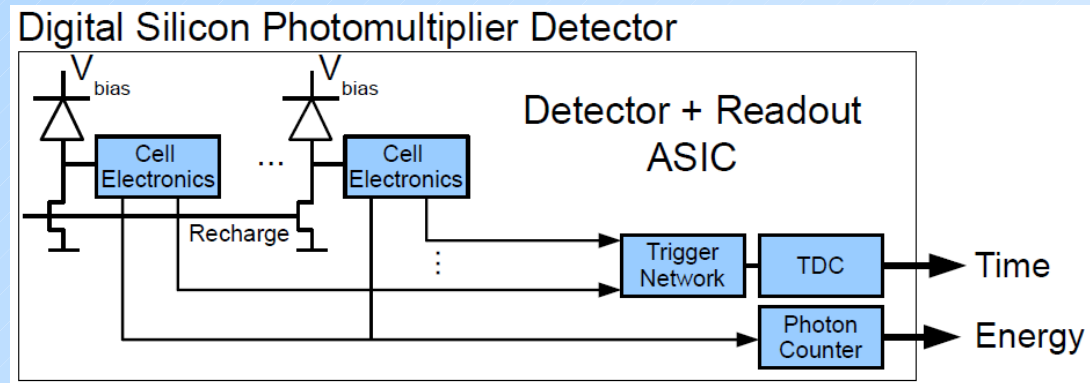
T. Krähenbühl (ETH Zurich) @ PD09



dSiPM-Digital SiPM (Philips)

Signal from each pixel is digitized and the information is processed on chip:

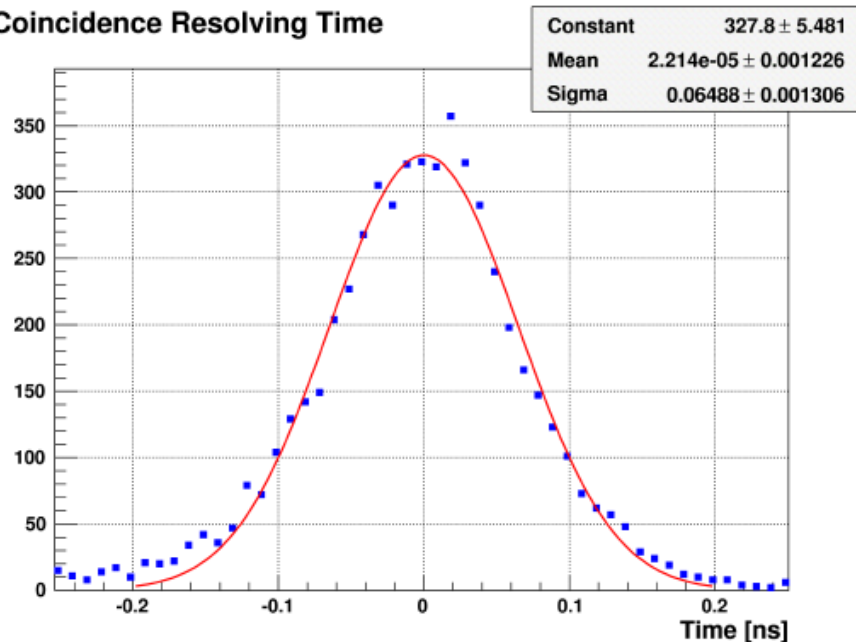
- time of first fired pixel is measured
- number of fired pixels is counted
- active control is used to recharge fired cells
- 4 x 2047 micro cells
- 50% fill factor including electronics
- integrated TDC with 8ps resolution



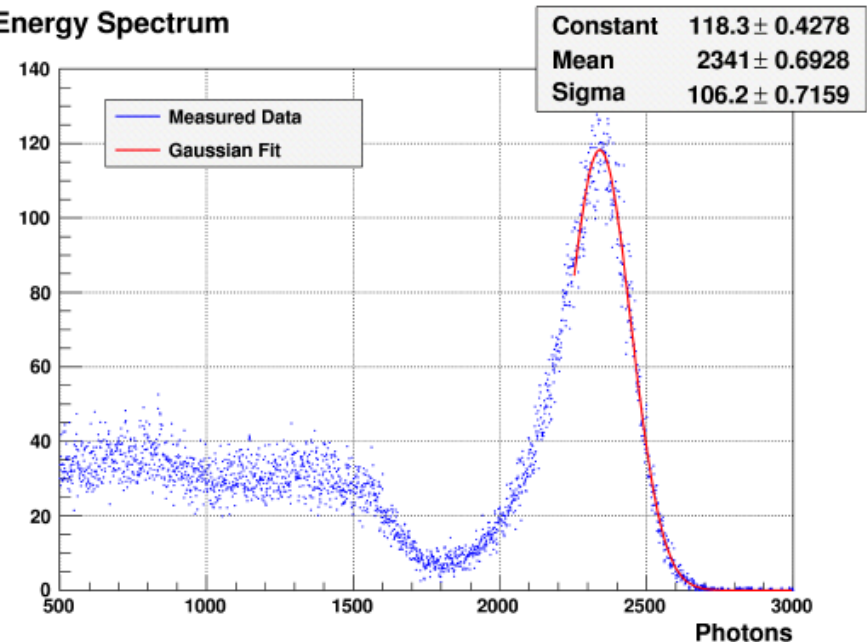
T. Frach (Philips) @ IEEE2009

dSiPM - TOF-PET application

Coincidence Resolving Time



Energy Spectrum



- 3X3x5 mm³ LYSO in coincidence, ²²Na source
- Time resolution in coincidence: **153ps** FWHM
- Energy resolution (excluding escape peak): **10.7%**
- Excess voltage 3.3V, 98.5% active cells
- Room temperature (31°C board temperature, not stabilized)

T. Frach (Philips) @ IEEE2009

Main sources of information

Conferences:

- TIPP2011, Chicago (<http://conferences.fnal.gov/tipp11/index.html>)
- RICH2010, Cassis (<http://rich2010.in2p3.fr/>)
- PD09, Kobe (<http://www-conf.kek.jp/PD09/>)
- TIPP09, Tsukuba (<http://tipp09.kek.jp/>)
- PD07, Kobe (<http://www-conf.kek.jp/PD07/>)
- RICH2007, Trieste (<http://rich2007.ts.infn.it/index.php>)

Overview papers:

- K. Arisaka, (NIM A442 (2000) 80)
- D. Renker and E. Lorenz (JINST-P04004)
- D. Renker (NIM A598 (2009) 207)
- J. Haba (NIM A595 (2008) 154)

and other conferences and related papers ...

BACKUP SLIDES